Juraj Chmelar

Size reduction and specification of granular petrol coke with respect to chemical and physical properties

Doctoral thesis
for the degree of doktor ingeniør

Trondheim, May 2006

Norwegian University of Science and Technology
Faculty of Engineering Science and Technlology
Department of Geology and
Mineral Resources Engineering

NTNU
Innovation and Creativity

NTNU
Norwegian University of Science and Technology

Doctoral thesis
for the degree of doktor ingeniør

Faculty of Engineering Science and Technology
Department of Geology and
Mineral Resources Engineering

ISBN 82-471-7899-0 (printed version)
ISBN 82-471-7898-2 (electronic version)
ISSN 1503-8181

Doctoral theses at NTNU, 2006:74

Printed by NTNU-trykk

Acknowledgements

This thesis is based on studies conducted at the Department of Geology and Mineral Resources Engineering and at the Department of Materials Science and Engineering, at the Norwegian University of Science and Technology (NTNU).

I would like to thank Professor Knut L Sandvik for introducing me into mineral processing and for his encouragement. I am very grateful to Professor Trygve Foosnæs for his guidance, enthusiasm, many fruitful discussions and support throughout this work. I thank Professor Harald A Øye for guidance and support.

Thanks are due to Dr. Arne Petter Ratvik at SINTEF Materials and Chemistry for his support, trust and guidance in this work. Anne Støre is thanked for help with the experiments and valuable discussions.

I would like to thank Hydro Aluminium Årdal for allowing me to conduct experiments at the plant. Special thanks goes to Dr. Hogne Linga and Dr. Lorentz Petter Lossius from Hydro Aluminium Årdal for their help and support through this work. Terje Jonny Berg is thanked for arrangement and shipment of coke samples for this work. Dr. Ramon Fernandez from Statoil also helped to supply some samples and I am therefore thankful to him. I would also like to thank Elkem Lista for allowing me to analyse samples at their facilities.

I am very thankful to the Department of Metallurgy at SINTEF Materials and Chemistry for help and encouragement during this work.

I am very thankful to Dr. Sean Gaal at SINTEF Materials and Chemistry for his support and help with several theoretical and technical problems during this work. A special thanks goes to Dr. Jacek Kolacz for his patience, help, encouragement and time he spent with me.

I am very thankful to all PhD students in the CarboMat program for their support and help. Great team!

Financial support for this work was provided from The Research Council of Norway and the Norwegian aluminium and ferro-alloy industries through the CarboMat program, which is gratefully acknowledged.

Finally, I want to thank my family and friends for their support. I am grateful to my beloved parents for their patience, understanding and encouragement through all those long years.

Abstract

Carbon required for the reduction of alumina by electrolysis in the Hall-Héroult process is supplied by the anode. Anodes are produced from a mixture of petroleum coke with coal tar pitch as the binder. The minimum theoretical carbon consumption is 0.334 kg C/kg Al. But due to current efficiency and oxidation losses the consumption is typically 400 kg C/kg Al.

Petroleum coke is a by-product from crude oil refineries, but as its value represents only about 2 per cent of the overall production it has a limited interest to the producers. Mechanical and physical properties of coke are influenced by the crude oil, processes within the refineries and calcining of the coke. Continuous high demand for calcined coke by aluminium smelters has created a difficult situation with respect to quality and availability, leading to the use of lower quality coke in aluminium smelters and potential disturbances in the production.

Understanding the consequences of varying calcined coke qualities is crucial for to possibly compensate and adjust process parameters in the subsequent use of the coke, in order to obtain economical production of aluminium.

In the present work, the subject of study was four different petroleum coke types, where three were derived from a single source (SSA, SSB and SSC) and one was from a blend of different cokes. All of the cokes had different chemical and physical properties. Single source cokes have homogenous chemical and physical composition in the whole size range while the blended coke had heterogeneous composition due to the mixture of different coke types used. The blended coke consisted of several different coke types (25) in order to meet the required specification.

This work also describes new characterisation/measurement methods which can contribute to a better understanding of variations in material properties due to physical and mechanical changes in the calcined coke feed materials.

Each step in the production of pilot scale anodes is described. A new method was developed for the characterisation of the mechanical strength of calcined coke. This method, the drop test, originates from the study of materials for road construction for the determination of the grain stability of rock materials. The method determines the coke grain strength in the entire size distribution. On the other hand, established measuring methods for calcined coke, HGI (ASTM D5003-95) and grain stability (ISO 10142), determine only the mechanical strength in a specific size range, +0.6-1.18 mm and +4-8 mm, respectively. In other words, both methods give limited information about coke mechanical strength distribution throughout the whole size range, which is especially important when blended cokes are used. Additionally, the results from the drop test are expressed in volume reduction, size reduction, impact force and amount of fines below 148 μm generated during the test. A good correlation between ISO 10142 and the drop test was found. The results show good correlation between the size and volume reduction and the specific grinding energy. The method can also determine the

grain strength of a specific size fraction which might be critical to further processing during anode production.

Totally, about 8 tons of four calcined coke types were processed during this work. The majority of this material was ground in the air swept ball mill, for production of the finest fraction, dust. The pilot scale air swept ball mill circuit is identical to the equipment used in industry today. This investigation showed the importance of process optimisation for the stable production of dust with the required specification (particle size and Blaine). Each coke exhibited different behaviour in the grinding circuit, due to different mechanical strengths, which is reported as a specific grinding energy. The mechanically weakest coke produced dust with the lowest specific grinding energy. The particle size variation in the coke used in the mill produced a significant disturbance in the product quality. It was found that the sweeping speed through the mill influences the particle size distribution in terms of the proportion of the finest particles. It also affected the particle roundness of the produced dust, which can influence the flowability of the coke when mixed with pitch. The ratio of ball sizes and the rotational speed of the mill influenced the particle size distribution, Blaine and specific grinding energy.

On-line particle size control was utilised during the dust production. This system allowed continuous control of the product size by regulation of the air classifier rotor speed. Three different dust sizes were produced in the air swept ball mill, which were all below about 200 μm but contained different proportions of material below 63 μm.

Sieved coke fractions together with dust were weighed according to a specified recipe and blended in a sigma blade mixer together with coal tar pitch. A vibration compactor was used for the production of green anodes under optimal conditions. The anodes were produced with three different pitch contents (15, 18 and 20 wt%) and three different dust sizes (45, 63 and 94 %, -63 μm).

Core samples of green anodes were investigated in an improved dilatometer for the determination of thermal expansion and shrinkage during baking. Improvements made to the dilatometer during this work contributed to better reproducibility, increased precision and a healthier working environment. An increase in the heating rate influenced the initial expansion, shrinkage and baking loss of the anode. The heterogeneous pitch distribution throughout the anode due to the forming force, friction between coke particles and between the paste and mould showed the importance of selecting a consistent sampling position. The results showed that the bottom samples have greater expansion due to a thicker pitch bridge layer while the top samples have reduced expansion. The sample packing material contributed to a higher initial expansion due to the reduced free surface area for binder volatiles release, and the shrinkage was reduced because of the radial thrusts from the packing material. Thermal dilation results showed differences between samples with varying pitch, dust size and coke type, which can be used to indicate the final properties of baked anodes. A good correlation was found between the thermal dilation after the pitch expansion and the dust content.

Green anodes were baked under controlled conditions and then characterised. The baked apparent density showed a good correlation with the pitch content and dust size. The results showed that 18 % pitch content and 63 % -63 μm produced the highest baked densities. The variation in coke type exhibited differences in baked density, specific electrical resistance, air permeability, CO_2 and air reactivity and modulus of elasticity.

Table of contents

1. Introduction

1.1 Aluminium production

Aluminium is produced industrially through a process patented independently in 1886 by Charles M. Hall and Paul L.T. Héroult. The process produces liquid aluminium by the electrolytic reduction of alumina (Al_2O_3) dissolved in an electrolyte consisting mainly of cryolite (Na_3AlF_6) at about 960 °C. The overall reaction can be expressed by Equation 1.1.

$$Al_2O_{3(dissolved)} + 1.5\,C_{(s)} = 2Al_{(l)} + 1.5\,CO_{2(g)} \qquad 1.1$$

Figure 1.1 presents a schematic drawing of an electrolysis cell with pre-baked anodes.

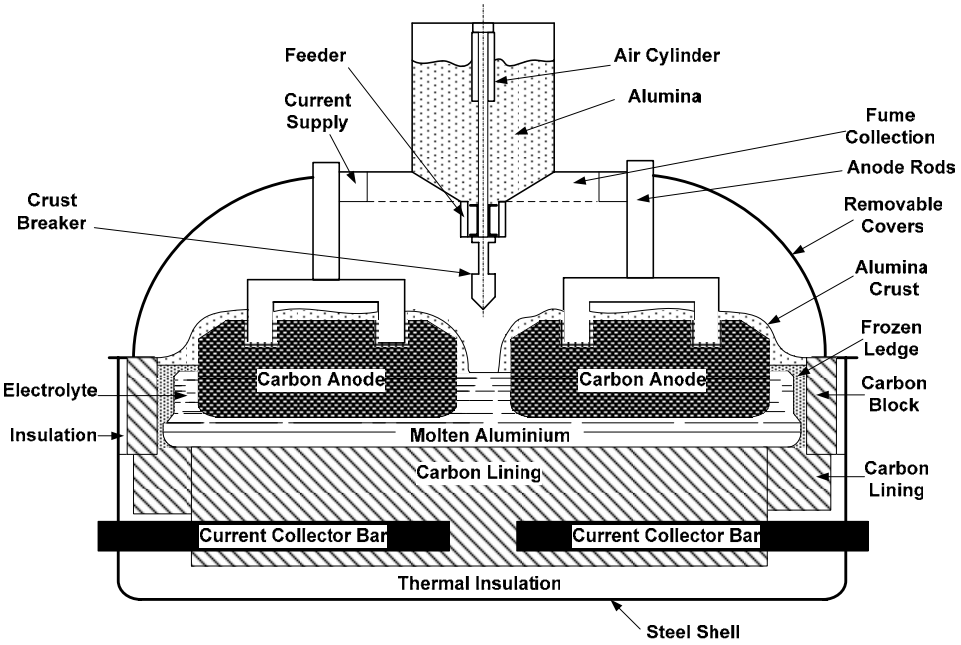

Figure 1.1 Electrolysis cell with prebaked anodes [Grjotheim, Kvande, 1993].

Carbon needed for the reduction of alumina is supplied by the anode. Today, there are two anode designs, prebaked and Söderberg anodes. Prebaked anodes are used more extensively due to several practical and environmental advantages.

The prebaked anodes are made from a mixture of petroleum coke aggregate and coal tar pitch as a binder. The mixture is formed (pressed or vibrated) at a pre-defined temperature and then placed in an anode baking furnace and heated to a temperature in excess of 1100 °C. For use in the reduction cell aluminium rods with iron studs are installed, which act as the electrical connection between the bus bar and the anode. Prebaked anodes are regularly replaced when they have reacted to about one quarter/one fifth of their original size, which takes approximately 25 days. The spent anodes are

called butts, which are cleaned and recycled as a raw material for the production of new anodes.

The prebaked anodes give lower carbon consumption per ton of aluminium compared to Söderberg anodes. However, replacement of anodes in the cell is a major disturbance in the operation of the cell, which is one of the main advantages of the Söderberg process, where anode paste is continuously supplied and baked, also eliminating the costs of anode forming, baking, butts upgrading and handling.

The Söderberg electrodes are manufactured from small briquettes composed of petroleum coke and coal tar pitch. The pitch binder content is about 25 wt%, which is considerably higher than the amount used in prebaked anodes (13 – 15 %) to ensure sufficient flow of the carbon paste. Briquettes are placed on top of the Söderberg anode block, where they are softened by the heat generated from the process. The paste passes slowly downwards through a rectangular steel casing and is baked into a solid composite.

One of the most problematic issues of Söderberg anodes is the environmental aspect. The high amount of pitch in the anodes leads to a release of potentially hazardous polycyclic aromatic compounds (PAH) during the process. The prebaked anodes release their volatiles during baking, which also create heat in the baking process. The PAH compounds are considered to be carcinogenic, as are all high molecular weight organic compounds [Meier, 2003]. However, it is possible to enclose Söderberg cells to provide control of the generated PAH compounds and thus comply with new environmental regulations, but it is an expensive solution.

1.2 Background

The most important requirements of products to manufacture anodes are; high chemical purity, high electrical conductivity, high mechanical strength, physical and chemical homogeneity, with a low reactivity to CO_2 and air (O_2) [Foosnæs, Naterstad, 1993]. The main raw material meeting the purity requirements is petroleum coke, derived from crude oil residues. The viscous hydrocarbon liquids are heated under pressure in a coking plant, where a phase transition from liquid to solid state takes place by cracking, de-hydrogenation and polymerisation. Today, the sulphur content and metal impurities in the petroleum coke are steadily rising as refineries use more high sulphur crude.

1.3 Coke production and characterization

Petroleum coke is a by-product of most oil refineries which has limited interest to the producer as its value is only about 2 percent of the overall production [Fernandez, 2003]. Therefore, the production yield of refineries is optimised towards the more economically valuable liquid and gaseous products. Mechanical and physical properties of the coke are influenced by this optimisation, with green coke production generally minimised to only about 4 to 6 volume % of the refinery output.

Figure 1.2 presents a flowchart of the production of green coke in the delayed coking process and calcining in a rotary kiln/rotary hearth furnace.

Today, the semi-continuous delayed coking process dominates the production of green coke. The heated residue of fractionated reduced crude oil is fed in shifts to the drums at a temperature of 485 °C to 515 °C and kept at a pressure of 1.0 to 6.5 bar. The coke is removed by blasting with high pressure water jets and is then transported to a storage system. A typical raw/green coke yield is between 15 and 50 % [Fernandez, 2003].

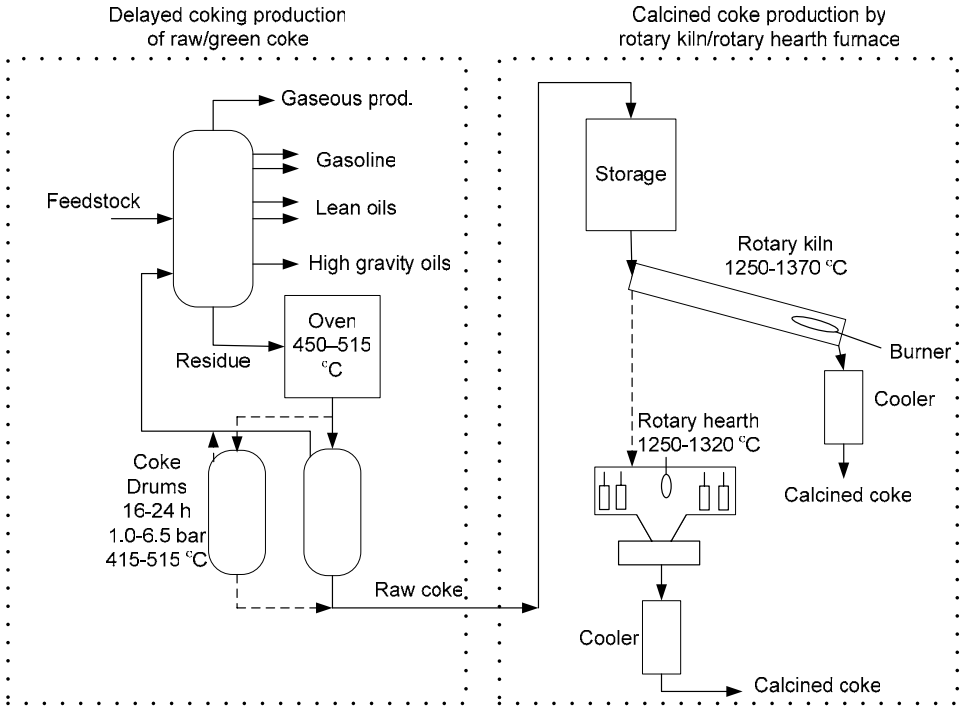

Figure 1.2 Coke production by delayed coking and calcining of green coke in rotary kiln or rotary hearth calciners [reproduced from Foosnæs, Naterstad 1993].

Today, there are two different calcining processes, the rotary kiln and the rotary hearth process.

The rotary kiln consists of a tilted refractory lined steel tube of up to 90 m length and 4.5 m in diameter. The kiln is heated by oil or gas from a burner placed at the outlet. The target temperature is maintained for 10 to 20 minutes by burning hydrocarbon volatiles and coke by air injection.

The carbon-hydrogen ratio is increased from a magnitude of 20 to 1000 when green coke is treated at 1250 °C to 1350 °C. The calcined petroleum coke is a hard, dense carbon material with low hydrogen content and good electrical conductivity. These

properties, combined with low metal and ash contents, make calcined petroleum coke suitable as a raw material for carbon anodes for the production of aluminium.

The chemical and physical properties of coke determine the performance of the anodes subsequently manufactured from it. Table 1.3.1 gives an overview of typical properties for petroleum coke in the green and calcined state.

The coke properties are mainly determined by

- Crude oil composition
- Coking process
- Calcining process

The real density of the calcined coke is determined by the final calcination temperature and the residence time [Fernandez, Meisingset, Balchen, 1996].

Table 1.3.1 presents typical data for green and calcined coke.

Table 1.3.1 Typical petroleum coke properties in the green and calcined state [Foosnæs, Naterstad 1993].

Properties	**Analytical Method**	**Unit**	**Green coke**	**Calcined coke**
Moisture	DIN51904	mass%	0.5-2.0	<0.1
Ash	ISO8005	mass%	0.04-0.5	0.04-0.6
Fixed carbon		mass%	85-95	95-99
Hydrogen	ISO N 837	mass%	3.0-4.5	<0.1
Sulphur	ISO N 837	mass%	0.2-4.0	0.2-0.4
Nitrogen	ISO N 837	mass%	0.1-0.5	<0.1
Volatiles		mass%	6.0-14.0	<0.3
Calcium	ISO N 837	ppm	25-500	50-600
Iron	ISO N 837	ppm	50-600	50-600
Manganese	ISO N 837	ppm	3-100	3-110
Nickel	ISO N 837	ppm	10-170	10-170
Silicon	ISO N 837	ppm	40-400	40-400
Sodium	ISO N 837	ppm	25-250	25-250
Titanium	ISO N 837	ppm	2-50	2-50
Vanadium	ISO N 837	ppm	5-300	5-300
Aluminium	ISO N 837	ppm	15-100	15-100
Real density	ISO 8004	kg/dm^3	1.5-1.8	2.0-2.13
Bulk density		kg/dm^3	0.68-0.76	0.79-0.92
Mean crystallite size L_c		nm	-	2.4-3.5
Specific el. resistivity	ISO 10143	μΩm	-	350-550
HGI	ASTM D5003	%	75-85	30-38
Grain Stability	ISO 10142	%	-	75-90

1.4 Current market situation

The variation in calcined coke quality is a consequence of the optimisation of crude oil processing, with a focus on the gaseous and liquid products. Continuous high demand for calcined coke by aluminium smelters makes the market situation difficult with respect to quality and availability. This critical situation puts aluminium smelters in a position where it is necessary to adapt, so that they may use a mixture of coke qualities in the production lines, depending on what is available. Therefore, it is necessary to optimise the process so that lower quality cokes can be used with minimal influence on the product quality.

Figure 1.3 presents the demand and supply of green coke used in the production of anodes from 1995 to 2007. It can be seen that the demand of green coke is expected to rise from 13.8 million tons in 2003 to 16.7 million tons in 2007. This increase is due entirely to demand from the aluminium smelting industry. Green cokes with low vanadium and sulphur content were available until 2002, but in 2003 the situation changed due to the lack of growth in new anode grade coke sources. The consequence of this was that non-traditional cokes with higher vanadium and sulphur content and a more isotropic structure have been blended with traditional cokes to meet the shortfall [Vogt et al., 2004].

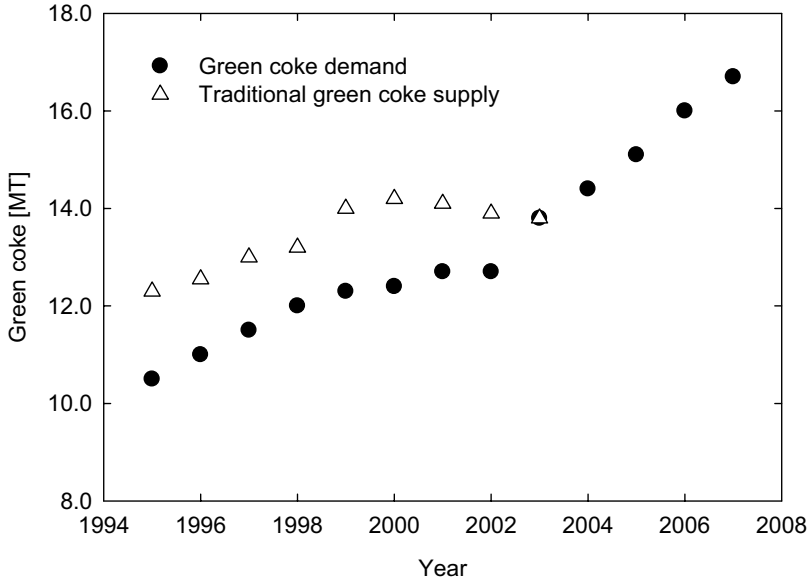

Figure 1.3 Green coke demand and availability [Vogt et al., 2004].

1.5 Scope of the work

Understanding the consequences of a varying calcined coke quality is crucial for anode production, as it is a key factor for stable and economical pot-line operation. The importance of using the correct coke composition in anode production with regard to

chemical and mechanical properties, price and availability has become increasingly important.

Additionally, it is critical to utilise and develop new characterisation methods which can track changes in the materials at different production steps. However, there are very few methods which characterise the green anode properties.

In this work, the variation of coke properties of four different coke types was investigated; three single source cokes and one blended coke. Each coke had different origins, chemical and mechanical properties, which made it possible to compare their relative performance. The mechanical strength of each coke was also investigated, adapting a method from road construction called the brittleness or drop test. This method determines the mechanical strength of the coke over its entire size distribution, thus providing information about the homogeneity of the coke. The drop test method measures the degree of crushed particles and volume reduction due to the impact. Results are compared with the conventional HGI and grain stability methods.

This work also shows the importance of controlling the grinding step for the production of a stable dust quality for use in anode production. Several different parameters were investigated in an air swept ball mill, for example; air sweeping speed in the mill, mill filling level, ball size charge composition, mill speed, return ratio and the effect of a heterogeneous feed. The ball mill was run with an integrated on-line particle size analyser, which maintained a stable product size over the entire grinding period. The product size was measured by laser diffraction, sieves and a Blaine apparatus. Different specific grinding energies were measured according to various mechanical properties of the investigated cokes.

An extended investigation on thermal dilation measurements and method optimisation was also performed on the produced green anodes. This investigation was performed in an improved vertical dilatometer, which showed a significant improvement in measurement repeatability, precision and better work environment. It was found that the heating rate, sampling position and packing material influenced the thermal dilation measurement. Furthermore, the effects of coke type (soft and porous versus hard and dense) and shrinkage were detected in the dilatometer.

Image analysis of green anodes was also performed, illustrating how the pore size distribution varies with the pitch content and dust size.

Part of the presented work has already been published [Chmelar, Brevik, 2004; Chmelar et al., 2005; Chmelar, Foosnæs, Øye, 2006]

2. Material Properties and Experimental Procedure

2.1 Petrol coke analyses

Each coke type was chosen according to its properties and availability. Three of the cokes were single source cokes and one was a blended coke.

The investigated cokes were received with the physical and chemical characterisation given in Table 2.1.1. The analyses were performed by the laboratory at Hydro Aluminium Årdal.

Table 2.1.1 Physical and chemical properties of the investigated cokes.

Properties	**Method**	**Unit**	**Coke**			
			SSA	SSB	SSC	Blend
Moisture	DIN51904	wt %	0.05	0.12	0.06	0.02
Ash	ISO8005	wt %	0.16	0.2	0.13	0.09
Sulphur	ISO 12980	%	1.18	1.04	2.89	2.01
V	ISO N 837	ppm	147	68	378	250
Si	ISO N 837	ppm	63	105	23	150
Fe	ISO N 837	ppm	105	189	71	200
Ca	ISO N 837	ppm	110	42	27	80
Ni	ISO N 837	ppm	82	44	170	150
Na	ISO N 837	ppm	55	28	43	60
Real density	ISO 8004	g/cm^3	2.07	2.065	2.07	2.086
Spec. el. resistivity	ISO10143	μΩm	490	473	487	500
Air reactivity	Hydro method	mg/cm^2h	79.7	26.1	126.8	96.6
CO_2 Reactivity	Hydro method	mg/cm^2h	24.5	10.2	10.4	11.0
Grain stability	ISO 10142	%	87.0	66.0	85.0	74
HGI	ASTM D5003-95	%	35	37	34	36
Porosity	Image analysis	%	16.8	21.1	17.1	20.5

SSA – Single Source A
SSB – Single Source B
SSB – Single Source C

The cokes differ in sulphur content, where SSC has the highest amount (2.89 %), SSA (1.18 %), SSB (1.04 %) and the blended coke (2.01 %). There is also a difference in the grain stability, where SSA and SSC are the mechanically strongest (87 and 85) while SSB is the weakest (66) and the blended coke has a medium strength (74). Porosity was analysed with an image analysis technique on a 0.5 to 1 mm coke fraction [Rørvik, Øye, Sørlie, 2001], using a 3 μm cut-off size. The SSA and SSC cokes have a very similar porosity of 16.8 and 17.1 %, while the SSB coke has the highest porosity together with the blend coke, of 21.1 and 20.5 %, respectively.

The highest content of vanadium and nickel was found in single source coke C with 360 and 170 ppm, respectively. Coke air reactivities show the expected strong correlation with the Vanadium content (Figure 2.1).

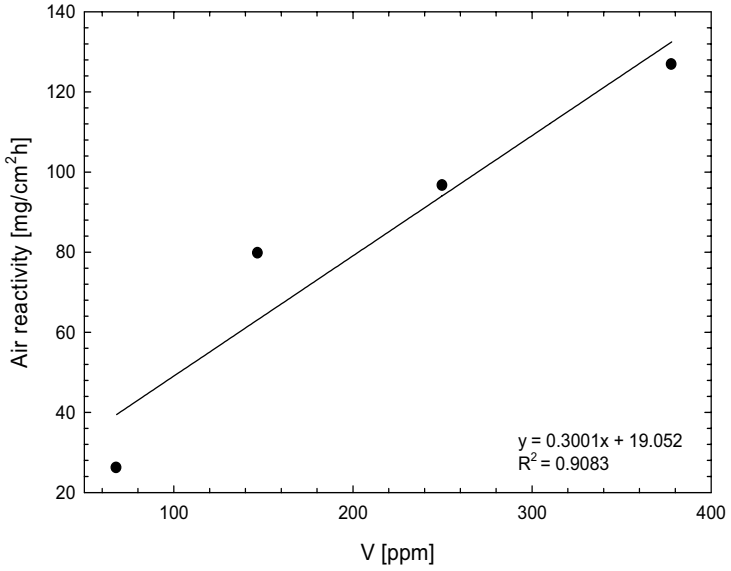

Figure 2.1 Correlation between the air reactivity and the V content for investigated cokes.

For the CO_2 reactivity, the values are equally low for cokes B, C and the blend coke, and highest for coke A. Low CO_2 reactivity is expected for coke B because of its low content of catalytic elements and a considerably anisotropic structure.

The specific electrical resistivity, although varying over a narrow range, correlates well with real density.

Table 2.1.2 lists physical and chemical properties of the applied pitch in this investigation.

Table 2.1.2 Physical and chemical properties of the applied pitch.

Properties	Unit	Value
Ash	wt %	0.20
S	ppm	0.54
Si	ppm	102
Fe	ppm	132
Zn	ppm	242
Coke remains	%	60.3
Toluen solubility	%	28.7
Spec. density	g/cm^3	1.32
Softening point	°C	120.3

2.2 Sample preparation

The sample preparation consisted of the five main production steps; sieving, grinding, mixing, forming and baking. Figure 2.2 presents a complete flowchart of the preparation process.

A representative sample of the received petroleum coke was analysed (Table 2.1.1) and sieved into various size fractions defined by the recipe. The -2 mm fraction was used to produce the dust in an air swept ball mill (section 4). All cokes were subjected to a drop test investigation where the mechanical strength of the coke grains was measured. The test description and results are presented in section 3.

A pre-defined recipe was used in all experiments. The appropriate amounts of the fractions and coal tar pitch were blended in a sigma mixer. The blended paste was compacted under controlled conditions (temperature, vibration frequency and time) in a vibration compactor to produce a green anode. Optimisation of the mixing and forming are described in the section 4. Measurement of the green apparent density was then performed before core samples were drilled from the green anodes for further characterisation.

A thorough investigation of the thermal dilation of the green anodes was performed using a dilatometer. The development and optimisation of this method is presented in section 5. Automated image analysis of green polished samples was also made to determine the pore size distribution, which is described in section 6.

The green anodes were placed in the baking oven, with petrol coke for support, and then baked with a defined temperature program and soaking time. Core samples were collected from the baked anodes for further characterisation of apparent density, air permeability, specific electrical resistance, CO_2 and air reactivity. The complete investigation is presented in section 6.

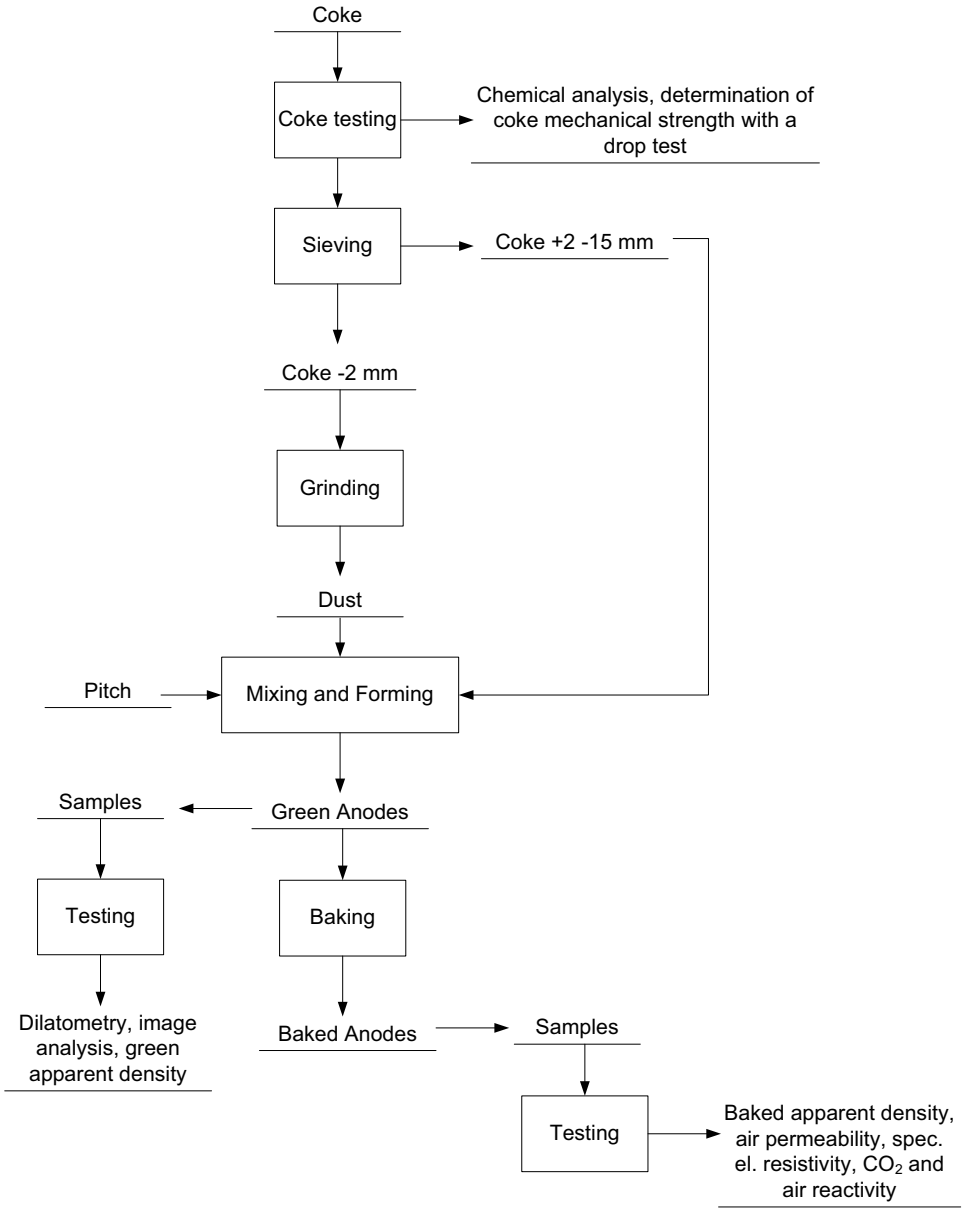

Figure 2.2 Experimental test procedure.

3. Development of a new method for coke grain strength measurement

Today, multiple source blend cokes often have to be used due to the petrol coke supply situation. Although specifications on sulphur and trace elements are met by blending, cokes with different chemical and mechanical properties have to be used. The blended coke often consists of up to 25 different coke qualities in order to meet the customers' specifications. Large variations in chemical and mechanical properties through the whole particle size distribution of the coke can therefore be expected.

Currently, two methods are used for characterisation of coke grain mechanical strength. The Hardgrove Grindability Index (HGI), according to ASTM standard D5003-95 and the grain stability test, according to ISO 10142.

These measuring methods do not represent the coke grain mechanical strength in the entire size range, but only in a narrow size distribution. This may give erroneous data interpretation and lead to problems during anode production, as for example excessive crushing of coke grains during mixing, under pitched anodes and poor chemical/physical properties of final baked anodes. Therefore a new method has been developed.

3.1 The HGI method

The HGI method (ASTM D5003-95) originates from the standard test for grindability of coal by the Hardgrove apparatus (ASTM D409). Prior to the test a representative sample of coke is crushed and sieved until all material is within the size range +0.60 -1.18 mm. Further, a 50 g representative coke sample from the crushed and sieved coke is placed in a grinding apparatus using two rotating disks with a groove and steel balls (8 steel balls 25.4 mm in diameter). The apparatus is turned for 60 revolutions by an electric motor. The total vertical force on the balls is 29.0 kg of weight added to the spindle, shaft, top grinding ring and gear. The coke is then retrieved, sieved and the amount of particles below 75 µm is used to determine the HGI value. A low HGI value describes a coke with a low grindability (hard coke) while a high value indicates higher grindability (soft coke) properties.

The HGI method describes the mechanical strength of the coke grains in the size fraction +0.60 -1.18 mm, which is the major constituent in the size fraction below 2 mm fed to the ball mill in most grinding circuits. The HGI method is used for characterisation of green cokes with results ranging between 75 and 85. Calcined coke HGI usually ranges from 30 to 38 and the resolution of this method is thus too low for reliable distinction between the mechanical strength of cokes with varying origins.

3.2 The grain stability test

The grain stability test (ISO 10142) is performed in a laboratory vibration mill having two grinding chambers, each filled with 1 kg of steel balls 10 mm in diameter. Coke (100 g, +4-8mm) is placed in each chamber and ground for 3.5 min. The amount of

material retained on a 4 mm sieve indicates the grain stability expressed in percent, with a high number indicating more mechanically stable coke grains.

The two methods analyse coke strength for two different size fractions. The HGI method uses very fine coke whereas ISO 10142 uses coarser coke.

The steel balls used in ISO 10142 are too small to crush the larger coke particles. Only the weakest particles which are porous and/or contain micro-cracks produced during calcination are crushed. However, during the test there is also a certain degree of autogenous grinding, where the large particles are ground against each other producing very fine particles.

3.3 HGI and grain stability comparison

HGI was measured for the three single source cokes and the blend coke. Figure 3.1 presents a graphical comparison of the HGI values for each coke. The HGI results indicate that single source coke C has the highest mechanical strength (34) while single source coke B is the mechanically weakest (37). Single source coke A and the blended coke have intermediate values of 35 and 36, respectively. However, the standard deviation values show that there are hardly no significant differences between the coke types.

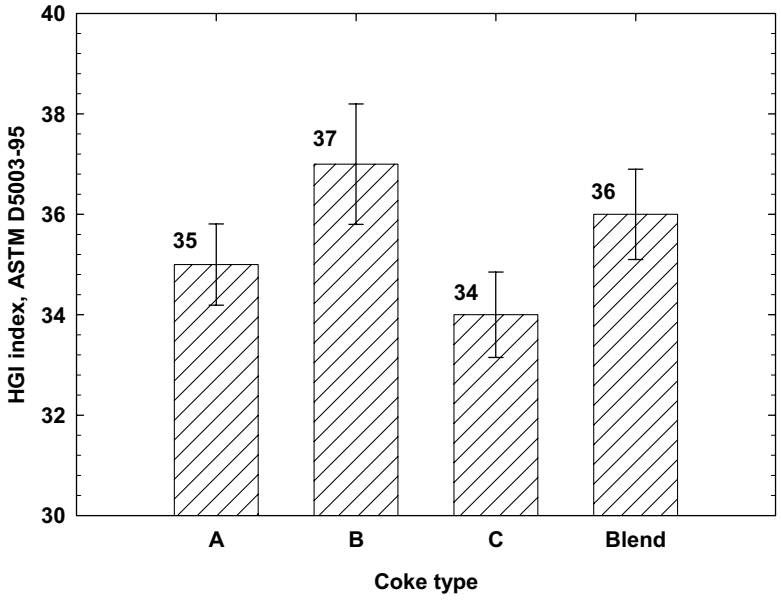

Figure 3.1 HGI results for the investigated cokes.

Figure 3.2 compares grain stability according to ISO 10142 for all four investigated cokes. This method shows that single source A has the highest grain stability with 87 % of the coke grains coarser than 4 mm, while coke C has 85 %. The weakest coke is

single source B with only 67 % of particles larger than 4 mm. The blended coke has a median grain stability value of 74 %.

This method shows that single source A coke is the mechanically strongest while the HGI method favours the single source C coke. The other coke results are the same as achieved by the HGI method. However, the resolution of the measurement is larger than obtained by the HGI method.

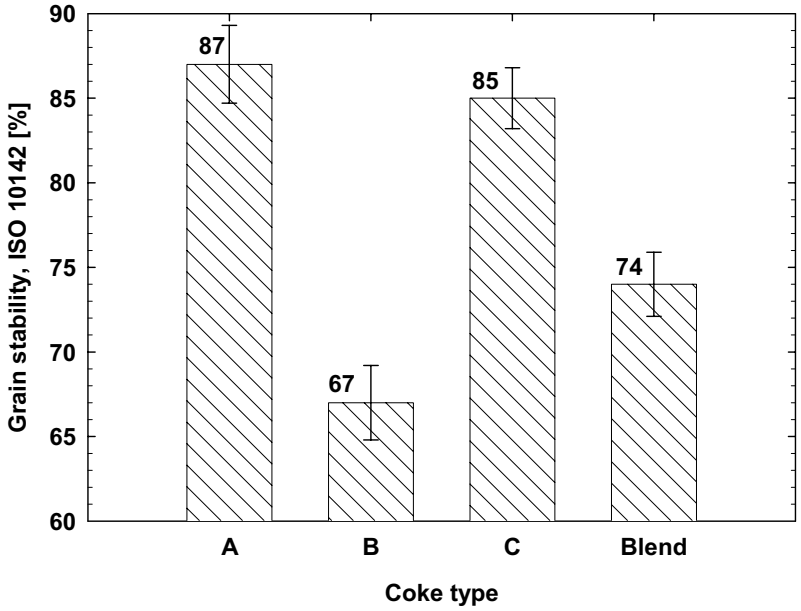

Figure 3.2 Grain stability data for the investigated cokes according to ISO10142.

3.4 Drop test method establishment

In this work a new method called the brittleness test or drop test was established to measure the coke grain strength. This method originates from the study of materials for road construction for the determination of the grain stability of rock materials [Statens vegvesen, 1980].

An earlier study [Ozkahraman, 2004] showed a good correlation between the drop test result and the Bond Work index. The Bond Work index (Wi) is a standard which gives a measure of the resistance of the material to crushing and grinding [Austin, Klimpel, Luckie, 1984].

Figure 3.3 presents a schematic drawing of the drop test device. A sieved coke fraction (+2-5 mm) of about 300 g is placed in a steel chamber 100 mm in diameter, which is closed with a lid. The chamber is fixed to the instrument base with two latches in order to prevent any movement during the testing. The lid rests freely on top of the coke material. The lid's peripheral diameter is slightly smaller than the internal chamber diameter to ensure free movement during the impacts.

The piston, having a weight of 14 kg, drops on the lid 20 times from the same height (25 cm) at a constant time interval, crushing and compacting the sample inside the cylinder. The material is then removed from the chamber and subsequently analysed by sieving.

This testing device was instrumented with a laser distance sensor for measurement of the volume reduction in the chamber during the test. The impact force is measured by an accelerometer installed on the top of the piston. Figure 3.3 and Figure 3.4 present the drop test instrument.

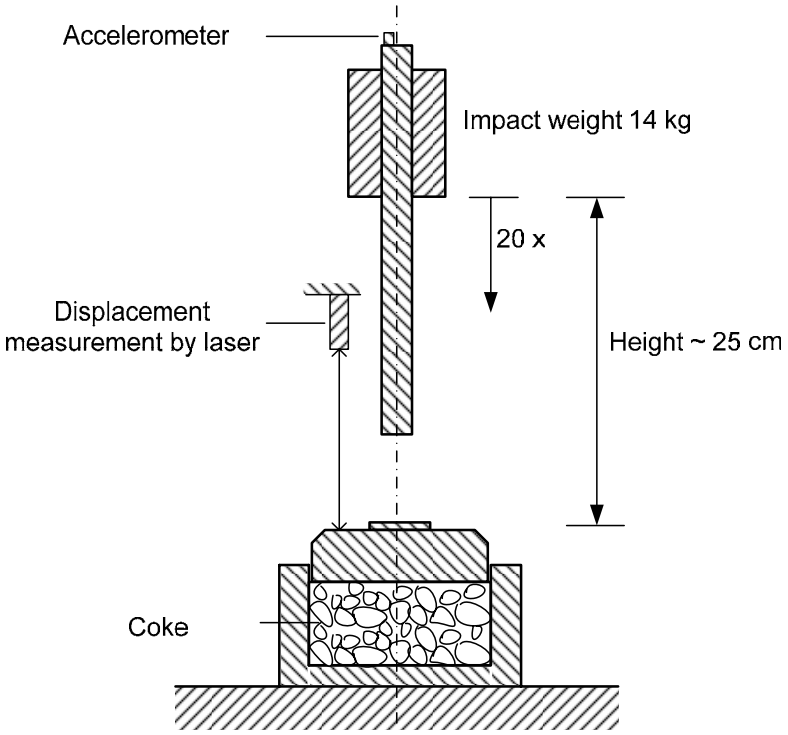

Figure 3.3 Drop test instrument.

Data from the accelerometer and laser are continuously logged by a computer. The logging program is written in the graphical language LabView 6.1. The data acquisition is performed with a DAQ card NI PCI-6024E and shielded connector block SCB 68 from National Instruments [National Instruments, 2003]. Figure 3.5 shows a photograph of the drop test instrument. Figure 3.6 shows the chamber with the lid and piston.

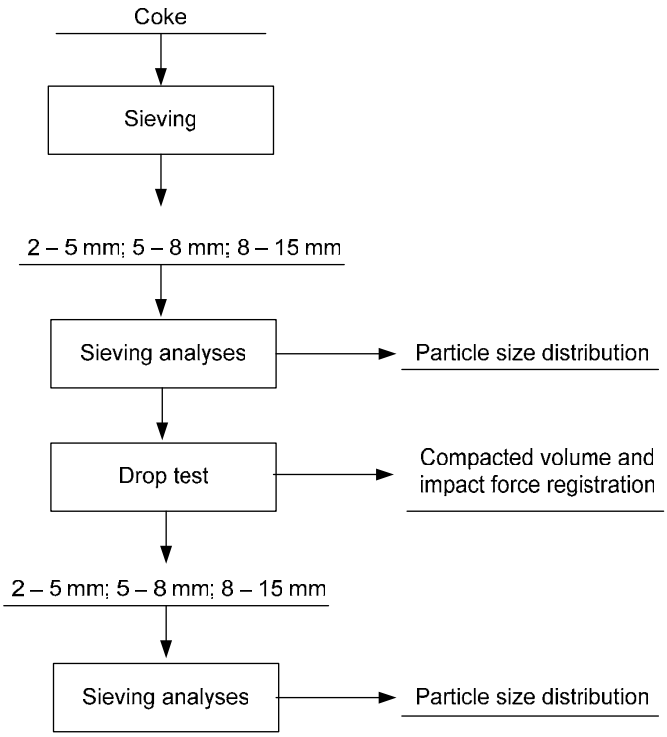

Figure 3.7 Testing procedure using the drop test device.

Figure 3.8 shows the volume compaction curve. The starting point 0 has a volume of 100 %. The maximum compaction is at impact 20; in this figure it is 36 % (100 % - 64 %).

The impact force is registered as the mean value for each impact (Figure 3.8). The PC program collects 100 samples per second which are used for the calculation. The curve has a scattered profile due to the unevenness of the contact area between the coke and the lid. A small deflection of the lid causes a variation in the impact force. These variations are closely linked to the compaction state of the material in the chamber. The compacted material absorbs the impact force but the lid slightly jumps up and might not be parallel with the coke surface and thus causes the force variations. The acceleration values fluctuate through the test but do not increase significantly with the number of impacts.

3.4.2 Test results

Three main parameters are determined by this method; the sieve analysis before and after the drop test, the impact force and the compacted volume.

The acceleration can be transformed to impact force by Equation 3.1. The only load weight used in this work was 14 kg. Figure 3.8 presents the impact force and the compacted volume after each impact.

$$F = m \times G \qquad 3.1$$

Where:

F – impact force [N]
m – weight of the load [kg]
G – acceleration [m/s^2]

The mean impact force is calculated from the 20 impacts (0 impact is omitted) and is presented in the graph. The impact force describes how well the coke particles are compacted in the chamber. A high impact force indicates a very compact coke composition with very little voids and porosity. However, low impact force values indicate that the coke composition has some porosity and voids that partly absorb the impacts.

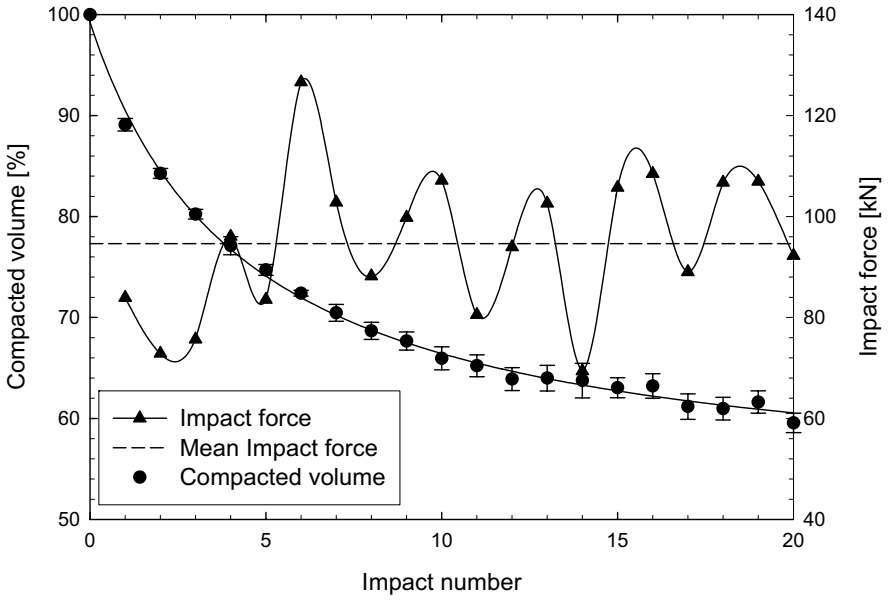

Figure 3.8 Drop test result expressed as volume reduction and impact force.

The largest volume reduction for the fractions is registered for the size range 8 – 15 mm. This is most probably due to large particles, porosity and voids. Single source coke B had the highest volume reduction (44 %), followed by the blended coke (40 %) and single source A and C had the same reduction (37 %), (Figure 3.9). The differences in the size range 5 – 8 mm were not as significant as in the size range 8 – 15 mm. The highest volume reduction was registered for the blended coke (33 %). The second was

single source B (31 %) followed by single source C and A (30 and 29 %), respectively. The finest fraction (2 – 5 mm) showed larger differences between the coke types. Single source B had the highest reduction (26 %) followed by the blended coke (24 %) and single source C and B (22 and 21 %), respectively.

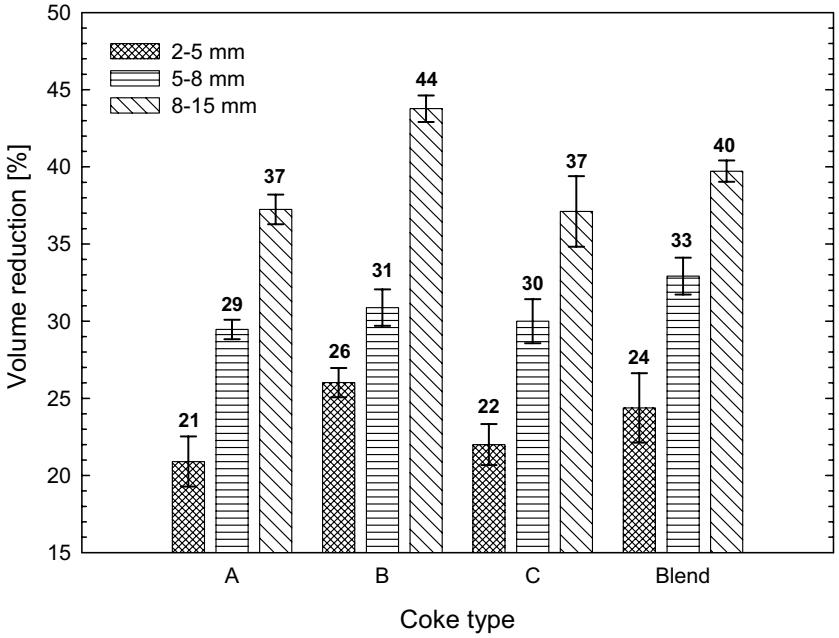

Figure 3.9 Volume reduction for four tested cokes (mean values).

The particle size distribution of each size fraction before the test was compared with the particle size distribution after the drop test. In order to compare the quantity of fines generated during the test, three sieve sizes were selected for each size fraction. It was 3.5 mm for the size fraction 2 – 5 mm, 7.0 mm for the size fraction 5 – 8 mm and 10 mm for the size fraction 8 – 15 mm. The size reduction numbers were calculated by determining the difference between the initial amount and the quantity after the test in each size fraction. For example, if the size fraction 2 – 5 mm contained 60 % of -3.5 mm fines before the drop test and after the drop test it contained 90 % (-3.5 mm) this will give a 30 % size reduction at 3.5 mm. Figure 3.10 presents the results of this comparison.

The weakest coke, exhibiting the largest size reduction, was single source B, however, the size reduction for the 7.0 mm fraction is slightly smaller compared to blended coke.

All four cokes have the same size reduction trend while the middle size (7 mm) has a lower size reduction ratio compared to the other sizes. The mechanically strongest coke is single source A in all size fractions. Single source C coke shows that the coarsest size range (10 mm) has a lower size reduction (23 %) compared to the finest size (3.5 mm) with 29 %. The other coke types, B and blend, had a larger size reduction in the coarsest

range. This may indicate that single source C has particles which are mechanically strong.

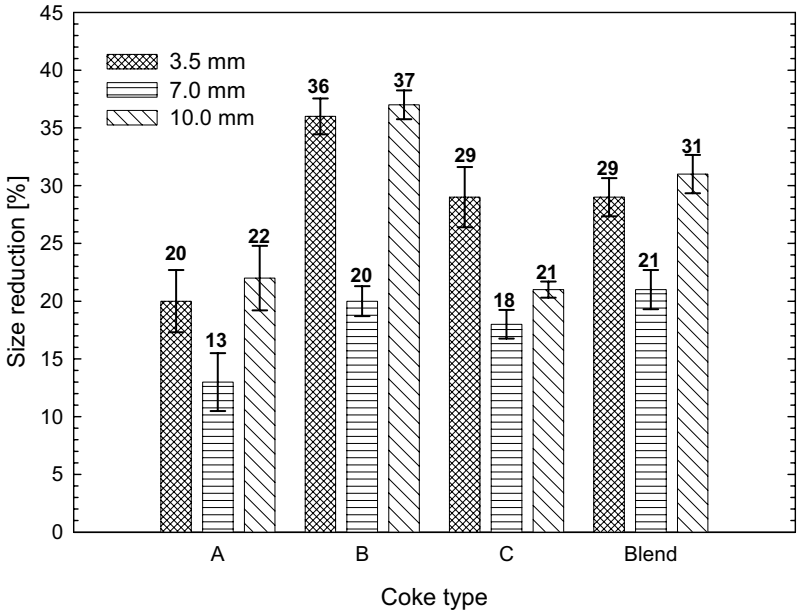

Figure 3.10 Size reduction in coke fractions expressed as difference before and after the drop test for the appropriate sieve sizes (3.5, 7.0 and 10.0 mm).

The sieve analysis after the drop test also included the 148 µm sieve in order to evaluate production of the finest fraction during the drop test. Figure 3.11 presents results and it can be concluded that single source coke B produced the largest amount of the -148 µm fraction from each size. The SSB coke contains about 2 to 5 wt % more of the -148 µm particles than the other investigated coke types.

Excessive fines generated while the anode is being mixed and formed will have a significant effect on the pitch consumption as particles below -148 µm have the largest surface area. This can result in under pitched anodes despite a correct prior calculation and dosage in the process.

Figure 3.12 shows the graph with the size and volume reduction plotted (8 – 15 mm size fraction) with a regression curve.

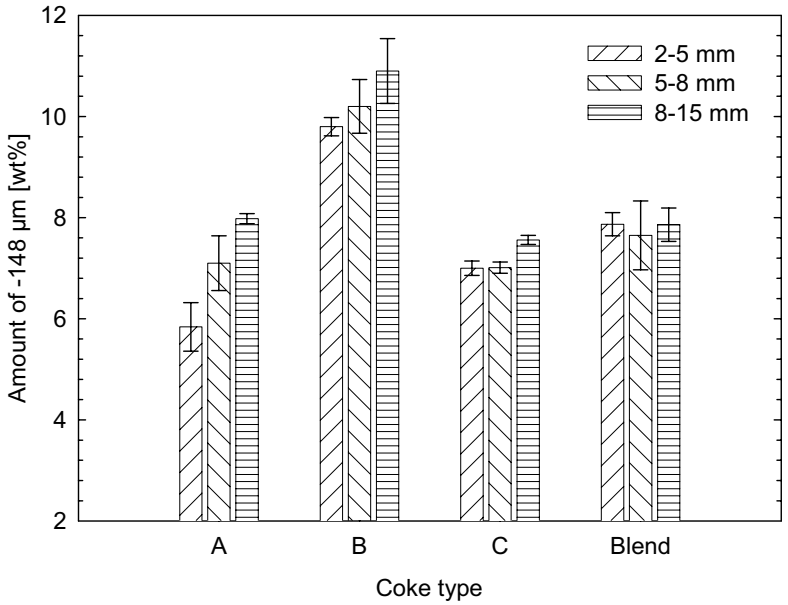

Figure 3.11 Amount of -148 µm particles produced during the drop test from each size fraction and coke type.

Figure 3.13 shows the mean impact force results for each size fraction and coke type. The impact force indicates how hard and/or how quickly the piston stops. If the coke bed is flexible (porous coke/mechanically weak) then the impact force will be low. On the other hand, if the coke bed is hard and dense the impact force will be high.

The highest impact forces were measured for the coarsest fraction (8 – 15 mm) and the lowest in the finest fraction (2 – 5 mm). The lowest impact force was measured for single source coke B.

The results also show that the impact force also can distinguish the differences between the investigated cokes, however there was a significant fluctuation in the results during the impacts which diminishes the validity. It is necessary to modify the lid design in order to avoid this effect.

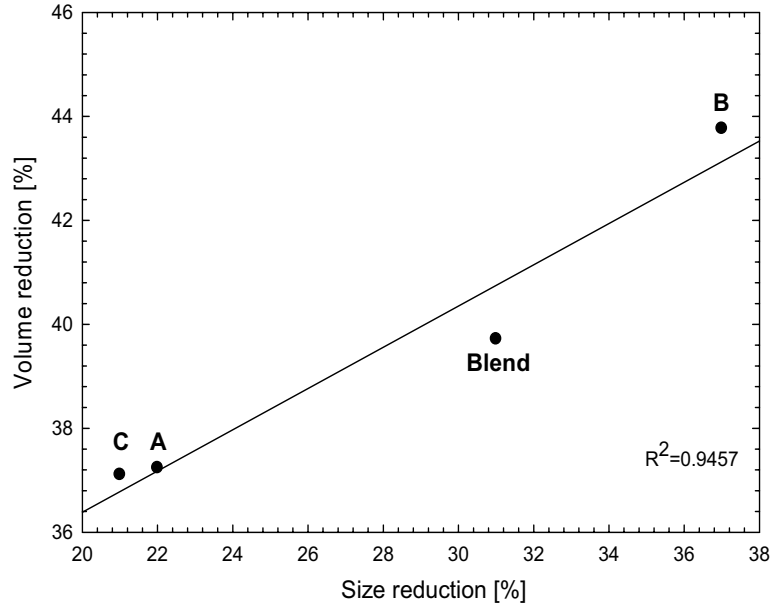

Figure 3.12 Relation between the size and volume reduction (8 – 15 mm size fraction).

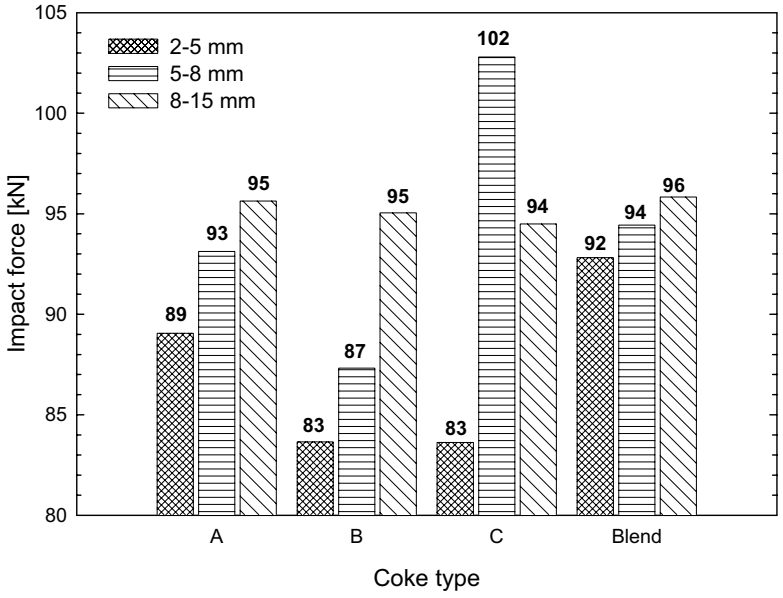

Figure 3.13 Average impact force values for each size fraction and coke type.

Results from the drop test are compared to the HGI and the grain stability results in Figure 3.14.

It was necessary to recalculate the grain stability results in order to make it easier to compare results. The grain stability method produces a number which corresponds to the amount of retained material on a sieve after the test. The higher this amount, the higher the mechanical strength. The recalculation was made according to Equation 3.2; in other words it expresses the amount of material passing through the sieve after the test.

$$MGS = 100 - GS \qquad 3.1$$

Where:

MGS – modified grain stability number [%]
GS – grain stability result according to ISO 10142 [%]

This recalculation reverses the grain stability results so that a lower value for MGS corresponds to a mechanically more stable coke.

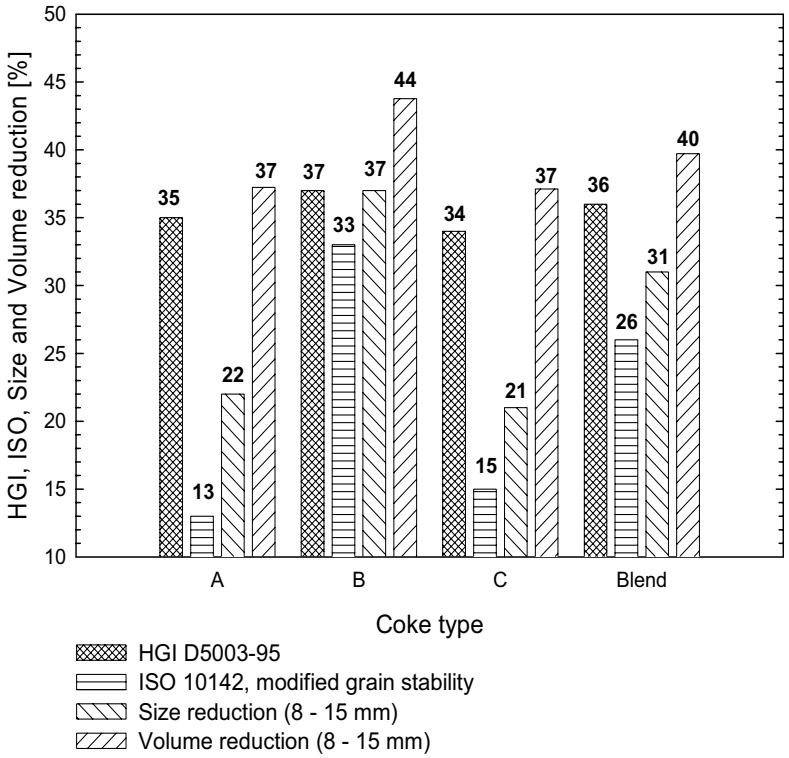

Figure 3.14 Comparison of HGI, grain stability and drop test results.

Figure 3.14 shows that the volume reduction correlates well with the results achieved by the HGI and the grain stability method. However, the HGI method indicates single source C as the mechanically strongest while the grain stability and the drop test methods both find single source A was the strongest. The three methods all indicate single source B as the weakest coke.

The size reduction results from the drop test show the same results as for the volume reduction. The results measured by different parameters correlate well. The size reduction results also found that the mechanically strongest coke is single source C. The size reduction results show large differences between the coke types compared to the HGI method.

Good correlations are easily found by plotting the volume or the size reduction values from the size fraction 8 – 15 mm against the grain stability, as shown in Figure 3.15 and Figure 3.16.

Conversely, no correlation was found between the grain stability and the impact force (values from the 8 – 15 mm size fraction) tests, as shown in Figure 3.17.

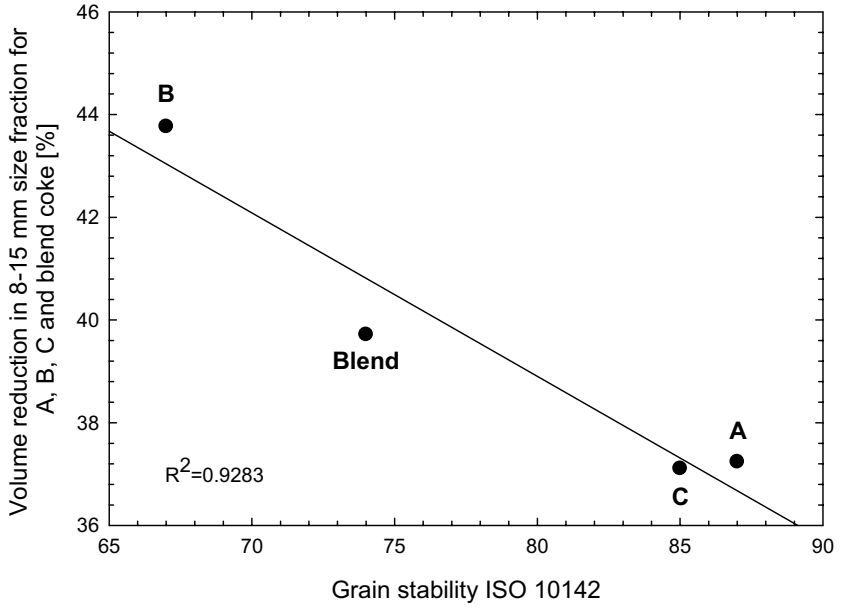

Figure 3.15 Volume reduction versus grain stability.

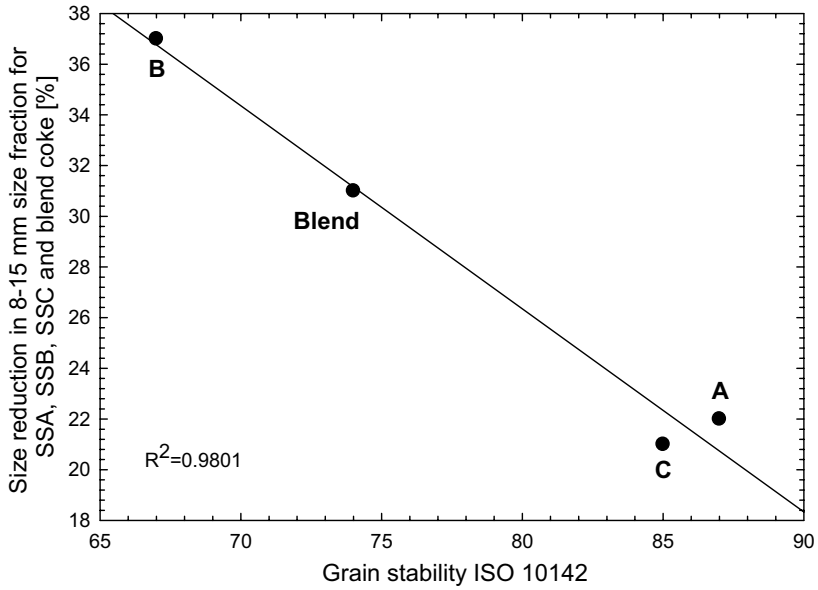

Figure 3.16 Size reduction versus grain stability.

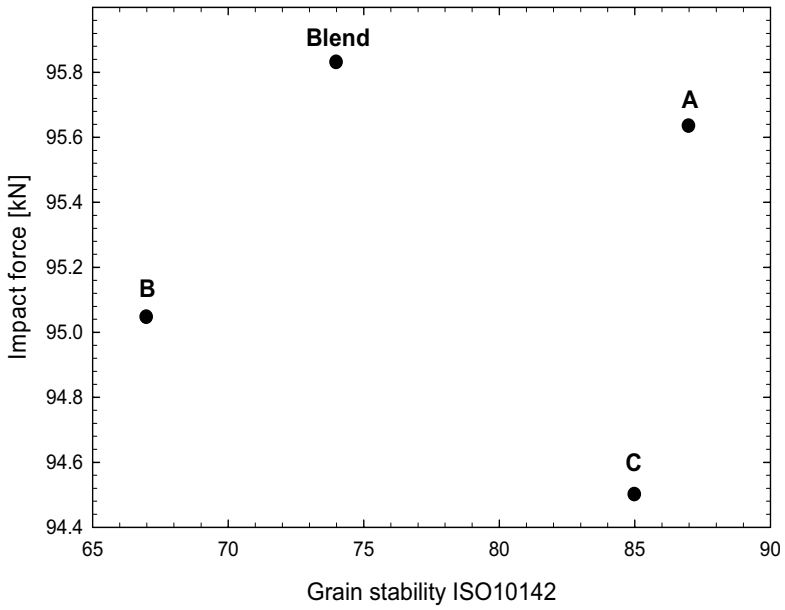

Figure 3.17 Impact force (measured for the 8 – 15 mm size fraction) versus grain stability.

The specific grinding energy of each coke was measured during the dust production in the air swept ball mill (see Section 4). These values (at Blaine number 3000) were used

to correlate the specific grinding energy and the size and volume reduction (size fraction 8 – 15 mm).

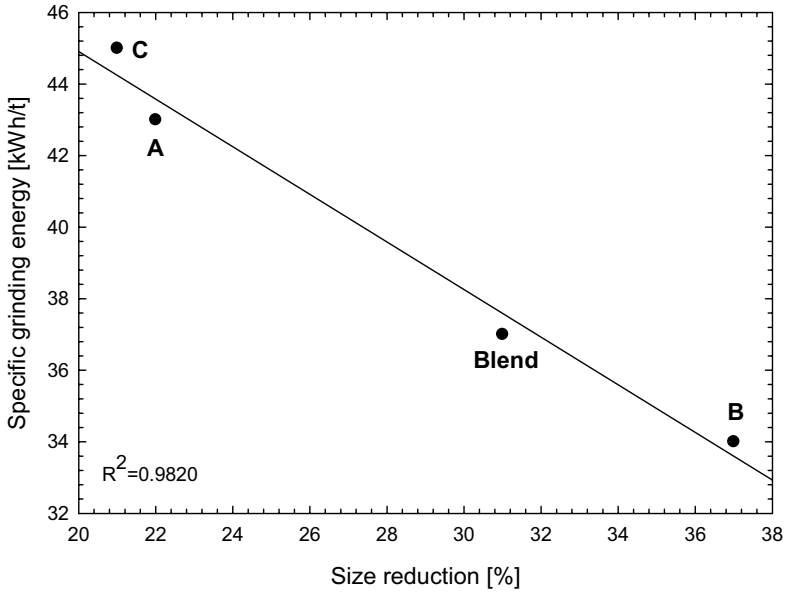

Figure 3.18 Specific grinding energy (at Blaine 3000) versus drop test size reduction (size fraction 8 – 15 mm).

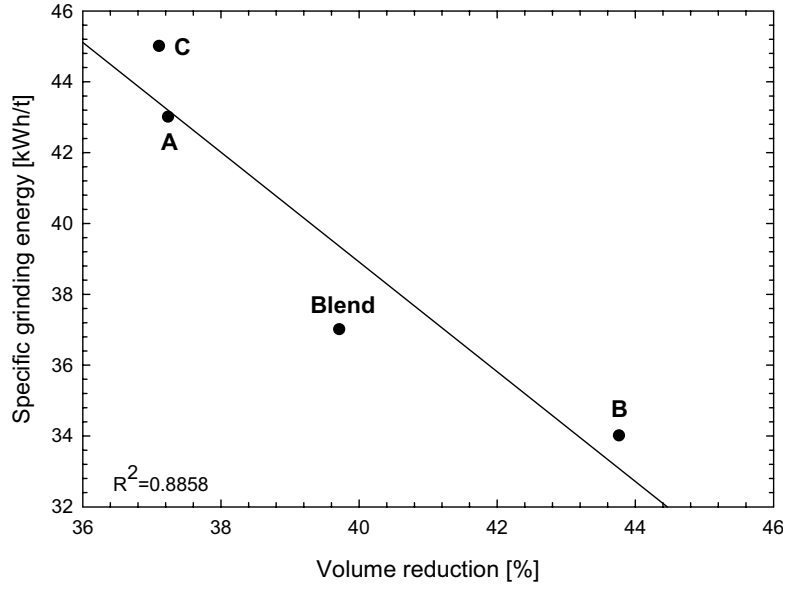

Figure 3.19 Specific grinding energy (at Blaine 3000) versus drop test volume reduction (size fraction 8 – 15 mm).

3.5 Discussion

The drop test method shows the suitability for the determination of the coke grain mechanical strength with respect to the entire size distribution and susceptibility to coke quality. If this method is compared to HGI ASTM D5003-95 and ISO 10142 the following advantages can be stated:

- It determines the grain strength in the entire size distribution (based on the results with sieved size fractions)
- It is possible to identify a mechanically weaker/stronger size fraction
- The results are expressed in the three parameters
    - Volume reduction
    - Size reduction
    - Impact force
- Certain size fractions correlate well with ISO 10142
- It is possible to predict the generation of fines due to mechanical loading of coke (mixing for example). The sieve analysis of -148 µm shows the amount of fines produced and thus indicates that extra pitch may be required.
- It is possible to determine the grain strength of a specific fraction which might be critical to further processing during anode production.

The results show that it is possible to correlate size and volume reduction and the specific grinding energy. This indication can predict and control grinding of coke in the ball mill circuit at the plant, especially when different coke types are used.

4. Anode production

4.1 Coke sieving and grinding in an air swept ball mill circuit

4.1.1 Sieving

The coke material was sieved with a Sweco sieving machine, which has a circular sieve 0.5 m in diameter. Several aperture sizes were used sequentially. The sieving capacity was optimised prior to sieving in order to achieve good separation efficiency, and was determined to be approximately 60 kg/h. The feed coke material was sieved into specific size fractions for further processing. The particle size distribution of all four received coke types is presented in Figure 4.1.

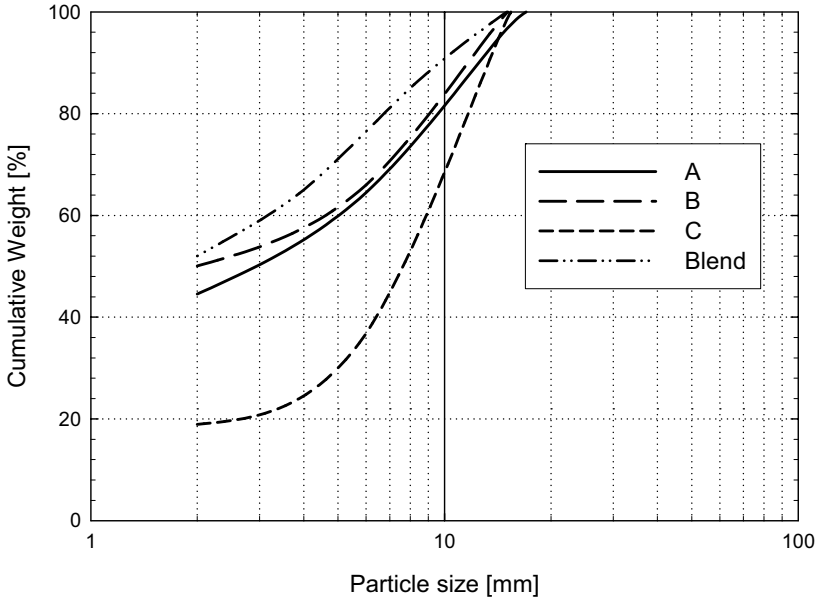

Figure 4.1 Particle size distributions as received of the investigated coke materials.

Figure 4.1 shows that coke C contains only 20 % of particles finer than 2 mm while coke B contains 50 % of this fraction.

4.1.2 Grinding

Ball mills are used to produce the finest fraction of the anode paste mixture from petroleum coke. There are two types of mill circuits currently used for industrial petrol coke grinding; air swept ball mills and grate discharge mills. The grate discharge mill is run in an open circuit thus there is limited control of dust size and capacity.

Air swept ball mill grinding is preferentially applied due to its advantages with regard to control of the product size and efficient removal of fine particles from the mill. Figure 4.2 presents a typical process flowchart for an industrial air swept ball mill grinding circuit. A typical capacity is between 3 and 10 t/h with a specific grinding energy in the range of 35 to 60 kWh/t.

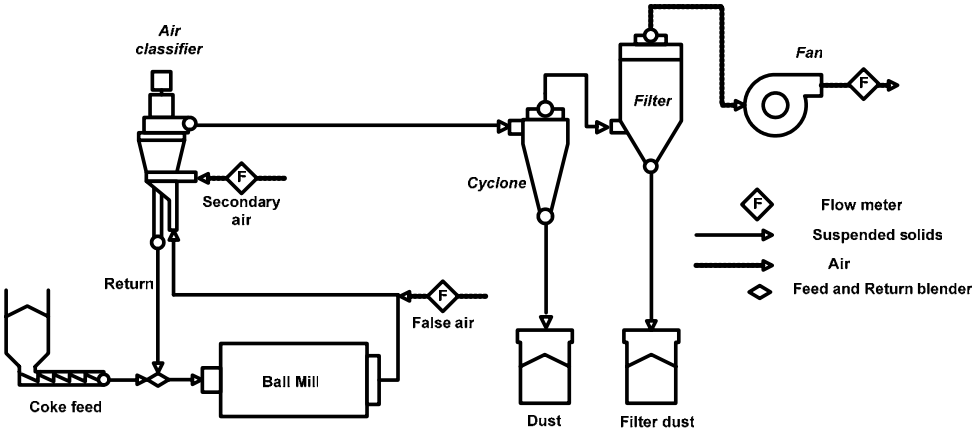

Figure 4.2 Air swept ball mill circuit with an integrated on-line particle size analyser.

The grinding circuit is sometimes equipped with an air cyclone before the filter where the major part of the dust fraction is removed, although the configuration depends on the requirements at the production site. Fine grinding has previously been studied by Kolacz (1997) in a pilot scale air swept ball mill grinding circuit which is further developed in this work.

4.1.2.1 Equipment

Figure 4.2 is a schematic drawing of an air swept ball mill circuit with an integrated on-line particle size analyser which was applied during this investigation [Chmelar, Foosnæs, Øye, Sandvik, 2005], (Appendix).

The ball mill is rubber lined and equipped with lifters. It has an internal diameter 0.56 m and a length of 0.8 m. The nominal power of this mill is about 3.5 kW. The mill is filled with steel balls (about 45 vol %) of different sizes (15 vol% of 24 mm, 15 vol% of 18 mm and 15 vol% of 11 mm diameter). The size distribution of the balls was regularly checked and the required amount of new balls added. Figure 4.3 shows a photograph of the balls and charge being removed from inside the mill. The rotational speed of the mill was adjusted with a frequency inverter.

Figure 4.3 Picture showing steel balls and coke material (before the ball size control).

A K-Tron Soder screw feeder supplied fresh feed material to the mill, with the feed rate regulated by the rotational speed of the screw. The feeder was placed on a weighing platform showing the weight loss as function of time, which was used to control the screw feeder speed. The ground product was then pneumatically transported to the forced vortex air classifier (the air classifier is now manufactured through Comex AS). The material is classified into two size fractions, above and below the specified particle size, which is expressed as d_{70} (d_{70} means that 70 % of the particles passes a specified size). The separation size is adjusted by both the air flow rate through the classifier and the rotor speed. Oversize material from the air classifier is returned to the mill via a mass flow meter, which measures the circulating load in the system. The mass flow meter consists of a vibratory feeder and a load cell, as can be seen in Figure 4.4.

The classifier air flowrate rate was adjusted by the fan speed. For improved efficiency the classifier was supplied with an extra air stream (secondary air) to clean the coarse material from the fines. The fines from the classifier were separated from the air first in a cyclone and subsequently in a Donaldson Torit type filter. The filtered air then enters the driving fan and is vented to the atmosphere. Compressed air is periodically blown back through the filter cartridges to remove the filter cake.

The torque of the rotating shaft driving the ball mill was measured to determine the required power and grinding energy. This was done by cradling the source (motor with chain transmission) and measuring the force of deflection. To determine the mill charge the complete ball mill unit was placed on a weighing platform, which directly measures the total mill weight. The fan (type Aerzen GMA 11.3 FA KII) creates the underpressure in the system for pneumatic material transport. The sweeping speed of the air in the mill was adjusted by the fan speed and/or by the false air valve. The valve adjustment does not affect the airflow through the air classifier and filter, only the

sweeping speed inside the mill. Figure 4.5 presents an inside view of the ball mill. Balls of different sizes, lifters and the grate are shown. It is also possible to see coke grains distributed between the balls.

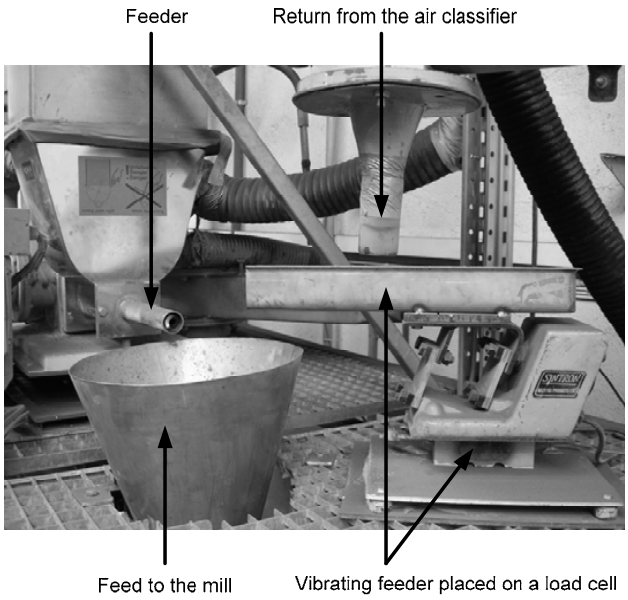

Figure 4.4 Equipment to feed coke and return oversize particles from the air classifier to the mill.

Figure 4.5 The inside of the ball mill.

Figure 4.6 presents an outline of the air classifier and a photograph is shown in Figure 4.7. The material was introduced from the bottom of the classifier through a vertical pipe directed at the lower section of the rotor. An inverted cone was attached to the mouth of this pipe for distributing the sample to the periphery of the rotor.

The fine particles entering the rotor leave the classifier through the top outlet due to the underpressure applied to the classifier. The coarse particles are unable to overcome the gravitational/centrifugal force and fall down to the bottom through an annulus section around the feed inlet. While leaving this chamber, a secondary air inlet at the bottom provides a rotating turbulent air current to rinse the coarse product. Thus, any fine particles entrapped or attached to the coarse material may be re-introduced to the rotor area by the lifting effect of the additional air. The amount and proportion of the secondary air was adjusted by an external vane.

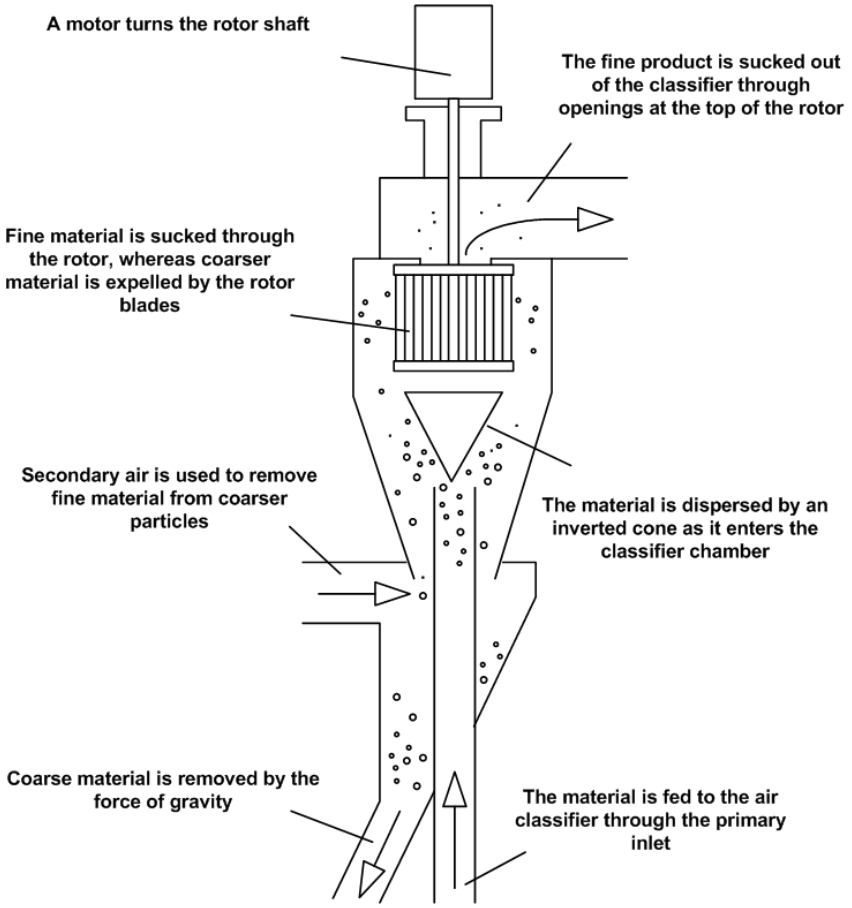

Figure 4.6 Principle of the air classifier.

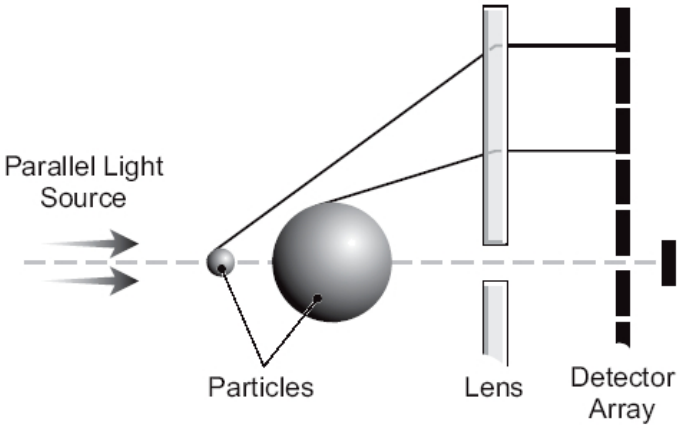

Figure 4.10 Light diffraction at particles and its detection [Malvern INSITEC, 1997].

The detection range of the unit is between 0.5 µm and 200 µm. The instrument continuously extracts material from the process line with a sampling probe, driven by suction from a venturi. The sample is pneumatically transported into the optical head where the particle size distribution is measured up to 4 times per second, and then the sample is pneumatically returned back to the process line. The venturi air is also used to disperse the material. Figure 4.11 demonstrates the principle of the venturi installed in the INSITEC instrument.

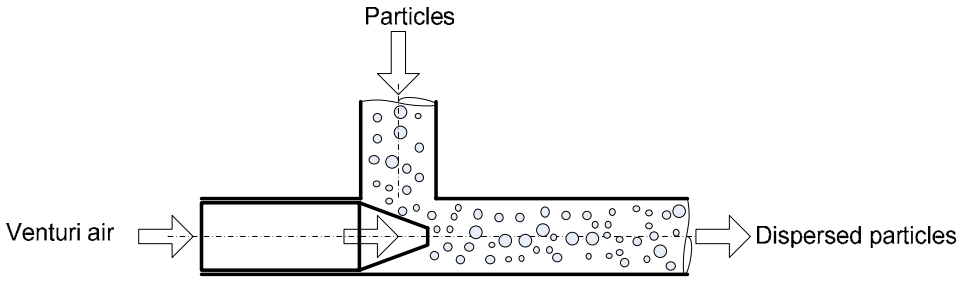

Figure 4.11 Principle drawing of the venturi.

Figure 4.12 presents a schematic drawing of the on-line analyser with air supply and sample transport.

The stainless steel sampling flute shown in Figure 4.13 is installed at the outlet of the air classifier. The position was chosen after several sampling tests in order to ensure laminar flow and an even material concentration at the sampling point.

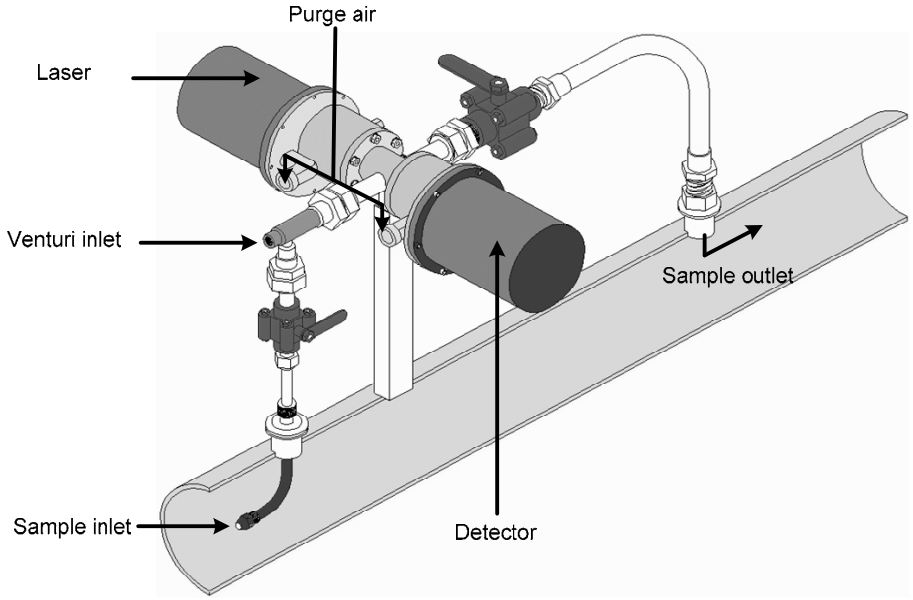

Figure 4.12 Air supply and sample transport in the on-line particle size analyser.

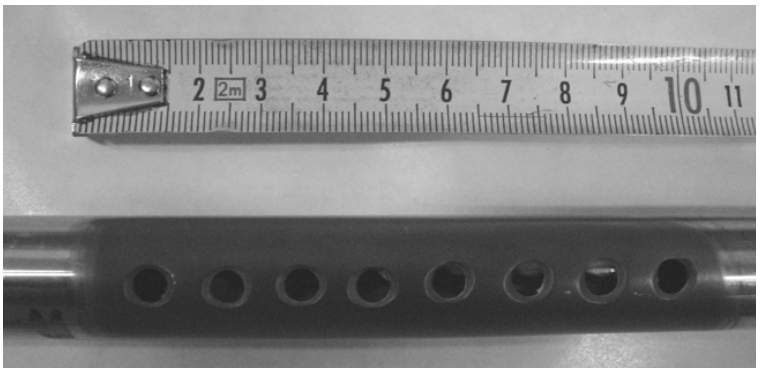

Figure 4.13 The sampling flute.

The grinding circuit was computer controlled. The control program was written in a graphical language, LabView 6.1 [Chmelar, Breivik, 2002]. Communication with the INSITEC program, RTsizer, is performed via the ActiveX component. The instrument control in the ball mill circuit was done with Field Point modules from National Instruments. During production the mill weight, mill torque, capacity, air classifier rotor speed and product size are continuously logged to the computer for further data analysis.

The rotor speed of the air classifier was adjusted with a frequency inverter in order to produce the specified product size. For example, if the set point was 64 μm at d_{74}, then

4.1.4 Blaine number measurement

The Blaine air permeability apparatus (Figure 4.17) is used by the cement industry for determining the specific surface area (cm^2/g) of portland cement. This method has become an effective tool for laboratory work and production control for coke dust size.

A powder sample is compacted in a cell with a plunger, to give a bed height of 15 mm. The cell is inserted into the tube where the inlet of the tube is open to the atmosphere. The apparatus is a means of drawing a defined quantity of air through a prepared sample bed of defined porosity. The number and size of the pores in a bed of defined porosity is a function of the particle size, which determines the rate of air flow through the bed (ASTM C204-84). The time required for the specified volume of air to pass through the bed is used to calculate the specific surface area. The calculated surface area is usually lower than those obtained by other measuring techniques and it is suggested that this is because the measured surface area is the envelope surface of the particles. However, the method is not suitable for fine powders since, for such powders, the flow is predominantly diffusion controlled [Allen, 1999].

R&D Carbon uses a semi-automatic test apparatus for Blaine measurement called "RDC-Blaine" where a sample of 70 g is used. In contrast to the cement industry, where the surface is calculated in cm^2/g, the result for coke is expressed as a dimensionless number (Blaine) [Smith et al., 1991].

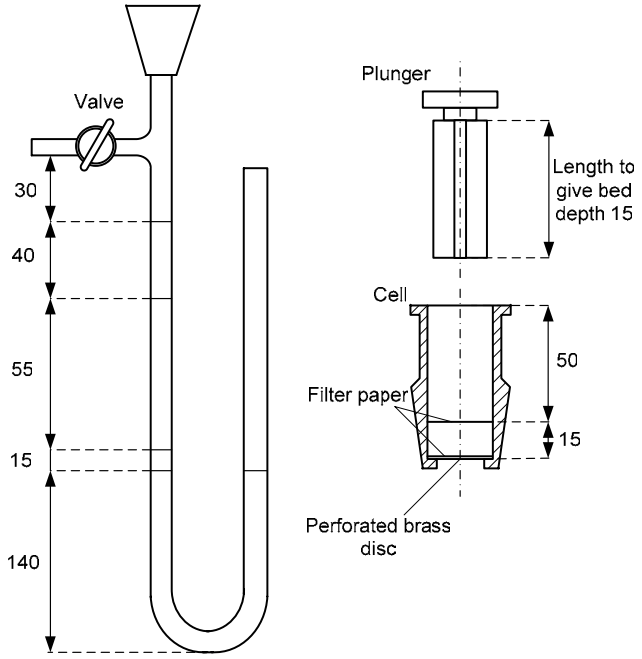

Figure 4.17 Blaine apparatus with cell and plunger. All dimensions are in millimetres.

All Blaine measurements in this work were carried out with the RDC-Blaine instrument at the Elkem Lista aluminium laboratory. Three measurements were used for the determination of Blaine number of each sample and an average is presented.

4.1.5 Influence of the mill operating parameters on the product

Coke grinding is affected by several parameters, e.g., coke mill filling, product size, feed size variations, sweeping speed/residence time. These parameters can have a significant influence on the product stability as well as on the specific grinding energy. Also, fluctuations due to coke material differences can be expected. The influence of the following parameters on the product specifications have been determined [Chmelar, Foosnæs, Øye, Sandvik, 2005];

- final product size
- quantity of coke circulating inside the mill
- air sweeping speed through the mill
- type and properties of mill feed material
- size and composition of balls inside the mill
- rotational speed of the mill

4.1.5.1 Product size variations

Three different grades of fines were produced for each coke type. These fines were used in a subsequent investigation of prebake anode production.

There are different ways to characterise the product size, however the most common is by sieve analysis and Blaine number measurement. Sieve analysis is performed with, e.g., 74 μm/200 mesh, where the product stream is sampled and a representative sample is analysed. The amount of the material passing through the sieve opening describes the product quality/stability. The other method combines the sieve analysis and the Blaine number. The Blaine number (ASTM standard C204-84) gives additional information about the product with respect to its size distribution profile.

Sieve analyses were made of the feed fraction (-2 mm) to the ball mill and results are shown in Figure 4.18. The particle size distribution of each coke is different. Single source coke C has the coarsest feed and single source coke B had the finest size distribution. A set point for the production of 60 μm at d_{70} was applied and calibration of the laser diffraction results with results from sieve analysis was carried out prior to experimental work.

Approximately 2 tons of each coke was processed separately in the ball mill circuit. It was necessary to process large amounts of the material in order to reach a steady state of the mill for each experiment. The steady state is indicated by a stable amount of return material at a constant feeding rate.

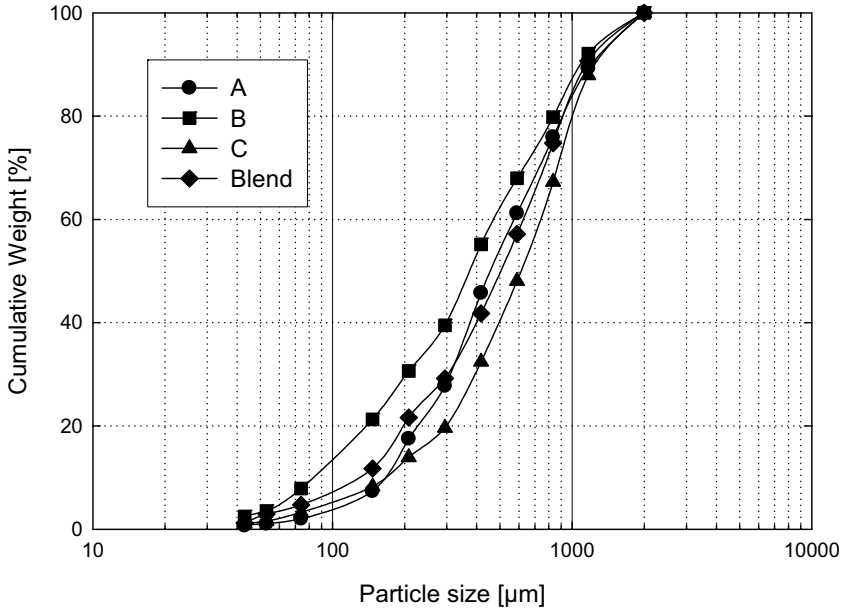

Figure 4.18 Particle size distribution of the feed coke materials to the air swept ball mill.

The grinding effect can be calculated according to Equation 4.3 [Sandvik, Digre, Malvik, 1999].

$$P = \frac{2 \times \pi \times n \times T}{60} \qquad 4.3$$

P – power [W]
n – mill speed [rpm]
T – torque [Nm]

The production capacity was then used to calculate the specific grinding energy in kWh/t. Figure 4.19 presents the calculated specific grinding energy for each coke.

Each material behaves differently due to its mechanical properties. Single source coke C had the highest specific grinding energy for each size fraction (Figure 4.19). However, single source coke B had the lowest specific grinding energy and thus is the easiest to grind. These results correlate well with ISO 10142 and the drop test method. The graph shows that there is a relation between the specific grinding energy and the Blaine number.

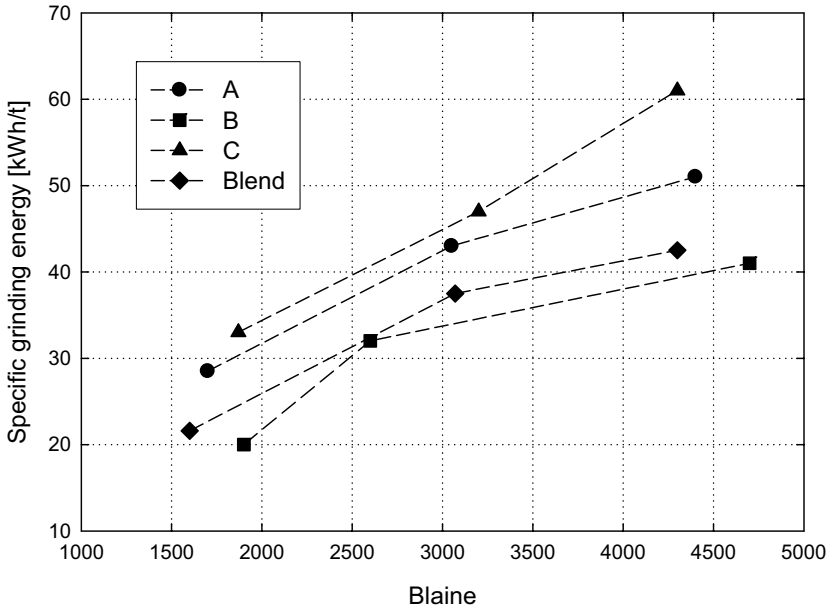

Figure 4.19 Specific grinding energy of four cokes versus the Blaine number.

4.1.5.2 The effect of coke mill filling

The ideal mill filling level produces the required material with the lowest specific grinding energy [Sandvik, Malvik, Digre, 1999]. Figure 4.20 demonstrates how the mill charge affects the specific grinding energy. The mill filling level was adjusted for this investigation by selecting a feed rate into the mill. The mill was allowed to reach steady state for each measurement. The same ball size composition was used for all investigations. The quantity of material in the mill was measured by weighing the mill during the experiment.

If the mill contains little material and the voids between the balls are only partially filled, the grinding is inefficient. In addition, a higher iron content can be expected in the product. Due to the different mechanical properties of the investigated cokes it was necessary to determine the optimal filling level for each coke (SSA, SSB, SSC and blend) and product size.

The optimum mill filling for this product size (Blaine 3000, 65 % -74 µm) was about 20 kg for each coke. A higher amount of coke in the mill will have a negative impact on the capacity as well as on the product size (unstable product with different particle size distribution curves). The grinding capacity of the mill is reduced when a too large quantity of coke is held within the mill [Carter, 1979].

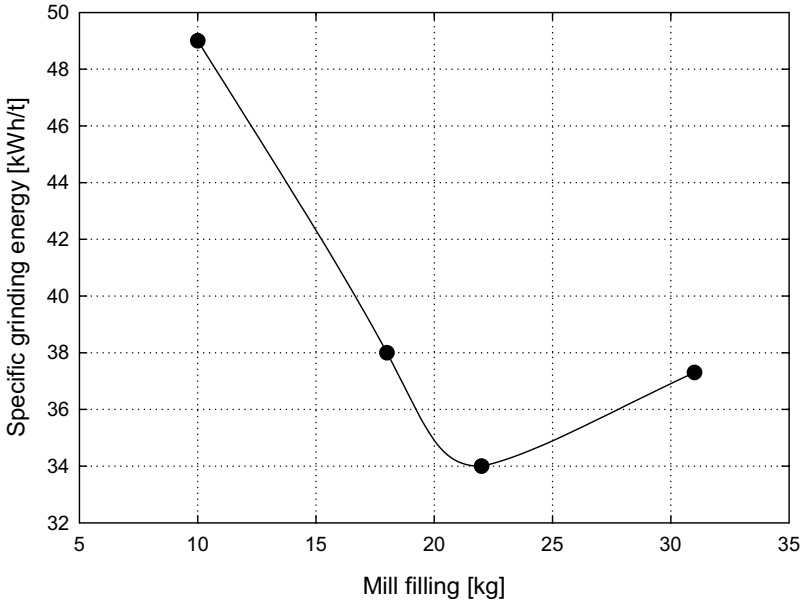

Figure 4.20 Relation between the mill filling and the specific grinding energy (single source A coke).

4.1.5.3 Effect of mill feed

Variations in the composition of the ball mill feed material often produce large variations in the production of fines for prebake anodes. Recycled fines and/or filter dust from the paste plant are common additions to the primary feed. Also, material segregation in silos will contribute to feed variation. Such a situation was simulated by placing two different size fractions in successive layers in the ball mill feeder. Figure 4.21 shows a feeder filled with two different grain size distributions. The fines layer had a particle size of 98 % at -74 µm and a Blaine number of about 4000. The circuit was run so that 68 % of -74 µm (sieve analysis) was produced. The air classifier rotor speed was adjusted to this product size and no size regulation was applied. Six samples were taken at equal time intervals for further analysis. Figure 4.22 shows the variation in Blaine number and the amount of -74 µm particles.

Figure 4.22 shows that there are large variations in the product size as well as in the Blaine number during operation. The variations in product size and Blaine number are also reflected in the process parameters, *i.e.*, the specific grinding energy as well as the return and the mill filling. The equipment was started at steady state ratio of conditions with a specific grinding energy of 33 kWh/t, mill weight 28 kg and return ratio of 31 %. During the experiment the specific energy, the return ratio and the mill weight decreased as the fine fraction entered the mill. The feed rate was not adjusted to keep a fixed mill weight in order to demonstrate how the feed size variation can affect both the product quality and the process performance. At the end of the experiment the specific grinding energy was 25 kWh/t, the mill weight 20 kg and a return of 15 %.

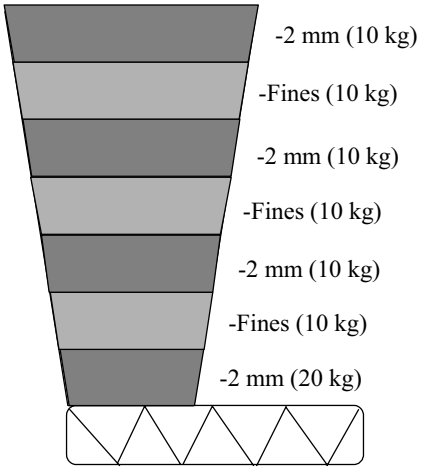

Figure 4.21 Feed size variations in the feeder hopper.

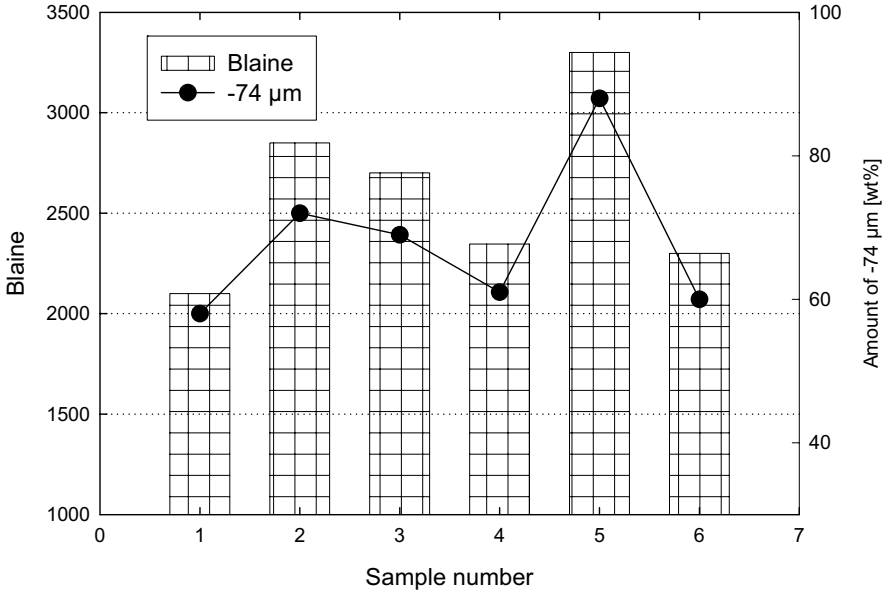

Figure 4.22 Blaine number and the amount of -74 µm particles (%) for six samples taken at different time intervals over the entire testing period.

4.1.5.4 The effect of the sweeping speed

The residence time of the particles inside the mill determines the degree of contact between coke particles and the steel balls. In air swept ball mills the particle residence time can be regulated by the air sweeping speed [Kolacz, 1995]. This speed can be regulated by applying false air at the mill outlet and will thus not affect the total air flow

rate of the circuit. A higher sweeping speed will remove coarser particles from the mill and thus shorten their residence time inside the mill, which will increase the amount of returned material. If the sweeping speed is low, the particles are ground finer (more energy transferred), causing the amount of return material to decrease. In order to investigate the effect of the sweeping speed three experiments were performed. Figure 4.23 shows how the sweeping speed affects the Blaine number and the amount of return material. At low sweeping speeds the return was 27 % and fines with a higher Blaine number of 3100 were produced. When high sweeping speeds were applied, the return increased to 55 % and the Blaine number dropped to 2100.

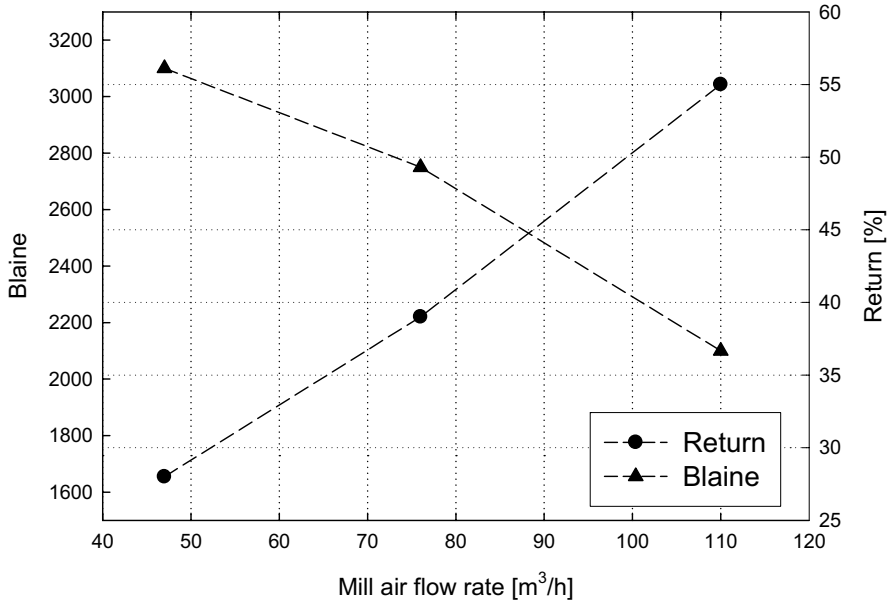

Figure 4.23 Effect of the sweeping speed on the Blaine number and the amount of return material.

Figure 4.24 presents particle size distributions of three materials produced at different sweeping speeds. The lower sweeping speed (47 m^3/h) resulted in more material in the finest range and thus a flatter size distribution curve and a higher Blaine number (3150) even though the top size was almost the same for all products. At the highest sweeping speed of 110 m^3/h less fines were produced in the finest range and the distribution curve was steeper compared with the lowest air flow rate (47 m^3/h).

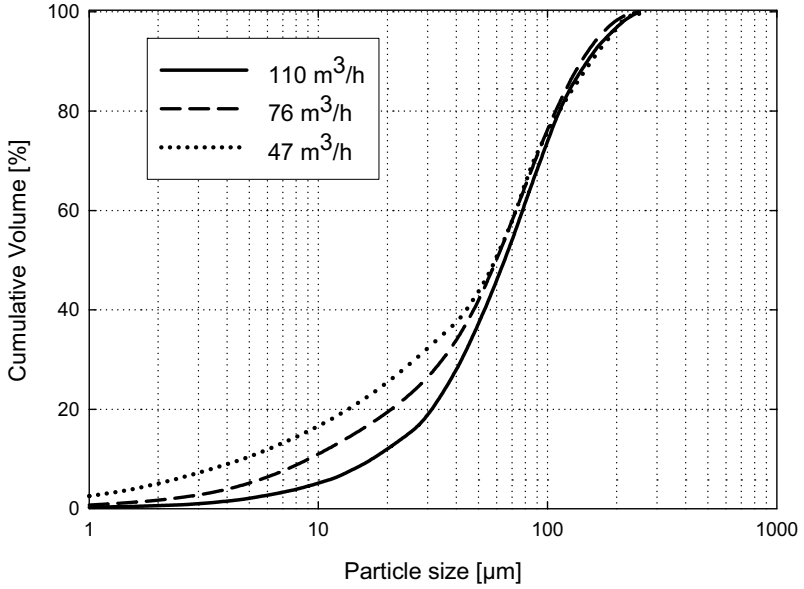

Figure 4.24 Particle size distribution of three products produced at different sweeping speeds (measured by laser diffraction analysis).

4.1.5.5 Mill speed

The effect of the critical speed was investigated in a batch mill. This mill is made of steel with an internal diameter of 0.4 m and a length of 0.2 m. The mill is not equipped with lifters and has no lining. It has a motor with a nominal power of 0.6 kW. The rotational mill speed is regulated by a gearbox.

The critical speed (n_c) is a theoretical speed at which the centrifugal force on a ball in contact with the mill shell at the height of its path equals the force on it due to gravity. The critical speed of the batch mill was calculated according to the following equation [Sandvik, Digre, Malvik, 1999].

$$n_c = \frac{1}{\pi} \times \sqrt{\frac{g \times 1800}{d}} = \frac{42.3}{\sqrt{d}} \qquad 4.4$$

n_c – critical speed [rpm]
d – mill diameter [m]
g – gravitation [m/s^2]

The specific grinding energy was calculated from the motor power measured during the test. Three experiments were carried out with speeds of 60 %, 70 % and 80 % of the critical rotational mill speed (n_c = 18.92 rpm). Representative samples were taken at regular intervals which correspond to a calculated specific grinding energy. All samples

were analysed by sieving. Figure 4.25 presents the relationship between the rotational speed and the specific grinding energy.
Figure 4.25 shows the effect of mill speed on product characteristics (particle size). The highest rotational speed of 80 % produced almost 15 % more fines than at 70 % of the critical speed. Note that since this test mill is not equipped with lifters, the higher rotational speed contributes significantly to the grinding effect.

The Blaine numbers shown in Figure 4.26 also follow the size reduction trend as shown in Figure 4.25. There was a difference of 400 Blaine number units between the 80 % and 70 % rotational speed at a specific grinding energy consumption of 40 kWh/t.

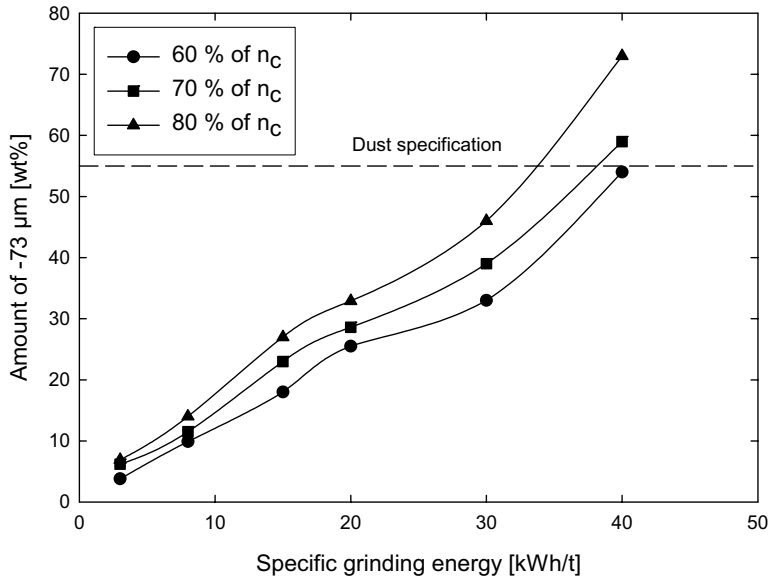

Figure 4.25 Product size (-73 µm) versus specific grinding energy as a function of the three mill rotational speeds expressed in percent of the critical speed (n_c – critical rotational speed of the mill).

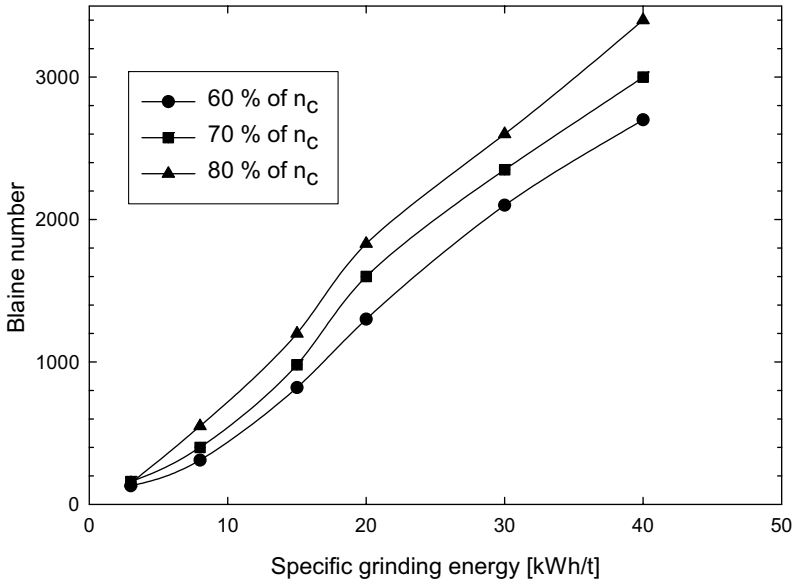

Figure 4.26 Blaine number as a function of the critical speed (n_c) and the specific grinding energy.

4.1.5.6 Ball size distribution

Three different ball size distributions were investigated in the batch mill in order to determine the influence on the product size. Table 4.1 presents the applied ball size distribution compositions. Ball size distribution 1 was run with a standard configuration [Nordberg, 1971 and Sandvik, Malvik, Digre, 1999]. The second ball size distribution was carried out using ball sizes of 10 mm, 15 mm and 20 mm. Finally, the third ball size distribution was run with 50 wt% of ball size distribution 1 but with an addition of 50 wt% of each ball size (10 mm, 15 mm and 20 mm). The diameter of each ball was measured manually by a vernier calliper prior to each investigation.

Table 4.1 Ball mill charge compositions.

Ball size [mm]	Ball size distribution 1 [wt %]	Ball size distribution 2 [wt %]	Ball size distribution 3 [wt %]
10	9.0	33.3	21.2
15	15.0	33.3	24.1
20	20.0	33.3	26.7
25	18.0		9.0
30	23.0		11.5
35	15.0		7.5

Figure 4.27 shows results with three different ball size distributions versus the calculated specific grinding energy. Ball size distribution 1 produced the highest amount

of – 73 µm particles. Ball size distribution 2 produced the lowest amount of -73 µm (52 %), which was mainly due to the lack of large balls and thus less energy available for grinding of the larger coke grains.

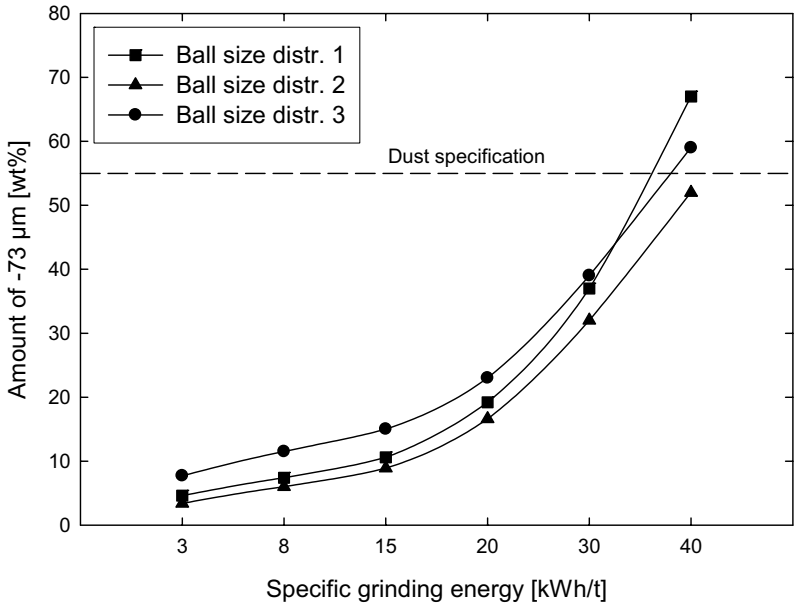

Figure 4.27 Product size versus specific grinding energy as a function of the three ball size distributions.

The collected samples were analysed with the Blaine instrument and the results are shown in Figure 4.28 as a function of the specific grinding energy. The highest Blaine number was achieved with ball size distribution 3 at a specific grinding energy of 40 kWh/t. However, this ball size distribution did not produce the product with the highest Blaine number for all sampling points when compared to ball size distribution 1. The increase in the Blaine number for the last two experiments was most probably caused by a larger quantity of smaller size balls compared to ball size distribution 1. The smaller balls are much more effective in grinding the fine particles. However, the lower amount of larger balls produced a lower Blaine number with a lower specific grinding energy consumption/grinding time.

This illustrates the importance of the correct proportion of balls in the mill to match both the feed material and the required product.

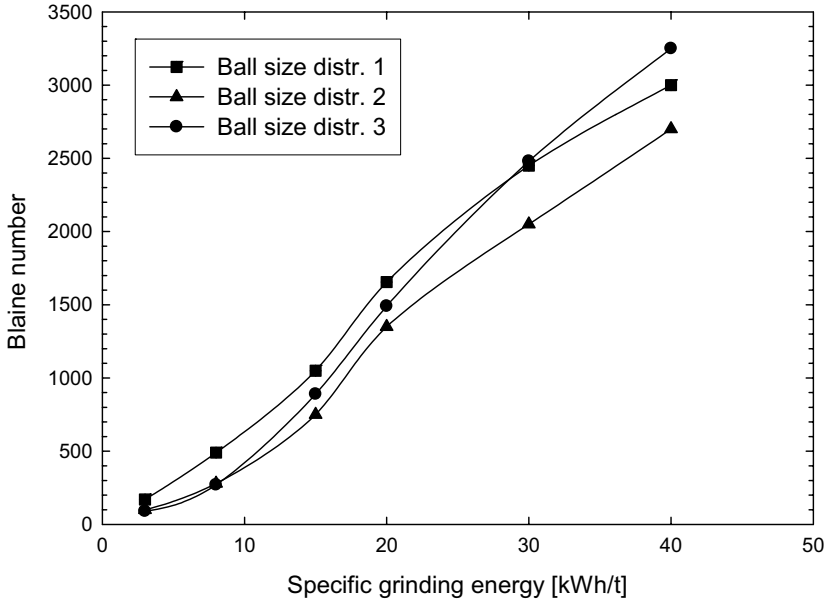

Figure 4.28 Blaine number as a function of the ball charge and specific grinding energy.

4.1.6 Morphological characterisation of the dust

In order to demonstrate the effect of the residence time (sweeping speed) on the mill product, image analysis of the produced samples was carried out. About 1 million particles from the product samples were analysed. The samples were taken at different times during grinding, which ensured statistical validity of the measurements. Figure 4.29 presents the Pharma Vision device for particle morphology measurement.

The measurements concentrated on the particle roundness. Roundness is characterised on a scale between 0 and 1. A perfect circle has a roundness of 1.0, while a very narrow elongated object has a roundness close to 0.

The sample was dispersed on a 100 x 100 mm glass slide using compressed air. The amount of the compressed air was optimised prior to measurements in order to achieve a mono layer of particles. Figure 4.30 presents the dispersion unit for sample preparation. The dispersion unit consists of a glass cylinder, a small funnel for the sample placement, compressed air nozzle, and a glass tube with a steel ball for sample transport and dispersion. The glass cylinder is sealed with the plate, thus particles and air can not escape to the ambient environment.

However, the mill production stability can be influenced by the following process and material parameters.

- Mill filling
  The amount of material in the mill mainly influences the specific grinding energy and product size. Additionally, the higher wear of steel balls for a low mill filling level can increase the amount of Fe in the product.

- Particle size distribution of the mill feed coke
  Experiments showed that the feed size can significantly influence the production stability (product size and Blaine).

- Sweeping speed
  High sweeping speed produced material with a lower Blaine number compared to a lower sweeping speed. This influenced the steepness of the product size distribution as well as the particle roundness. In other words, a long residence time of the particle in the mill at a low sweeping speed will contribute to excessive production of the finest particles and will produce more round particles.

- Mill speed
  The mill speed influences the grinding mechanism (cataracting and/or cascading).

- Ball size distribution
  The ball size distribution can determine the product size and Blaine number, as small balls are effective at producing fine particles, while the larger balls are required for larger particles.

On-line particle size control contributed to the stable and controlled production of specified product sizes.

4.2 Mixing and forming

4.2.1 Mixing

The prepared coke fractions were weighed according to the specified recipe and blended in the sigma blade mixer together with coal tar pitch.

The sigma blade mixer consists of a double blade mixer with two horizontal impellers. The blades can rotate in both directions; towards each other or away from each other. The rotational speed of the blades can be regulated with a gearbox or a frequency inverter. The blades are formed in a sigma shape. Figure 4.35 illustrates the operating principle of the mixer. This configuration is commonly used with highly viscous materials [Uhl, Gray, 1967].

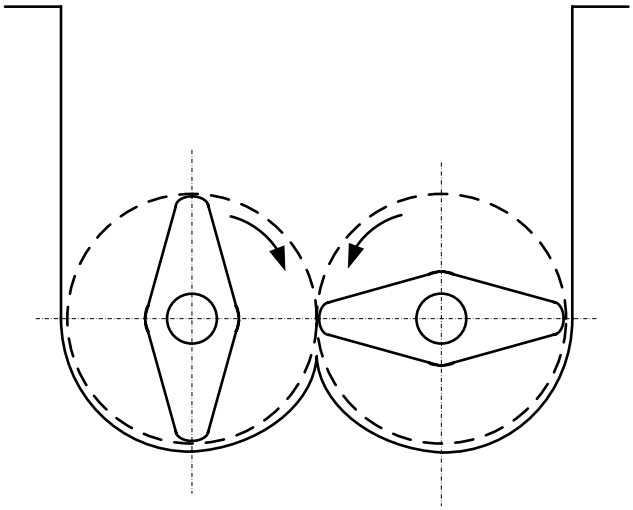

Figure 4.35 Principle of the sigma blade mixer.

Figure 4.36 shows the configuration a single sigma blade.

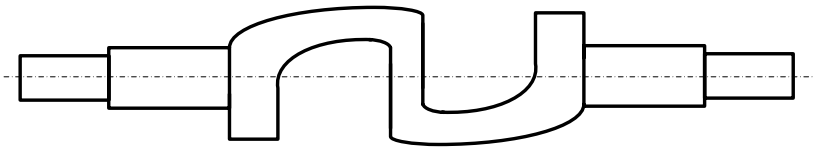

Figure 4.36 Drawing of the sigma blade.

Figure 4.37 shows a picture of the sigma mixer produced by Werner & Pfleiderer, which was used in this work. It shows a detailed view of the mixer, where the two sigma blades can be seen. The mixer shell is heated by oil to 210 °C [Sigma Mixer technical manual, 1991].

5. Method development for thermal dilation of green anodes

5.1 Background

The anode can be subjected to significant stresses during baking, mainly due to thermal expansion, shrinkage and inherent temperature gradients, which can affect critical properties of the anode. Understanding these physical and chemical changes is important for both the economic viability of the process and optimal process control.

Dilatometric equipment has been developed to study the dimensional changes during baking of green anodes, showing that these changes are influenced by sample orientation parameters (both parallel and perpendicular to the direction of forming), type of filler, specimen dimensions and heating rate [Fitzer et al., 1973].

Two studies [Letizia, Calderone, 1980] and [Martirena, 1983] point out that grain size distribution, pitch content, heating rate and the use of packing mass have significant influence on the dimensional changes during baking. These changes are affected by different types of packing mass, due to the different radial thrusts on the sample and the plasticity of the carbon specimens.

Table 5.1 presents an overview of the significant transitional changes related to the physical-chemical changes and the major practical phenomena.

Table 5.1 Physical-chemical transitions by heat treatment [Foosnæs, Naterstad, 1993].

Temperature zone [°C]	Physical-chemical changes	Major practical aspects
0 – 200	Thermal expansion of pitch. Release of residual tensions caused by forming and cooling	Reduced density. Slight release of aggregate interlocking.
150 – 350	Redistribution of pitch into voids by pitch expansion. Post impregnation of the coke aggregate.	Risk of stud hole slumping/damage. Permeability, mechanical strength and resistivity are affected.
350 – 450	Release of light binder volatiles.	Slight reduction in density of the aggregate packing.
450 – 600	Coking: Transition from plastic to solid matrix. Release of the majority of non-coking volatiles.	Dilatometric tensions by thermal gradients causing expansion and contraction within the same block. Release of tensions by micro/macro cracks depending on the thermal gradient.
600 – 900	Post-coking: Release of heavy cracked volatiles, methane, hydrogen and annealing of tensions	No particular effects within the range of ordinary heating rates.
900 – 1200	Crystalline reorientation and growth of the binder coke and possibly of the lowest calcined aggregate coke.	Dilatometric tensions by contraction. Macro cracks may arise if the previous average calcining level is largely exceeded (>100 °C) for the coke.

Figure 5.1 presents an example of the thermal dilation of a green core sample 50 mm in diameter and 50 mm long, containing 15 % pitch. No packing material was used to

support the sample. The sample was heated at 60 °C/h to 950 °C, then soaked for three hours under a nitrogen atmosphere.

Thermal dilation changes are expressed in per cent of the original sample height. However, the calculation also includes a correction for the dilation of the equipment.

The initial expansion at about 100 °C is due to the release of residual stresses from the forming and cooling process. The sample expands further (up to 0.55 % of its initial height) because of trapped volatiles. A further increase in the temperature leads to slumping caused by the plasticity of the sample. The sample expands slightly at about 300 °C due to trapped light binder volatiles. There is a sudden height increase at about 400 °C which is most likely a consequence of the residual pitch expulsion from the coke pores. The sample height is then reduced after the release of volatiles and at about 450 °C the transition from a plastic to a solid matrix starts. The major release of non-coking volatiles takes place up to about 600 °C. The post coking process starts at about 600 °C and continues until 900 °C, accompanied by the release of cracked volatiles (methane, hydrogen) and sample height reduction.

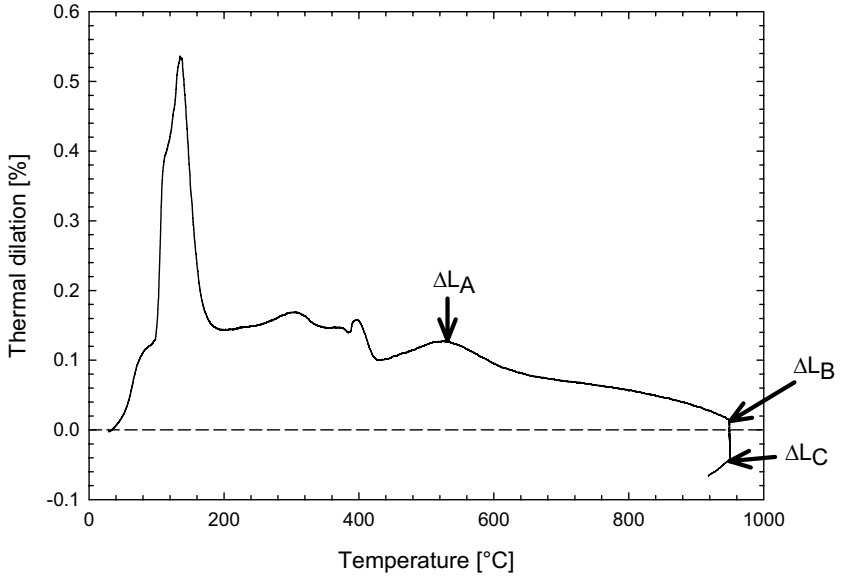

Figure 5.1 An example of thermal dilation measurement of a green sample versus temperature.

The ISO 14428 standard describes the determination of expansion and shrinkage of ramming pastes during baking. The standard describes the experimental procedure, equipment used for testing and how to calculate and interpret results.

According to ISO 11428, the sample was packed in a mass of carbon particles (electro-calcined anthracite or graphite), then heated in nitrogen at 180 °C/h to 950 °C, where it was soaked for three hours.

The maximum thermal shrinkage before and after soaking at 950 °C was calculated from the following Equations 5.1 and 5.2

$$\Delta L_{before} = \Delta L_A - \Delta L_B \quad 5.1$$

$$\Delta L_{after} = \Delta L_A - \Delta L_C \quad 5.2$$

Where:
ΔL_{before} is the maximum thermal shrinkage [%] before the sample reaches 950 °C
ΔL_{after} is the maximum thermal shrinkage [%] after soaking for 3 hours at 950 °C
ΔL_A is the maximum thermal expansion [%] before the sample starts to shrink
ΔL_B is the thermal expansion [%] immediately before the sample reaches 950 °C
ΔL_C is the thermal expansion [%] after soaking at 950 °C for 3 hours

Figure 5.1 presents the positions of the thermal dilations value of ΔL_A, ΔL_B, and ΔL_C on the example thermal dilation curve.

However, ISO 11428 does not consider the significant changes that occur before the sample reaches 450 - 500 °C.

Thermal dilation of the sample is calculated from the following equation

$$TD_t = \frac{\Delta l_t}{l} * 100 \quad 5.3$$

Where:
TD_t is the thermal dilation [%] at a given temperature t
Δl is the thermal dilation [mm] at a given temperature t
l is the height [mm]of the sample before testing

5.2 Original dilatometer

A dilatometer which was constructed in 1995 at NTNU was used for this investigation. It was a vertically arranged system with a water cooled cylindrical furnace. Two thermocouples were installed, one close to the heating elements of the furnace and another from the base contacting the bottom of the quartz tube. Figure 5.2 presents a schematic drawing of the original dilatometer.

A core sample 50 mm diameter and 50 mm long was placed on the graphite washer in the cylindrical quartz tube. A quartz push rod rested on top of the sample, and follows the sample movement, transferring it to the linear transducer. The sample is covered with a packing material (typically graphite particles).

The quartz tube, 60 mm in diameter and 600 mm long, was polished at the bottom (both inside and outside) and the top in order to achieve maximum alignment of the sample

position versus the quartz push rod. The quartz pipe rested freely in the furnace on an alsint pipe supported from the bottom of the furnace.

Nitrogen to purge the chamber was injected through the furnace lid. The furnace can be heated at a constant rate by a temperature controller. A computer registers the temperature and dimensional changes at a specified time interval during the measurement. Microsoft Excel is used for logging and visual presentation of the data.

The original dilatometer was always used with a packing mass. This was mainly due to insufficient purging and the description in the ISO 14428F standard. Most of the published works also used a packing mass around the samples.

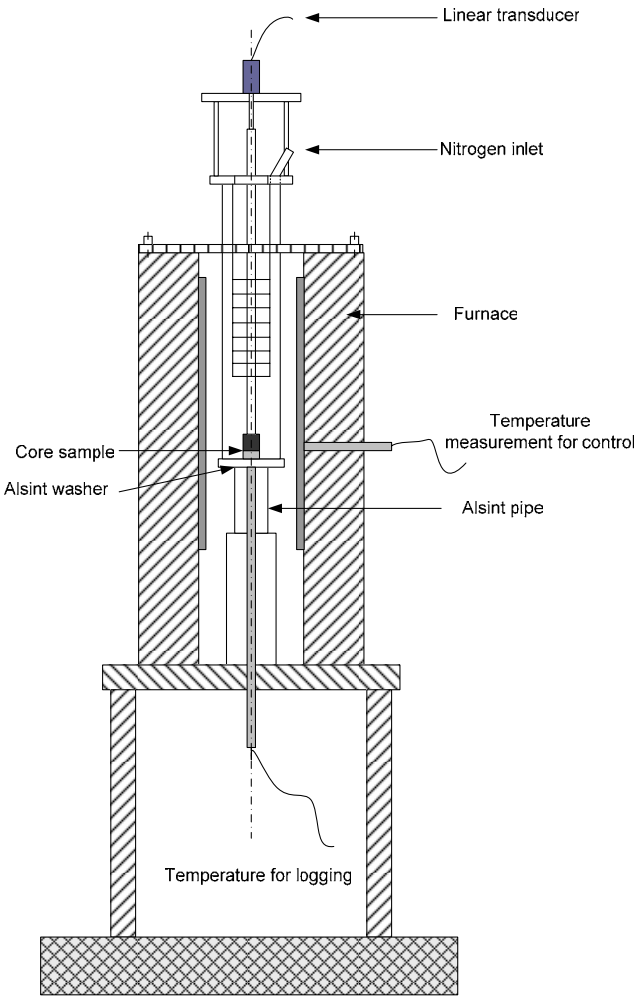

Figure 5.2 Original dilatometer.

Finally, the baking loss of the samples was measured and is presented in Figure 5.19. The baking loss increases with increasing heating rate.

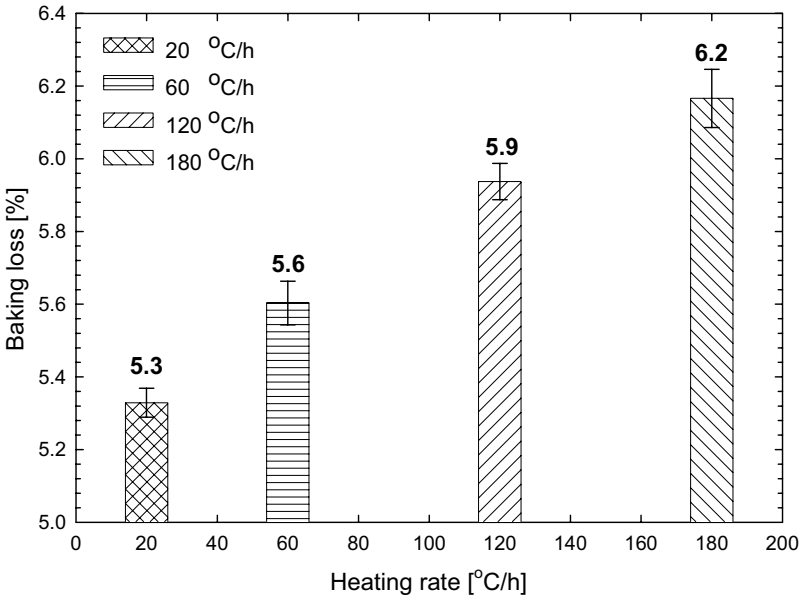

Figure 5.19 Baking loss of the samples at different heating rates.

5.5.3 Sample preheating treatment

During the measurement of the coefficient of thermal expansion (CTE) for ramming paste the sample is preheated to about 400 °C [Sørlie, Øye, 1994]. This pre-treatment prevents excessive slumping when samples with a higher pitch content are heated.

The aim of this investigation was to find the influence of the sample preheating and thus the removal of the initial expansion on the final shrinkage.

Green anode samples of known granulometric composition and pitch content were investigated in the dilatometer with and without preheating. Two pitch levels, 15 % and 18 %, were used. Three samples were run for each composition. The sample preheating was carried out with a heating rate of 20 °C/h and a soaking time of one hour at 400 °C. Packing coke was used to prevent oxidation. The samples were cut into the correct dimensions after the preheating treatment.

All samples were run in the dilatometer with a heating rate of 60 °C/h. Figure 5.20 compares thermal dilation curves for samples with and without preheating and a pitch content of 15 %.

There is a significant difference between the thermal dilation curves of the preheated sample and untreated sample. The preheated sample lost its initial maximum expansion

due to removal of the volatile pitch components. The major difference between the samples is the expansion in the temperature range from 400 °C to 600 °C. The preheated sample reaches a maximum expansion at 460 °C while the untreated sample has a corresponding maximum at 570 °C.

Figure 5.20 shows a comparison of the thermal dilation with the calculated shrinkage ΔL_{before} and ΔL_{after}. The preheated sample has more shrinkage when compared to a normal sample.

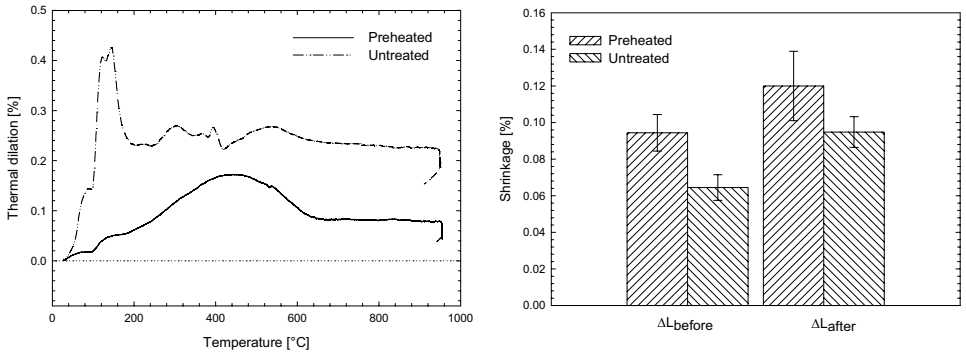

Thermal dilation Shrinkage

Figure 5.20 Comparison of the thermal dilation and shrinkage of samples (15 % pitch content) with and without preheating.

Figure 5.21 presents results from samples with 18 % pitch content. The untreated sample significantly changed its thermal dilation profile due to the higher pitch content. There was a small expansion at 120 °C, but with increased temperature the sample slumped extensively. Around 250 °C the sample stopped slumping and maintained its height until about 400 °C. There was a small decrease in the height followed by expansion until about 530 °C. The sample height was slightly reduced during the post coking process. The preheated sample had a similar thermal dilation profile as the 15 % sample. The preheated sample reached a maximum at 450 °C, while the untreated sample exhibited a maximum at 575 °C.

The calculated shrinkage ΔL_{before} and ΔL_{after} shows that the preheated samples exhibit significantly higher shrinkage compared to untreated samples.

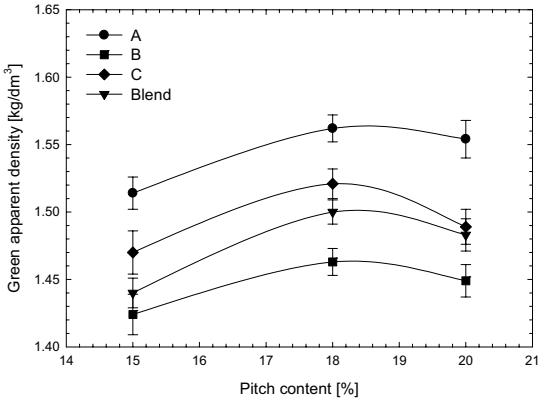

45 % dust size

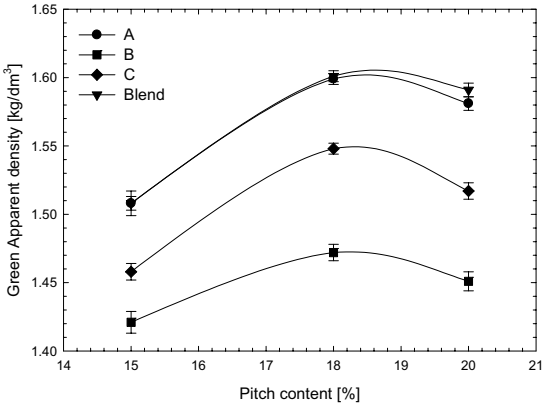

63 % dust size

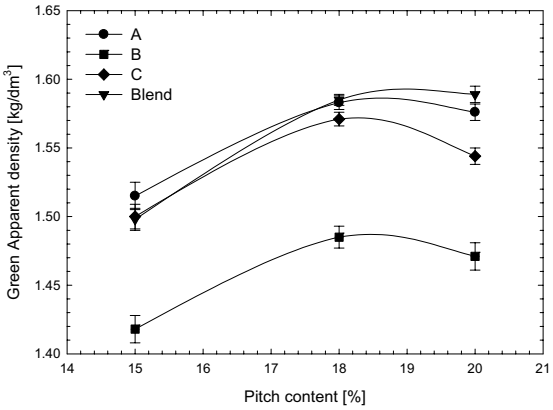

94 % dust size

Figure 6.2 Green apparent density versus pitch content for different cokes with the dust sizes 45, 63 and 94 % (45, 63 and 94 % -63 µm particles).

Figure 6.3 shows the green apparent densities for all four cokes at different dust sizes and pitch contents. The optimal pitch content for single source coke A was about 18 %. The dust size of 64 % was an optimal amount in order to obtain the highest density. The increase of dust size to 94 % reduced the density from 1.6 kg/dm^3 (dust size 63 % at 18 % pitch content) to 1.58 kg/dm^3 (pitch content 18 %). The lowest dust size of 45 % produced the lowest densities at 18 and 20 % pitch content. However, there were no significant density differences at 15 % pitch content.

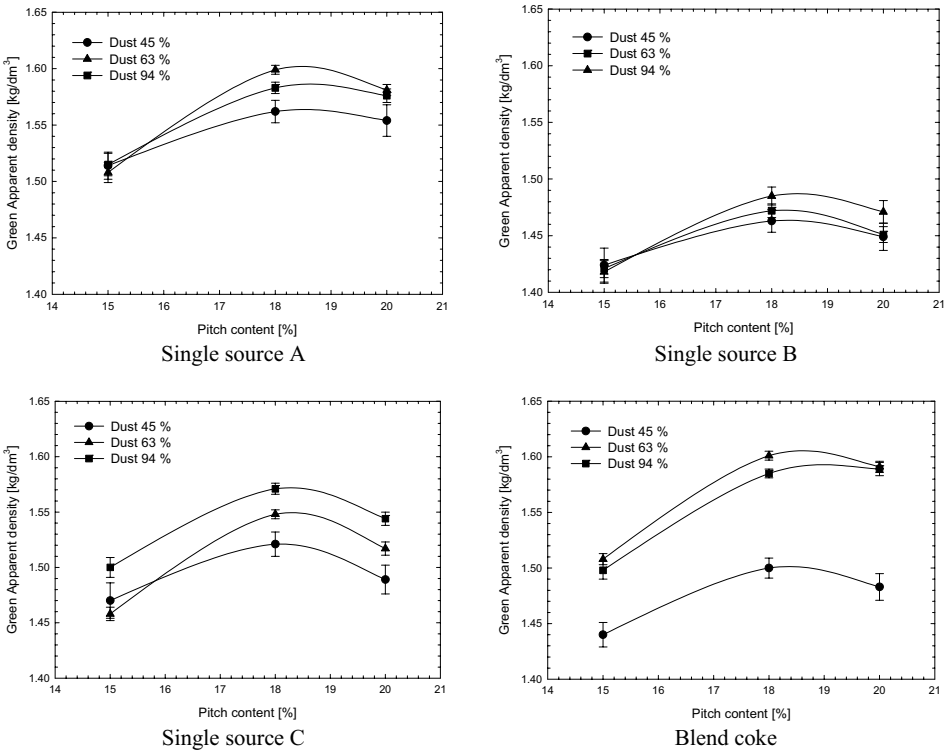

Figure 6.3 Green apparent density versus pitch content for single source A, B, C and blend coke with different dust sizes.

Green anode samples made from single source coke B showed the lowest green apparent density values of all cokes for each pitch and dust size. The highest density (at 18 and 20 % pitch content) was achieved with dust containing 94 % -63 µm.

For single source coke C the highest dust size of 94 % had the greatest effect on the green apparent density for each pitch content. The lowest densities were measured in anodes made of dust size 45 % except at the lowest pitch content (15 %) where the dust containing 63 % -63 µm produced a lower density.

The results for the blended coke show that 63 % dust was an optimal size for the highest green apparent density. The lowest densities were produced when using the 45 % dust size.

6.1.2 Thermal dilation investigation

Thermal dilation investigations were carried out for anodes made from single source cokes A, B and C. The effect of dust size and pitch content on the thermal dilation and the calculated shrinkage was investigated. The blend coke samples are not included in these experiments as the samples were used in the method development and optimisation. Two core samples were used for each test and the calculated average is presented. The core samples were taken from the same position in the pilot anode. The same heating rate of 60 °C/h was used for all samples.

Additionally, the roundness of the dust particles for each coke type was investigated. The results are presented in Table 6.1.1

Table 6.1.1 Roundness results**.**

Properties	Method	Unit	SSA	SSB	SSC
Dust roundness	Image analysis	45*	0.60	0.72	0.62
		63*	0.67	0.76	0.66
		94*	0.74	0.87	0.76

* dust size expressed in % of particles passing a 63 μm sieve

The differences in the mechanical strengths of the investigated cokes resulted in different shapes of the produced fine particles. The SSB coke has higher roundness values compared to the SSA and SSC cokes. The standard deviation of particle roundness was about 5 % for Dust 45, 4 % for Dust 63 and 3 % for Dust 94. The binder matrix using SSB coke is expected to flow more easily while in the SSA and SSC cokes the flowability is probably reduced due to irregularly shaped interlocking particles. However, the SSB coke has a similar roundness factor in Dust 45 as SSA and SSC have in Dust 94.

6.1.2.1 Single source A coke, pitch content versus dust size variation

Figure 6.4 presents thermal dilation comparisons for single source coke A with 15 % pitch content and different dust sizes.

The sample with the lowest dust size (45 %) expanded least at 170 °C, while the sample with the higher dust size (63 %) had the highest expansion. This sample also has the highest expansion at 330 °C due to release of light binder volatiles. The highest dust size delayed the expulsion and the sample reached its greatest height at 190 °C. This sample did not slump as the others with the lower dust size, due to lower viscosity.

The calculated shrinkage shows that as the dust size increases it reduces the ΔL_{before} and ΔL_{after}.

Increasing the pitch content to 18 % contributed to slumping of the samples even with the highest dust size (94 %). The sample with the lowest dust size (45 %) started to slump at a lower temperature compared to the higher pitch content samples (18 and 20 %) which showed an additional expulsion peak at about 170 °C.

The highest dust size (94 %) sample shows a different thermal dilation curve, especially between 250 and 600 °C. The sample expanded significantly from 480 to 600 °C as the non coking volatiles were released. Increasing the dust size contributed to greater shrinkage of the samples. However, a pitch content of 15 % produced the opposite trend. Additionally, samples with 15 % pitch content did not slump, but kept its thermal dilation changes within -0.25 % of the initial height. On the other hand, samples with 18 % pitch content expanded to about 0.8 % but slumped to about -1 % of the initial height.

The samples with the highest pitch content (20 %) slumped significantly while heating between 140 and 300 °C**.** The lowest height reduction was measured with the lowest dust size (45 %).

6.1.2.2 Single source B, pitch content versus dust size variation

Figure 6.5 presents a comparison of the thermal dilation at varying dust sizes with 15, 18 and 20 % pitch content. The lowest dust size gives the highest expansion. The finer dust size decreases the thermal dilation, especially between 250 and 350 °C.

On the other hand, the finer dust size contributes to a higher shrinkage. The curves for a pitch content of 18 % shows that the finer dust size decreases the expulsion. This was also found with 15 % pitch content. However, the thermal dilation curves are more complex when compared to 15 % pitch content. The profile development is very similar for each dust size, but with different expansion/slumping. The maximum expansion was found with the 45 % dust size. Additionally, there is an expansion at 200 °C which is missing in the other two dust sizes.

Samples with 63 and 94 % dust size slumped after expanding at about 150 °C. There is a temperature shift in expansion at 160 and 310 °C between the three dust sizes. The lowest dust size (45 %) starts to expand at a lower temperature while the other samples are delayed. The highest pitch content contributed to extended slumping for all three dust sizes. The shrinkage results show no clear trend for the pitch content.

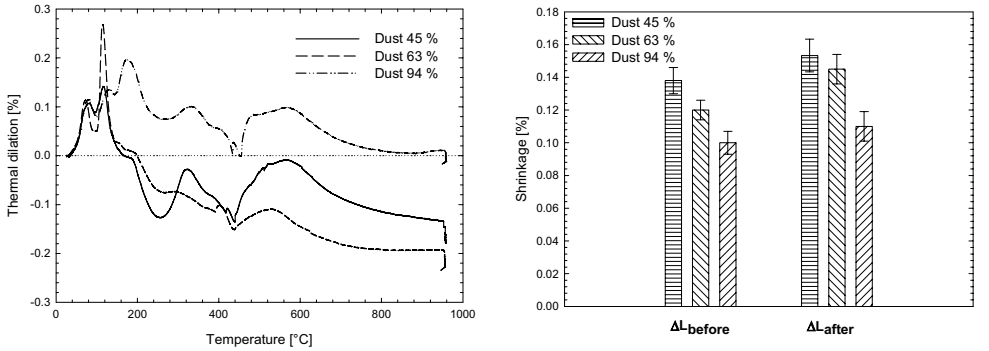

15 % pitch content

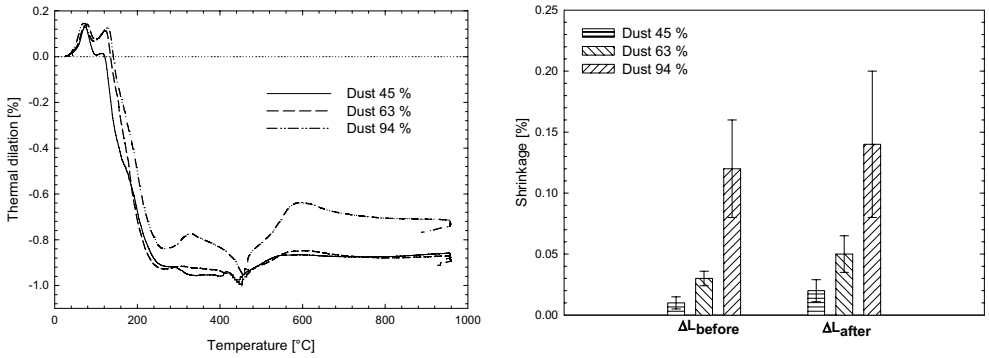

18 % pitch content

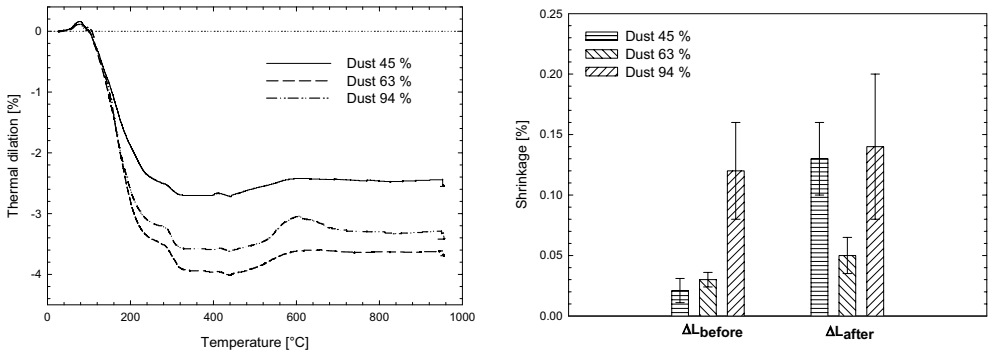

20 % pitch content

Figure 6.4 Thermal dilation with shrinkage of single source coke A with 15, 18 and 20 % pitch content and different dust sizes.

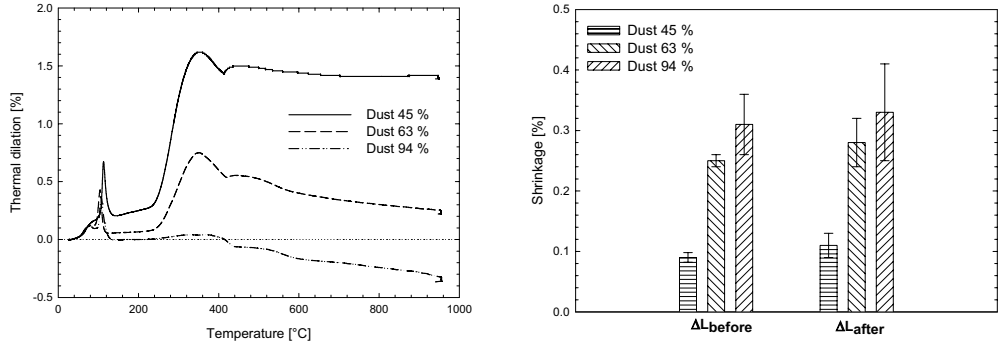

15 % pitch content

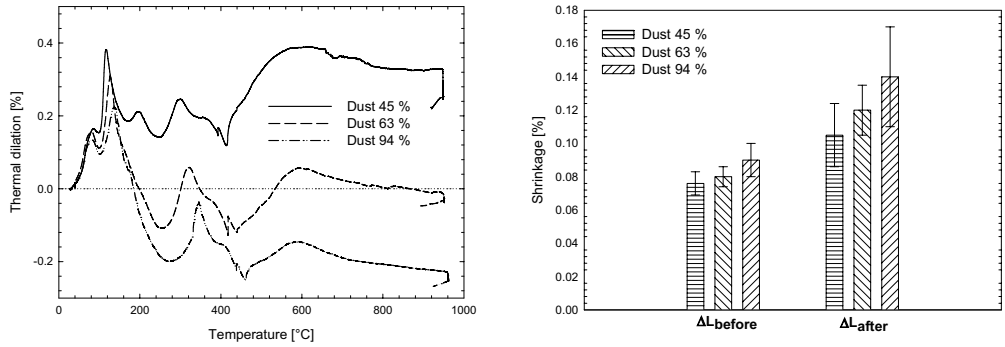

18 % pitch content

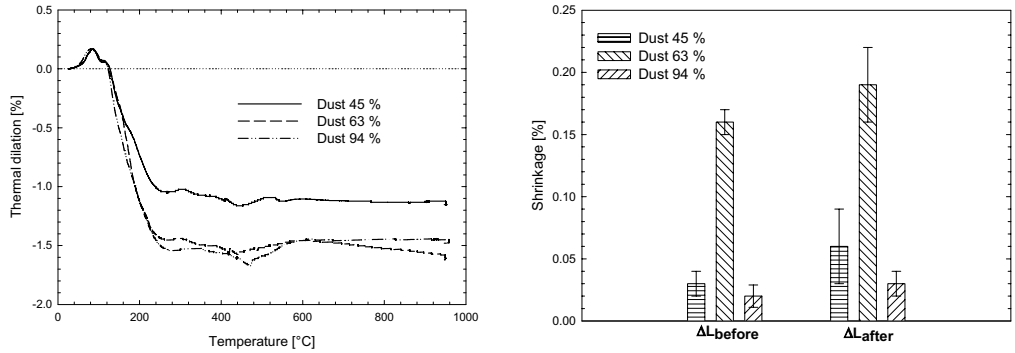

20 % pitch content

Figure 6.5 Thermal dilation with shrinkage of single source coke B with the 15, 18 and 20 % pitch content and different dust sizes.

6.1.2.3 Single source C, pitch content versus dust variation

Figure 6.7 presents results with 15, 18 and 20 % pitch content and different dust sizes. It can be seen that the finer dust size contributes to more sample expansion (at 15 % pitch content). All three dust size curves have a similar profile, but there is a temperature shift

6.1.2.4 Coke comparison with regard to the dust size

This comparison shows the effect of dust size with a constant pitch content (15 %) on the thermal dilation test. Figure 6.8 presents results for the thermal dilation of single source coke A, B and C with 15 % pitch and 45, 63 and 94 % dust size.

Dust size 45 produced samples with very similar shrinkage despite a large expansion for the SSB coke, first at about 110 °C, then strongly at 240 °C, followed by slumping at about 350 °C. The expansion at 350 °C is probably caused by a denser matrix where binder volatiles were trapped and rounder particles produced higher flowability in the paste. At this dust size the SSB coke had the lowest shrinkage for both ΔL_{before} and ΔL_{after} and it seems that 15 % pitch is close to optimum for SSB at this grain composition. During the mixing process more fine particles were generated in the mechanically weak SSB coke, thus generating a higher surface area. It is expected that some of the largest grains in the coarse and medium fractions were crushed during mixing, thus reducing the samples overall strength.

The SSB coke with Dust size 63 has a similar dilation profile (as with Dust size 45); however both the initial expansion at 110 °C and the expansion at 350 °C are lower, although it reached the highest shrinkage of all cokes for this dust size. The lower expansion is considered to be due to the larger surface area of the particles and thus a thinner binder layer with lower adhesion strength. The SSA coke initially expanded more at 160 °C for this size fraction after a significant residual stress release at 70 °C. The higher expansion is caused by a denser structure with a higher volume of trapped volatiles in the voids and pores. The SSC coke with Dust size 63 has nearly identical initial expansion (110 °C) as with Dust size 45, however the whole thermal dilation profile is higher. Dust size 63 produced the best composition with 15 % pitch content, considering green apparent densities for both SSA and SSC.

The finest dust size of 94 % below 63 µm changed the thermal dilation profile of the SSB coke dramatically. The secondary expansion at about 350 °C (also observed with Dust size 45 and Dust size 63) was diminished and the sample shrunk extensively from 500 to 950 °C. For this composition visible cracks were observed at the periphery. The paste became under-pitched with Dust 94 and thus no significant expansion occurred because of a limited amount of trapped volatiles in the voids and pores. The highest initial expansion is observed for the SSC coke at about the same temperature (160 °C) as measured with Dust size 63. The higher thermal dilation might be caused by more trapped volatiles in a denser structure when the finest dust size is applied. However, the SSA coke does not have a large initial expansion, but instead three subsequent peaks from about 70 to 190 °C. The highest shrinkage was found for the SSB coke, while the lowest for the SSC coke.

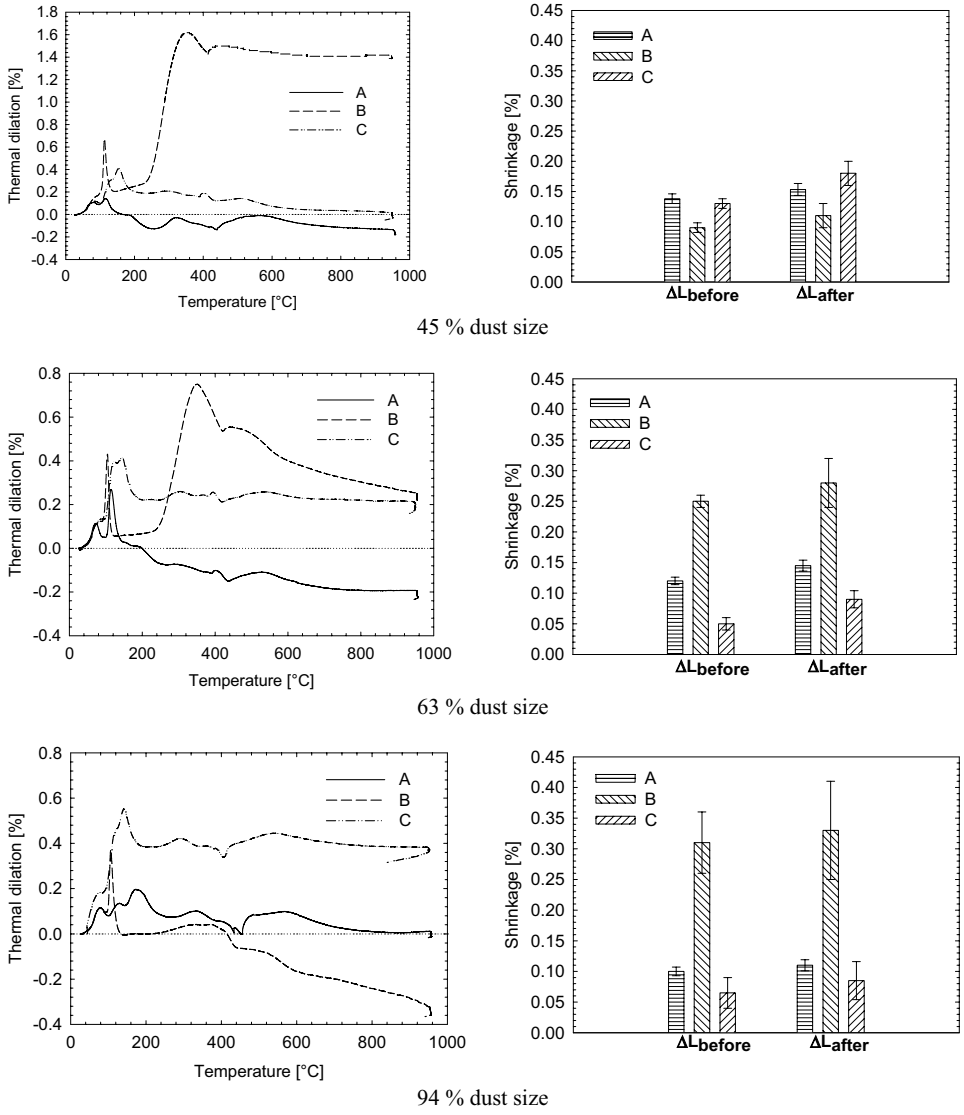

Figure 6.8 Thermal dilation of single source A, B and C coke with 15 % pitch and 45, 63 and 94 % dust size.

Figure 6.9 presents four graphs where the first three (SSA, SSB and SSC) are plotted correlations between the dust size and the residual sample dilation. Residual sample dilation is defined as the thermal dilation after the initial expansion when the height flattens out. The fourth graph presents the green apparent densities for each coke and dust size, and indicates that 15 % pitch is optimum for SSB coke with Dust 45, while the optimum for SSA and SSC cokes with 15 % pitch is Dust 63.

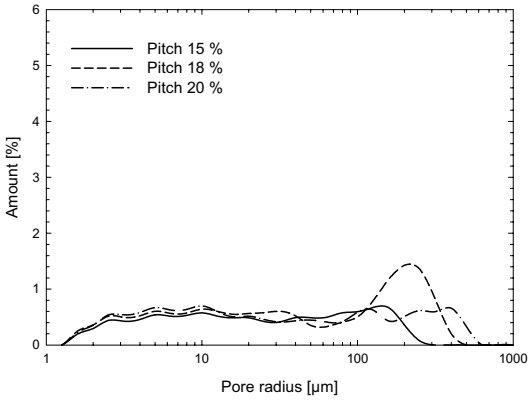

45 % dust and different pitch contents

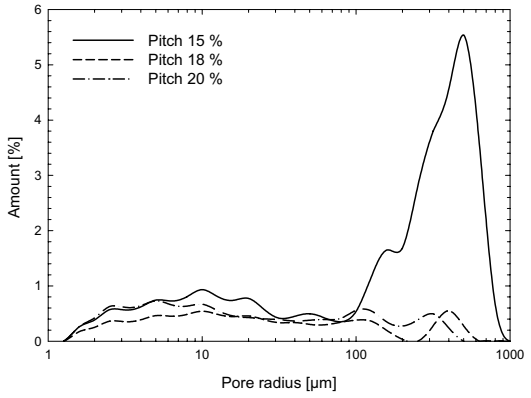

63 % dust and different pitch contents

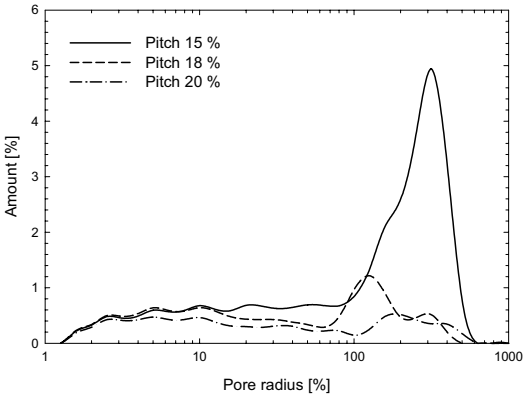

94 % dust and different pitch contents

Figure 6.13 Pore size distribution of the samples with 45, 63 and 95 % dust size and 15, 18 and 20 % pitch contents (Single source A).

6.1.4 Discussion

The green apparent density results showed that single source B coke exhibited the lowest values. The finer dust size contributed to the increase of the green density. A pitch content of 18 % produced the highest densities at each dust size. Single source coke B was mechanically weakest among the investigated cokes, thus during the mixing and paste preparation an excess of fines were generated as large particles were crushed, which negatively contribute to the density. Single source A and C coke reached the highest densities with dust size 45 %. Dust size 63 and 94 had the highest densities with coke A and the blended coke.

The thermal dilation method results showed the effect of dust size and pitch content. The results at the pitch content of 18 and 20 % indicate significant sample slumping after initial expansion (about 170 °C). However, the SSB coke does not show this slumping at 18 % pitch content, due to an excess of fines (surface area) generated during the mixing. Additionally, SSB had the highest porosity. The preheating treatment should be considered for the samples with 18 and 20 % pitch content in order to avoid the slumping.

The newly defined term “residual sample dilation” showed a good correlation with the dust size for each coke. However, the SSB coke had an opposite trend than SSA and SSC coke. Also, shrinkage of the SSB coke increases with the dust size while it decreases for SSA and SSC coke. Crack formation on the surface of SSB samples was observed after the thermal dilation investigation. The most probable reason why the SSB coke had an opposite trend is the excess of fines and the lack of large coke grains due to crushing during the mixing, thus a binder deficit resulting in reduced overall strength and crack formation.

Thermal dilation analysis can contribute to the following conclusions:

- Final degree of anode shrinkage
- The pitch content level
- Residual sample dilation can indicate the dust size
- Porosity development
- Crack formation on the surface by visual observation after the testing
- Heating rate optimisation

The image analysis of green anodes showed possibilities to analyse the degree of porosity in the sample. The pitch content and proportion of fine dust can be visualised and quantified. This technique can contribute to a better control of the paste quality.

6.2 Characterisation of baked anodes

6.2.1 The baking process

All green anodes were baked with the same heating rate. The anodes were first heated to 550 °C with a heating rate of 20 °C/h, then to 1100 °C at 100 °C/h. Three hours soaking time at 1100 °C was applied. The anodes were then cooled to room temperature. Figure 6.14 shows the baking temperature profile versus time.

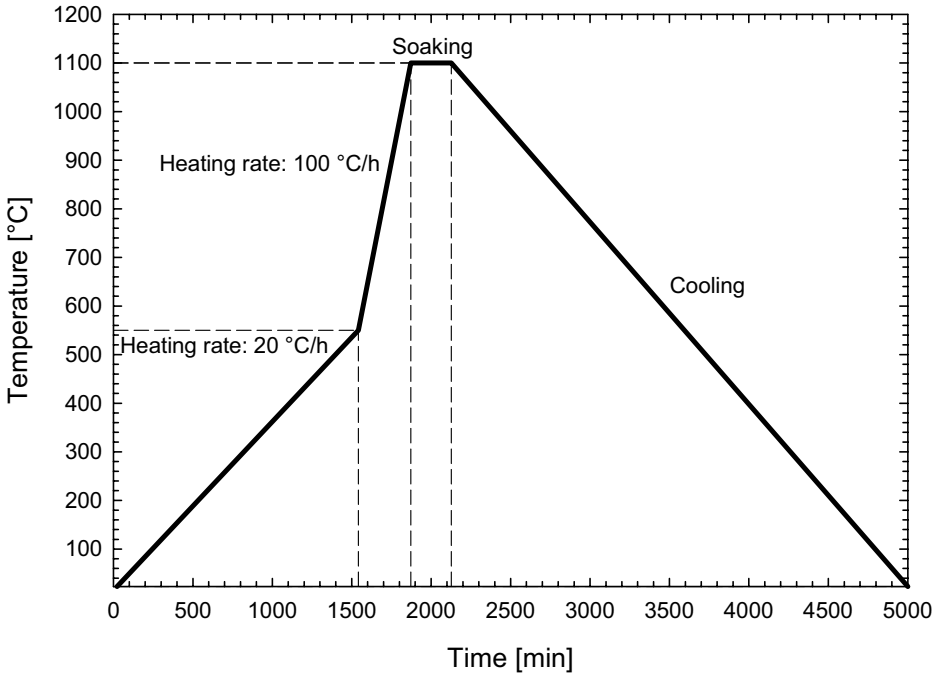

Figure 6.14 Anode baking temperature versus time.

Four pilot anodes were baked simultaneously. They were placed two by two in metal containers and packed with coke. The coke had a particle size from 5.0 to 15.0 mm. The containers were placed on top of each other and positioned in the centre of the oven.

A reference coke was used for determination of the mean crystallite size (L_c) according to ASTM D 5187-91 to verify even baking level (the combined effect of temperature and time) for the pilot anodes. This method determines the mean crystallite thickness of a representative, pulverised sample of calcined petroleum coke by interpretation of an X-ray diffraction pattern.

Figure 6.15 shows the results of these experiments. Four reference petroleum coke samples were placed in small holders with a lid and inserted into each anode. The results show that there are only small differences between the L_c values of the samples

from the top and the bottom. In other words, it can be concluded that all four anodes were baked at nearly identical conditions (temperature/time).

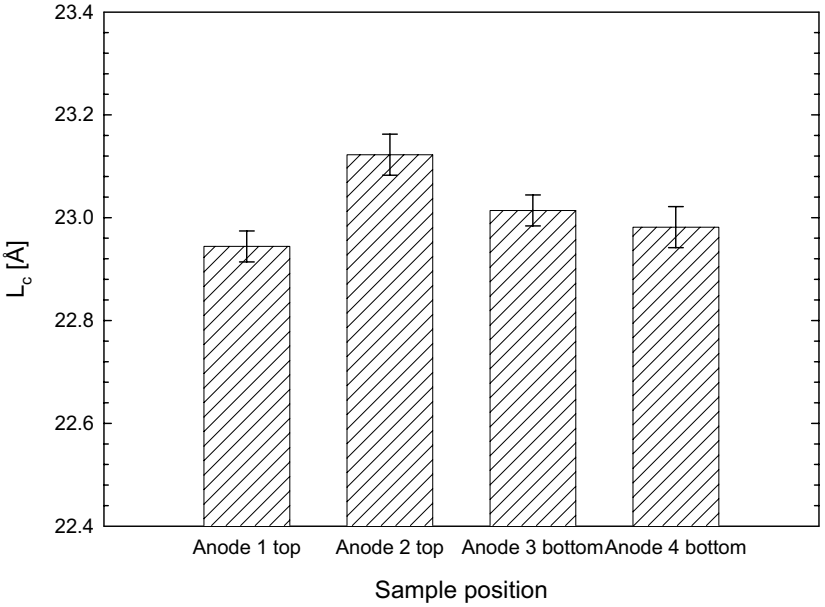

Figure 6.15 Crystallite size (L_c) of the reference coke baked together with anodes in different oven positions.

Figure 6.16 presents a photograph of the baked anodes. The baked anodes were cleaned by removing the packing coke and the dimensions were measured for determination of the baked apparent densities.

Figure 6.16 Photograph of the baked anodes.

6.2.2 Properties of baked anodes

All baked anodes were sampled and the following parameters were measured and presented in Table 6.2.1:

- Baked apparent density
- Specific electrical resistance
- Air permeability
- Modulus of elasticity
- Air and CO_2 reactivity

Baked apparent density was measured for each anode and the Figure 6.17 shows the average value of two samples with the calculated standard deviation. The specific electrical resistance was measured according to the ISO 11713, with analytical equipment from R&D Carbon. Core samples of 50 mm diameter and length 100 mm were measured 4 times (4 times around the sample periphery with 45° shifts). The modulus of elasticity was measured according to the ASTM C1198 standard. The measurement of CO_2 and air reactivity was performed by the thermogravimetric method at the Hydro Årdal laboratory.

Figure 6.17 presents the results of baked apparent density measurements of anodes with 45, 63 and 94 % dust size. Both the green and the baked densities are low and an unfortunate scatter in the data is noted. The anode paste was mixed in the sigma mixer, thus an uncontrollable aggregate crushing probably plays an important role. A large reduction in density during baking was observed; on the average the density is reduced by 0.096 g/cm^3. A coarse inspection of the data shows that the density reduction largely increases with increasing pitch content at each dust size, thus indicating that samples with 15 % pitch are slightly underpitched, and slightly overpitched at 20 %. The highest densities were measured for single source coke A, while the lowest were found for

single source coke B, which also is the mechanically weakest coke. This is surprising, as full scale anodes produced from cokes A and B show approximately the same density values.

The highest values of baked apparent densities were achieved with about 18 % pitch content for each investigated coke type and this is probably close to the optimum pitch content. The results for samples with 45, 63 and 94 % dust size were investigated. The increase of dust size to 63 % contributed to higher baked apparent densities for each coke type and pitch content. There is a significant increase of density for coke A and the blended coke for a pitch content from 15 to 18 %. However, coke B and C have only a slight increase in density in this pitch content range. The highest dust size (94 %) had a negative influence on the baked densities, especially for the blend coke.

The air permeability (Figure 6.19) is a factor of more than 10 higher than usually found for full scale anodes. Although low densities, the permeability is unrealistically high and probably due to erroneous measurements. A correlation between baked density and permeability is generally expected, but can not be found here. Neither is a reduction in permeability observed with increasing fineness of the fines fraction. The specific electrical resistance (Figure 6.18) is high, but not unusual for laboratory made anodes. No correlation is found, however, with experimental variables. Reactivities (CO_2 and air) do not correlate with the corresponding reactivities of the pure cokes or the experimental conditions.

Table 6.2.1 Properties of green and baked anodes.

Coke [type]	Dust size [% of -63 µm]	Pitch [%]	Green app.density [kg/dm^3]	Stdv	Baked app. density [kg/dm^3]	stdv	Air permeability [nPm]	stdv	Spec el. res [µΩm]	stdv	E modul [GPa]	CO_2 reactivity [mg/cm^{2}h]	air reactivity [mg/cm^{2}h]	Soot index [%]	Shrinkage, ΔL_{after} [%]
SSA	45	15	1.514	0.012	1.45	0.012	14.5	0.8	77.3375	1.9	5.2	20.1	28.2	18.4	0.1533
SSA	45	18	1.562	0.01	1.47	0.01	6.21	0.3	72.56	1.5	5.9	23.4	25.7	26	0.02
SSA	45	20	1.554	0.014	1.43	0.014	8.2	0.5	72.9	1.55	5.9	32.9	-	33.3	0.13
SSB	45	15	1.424	0.015	1.35	0.015	10.35	0.74	66.8	1.68	6.6	30.8	45.7	24.9	0.11
SSB	45	18	1.463	0.01	1.36	0.01	5.86	0.31	65.325	1.2	6.5	26.8	38.4	19.1	0.14
SSB	45	20	1.449	0.012	1.33	0.012	7.98	0.38	65.9	1.48	6.9	27.2	29	26.9	0.06
SSC	45	15	1.47	0.016	1.39	0.016	8.5	0.58	69.5	1.53	6.9	13.7	49.2	4.9	0.18
SSC	45	18	1.521	0.011	1.43	0.011	6.945	0.31	66.67	1.13	6.7	15	53.4	5.7	0.04
SSC	45	20	1.489	0.013	1.41	0.013	10.3	0.75	67.5	1.25	6.1	13.8	46.4	3.3	0.05
Blend	45	15	1.44	0.011	1.38	0.011	14.9	0.89	79.5	1.49	5.6	17.1	27.4	8.2	-
Blend	45	18	1.5	0.009	1.41	0.009	8.1	0.45	67.9	1.36	5.7	18.8	26.3	8.8	-
Blend	45	20	1.483	0.012	1.38	0.012	9.35	0.78	68.9	1.41	4.7	16.9	27.4	5.8	-
SSA	63	15	1.508	0.009	1.395	0.009	12.9	0.71	86.175	1.37	4.1	21.4	29.5	23	0.15
SSA	63	18	1.599	0.004	1.489	0.004	8.1	0.48	76.66	1.27	5.1	22.3	30.5	18.4	0.05
SSA	63	20	1.581	0.005	1.45	0.005	9.8	0.52	76.85	1.31	5.4	31.3	35.7	31.2	0.1
SSB	63	15	1.421	0.008	1.374	0.008	9.9	0.62	65.28	1.21	6.8	24.9	40.6	22.6	0.33
SSB	63	18	1.472	0.006	1.4	0.006	6.93	0.39	64.5	1.19	6.7	24.3	44.9	19.7	0.1
SSB	63	20	1.451	0.007	1.378	0.007	8.9	0.47	66	1.22	6.5	24.9	44.8	21.2	0.19
SSC	63	15	1.458	0.006	1.39	0.006	7.89	0.42	69.1	1.28	6.8	15.8	44.3	7.2	0.09
SSC	63	18	1.548	0.004	1.42	0.004	6.945	0.35	65.7	1.2	6.6	13.2	50.3	3.9	0.09
SSC	63	20	1.517	0.006	1.395	0.006	10.9	0.62	68.5	1.29	6	12.1	45.5	5.5	0.038
Blend	63	15	1.508	0.005	1.42	0.005	14.1	0.79	73.8	1.255	6.1	16.5	30.7	9.3	-
Blend	63	18	1.601	0.004	1.5	0.004	7.99	0.51	66.9	1.18	6	20.8	32	13.8	-
Blend	63	20	1.591	0.005	1.481	0.005	10.2	0.68	68	1.205	5.5	20.6	34.4	12.4	-
SSA	94	15	1.515	0.01	1.429	0.01	10.1	0.78	79.5	1.29	5.5	15.5	26.2	15	0.11
SSA	94	18	1.583	0.005	1.493	0.005	8.705	0.52	74.9	1.22	4.8	20.2	32.3	32.3	0.14
SSA	94	20	1.576	0.006	1.47	0.006	9.5	0.59	77.6	1.23	4.4	30	-	31.8	0.37
SSB	94	15	1.418	0.01	1.345	0.01	14.1	0.82	71.8	1.266	6.1	27.4	35.6	19.5	0.28
SSB	94	18	1.485	0.008	1.378	0.008	9.9	0.51	67.5	1.255	5.5	17.9	33.7	9	0.11
SSB	94	20	1.471	0.01	1.356	0.01	10.8	0.74	68.4	1.259	5.3	25	42.4	20.6	0.03
SSC	94	15	1.5	0.009	1.41	0.009	8.2	0.69	66.66	1.15	6.3	15.5	NA	7.1	0.085
SSC	94	18	1.571	0.005	1.44	0.005	7.495	0.49	64.78	1.12	6.5	17.3	42.7	6.4	0.208
SSC	94	20	1.544	0.006	1.42	0.006	10.9	0.74	65.8	1.14	6	16.2	49.3	3.6	0.085
Blend	94	15	1.498	0.008	1.405	0.008	10.65	0.79	70.5	1.169	6.1	20.3	29.4	10.4	-
Blend	94	18	1.585	0.004	1.499	0.004	7.3	0.47	65.4	1.12	5.8	26.4	24.2	12.5	-
Blend	94	20	1.589	0.006	1.475	0.006	9.8	0.59	66.4	1.145	5.3	37.1	30.9	25.1	-

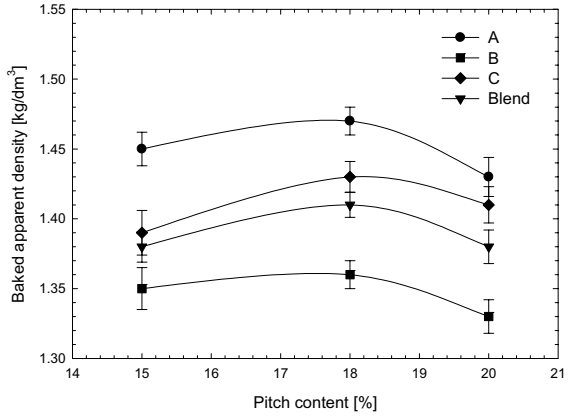

Dust size 45 %

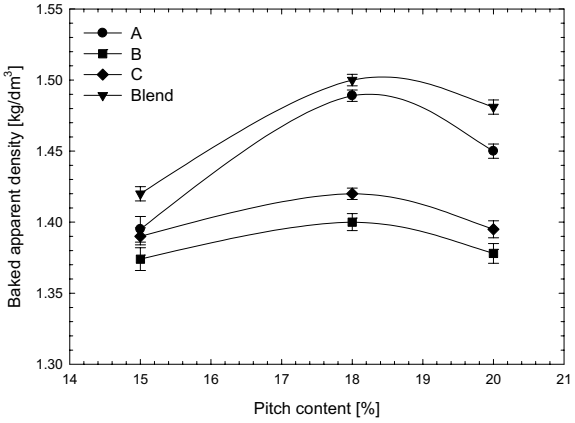

Dust size 63 %

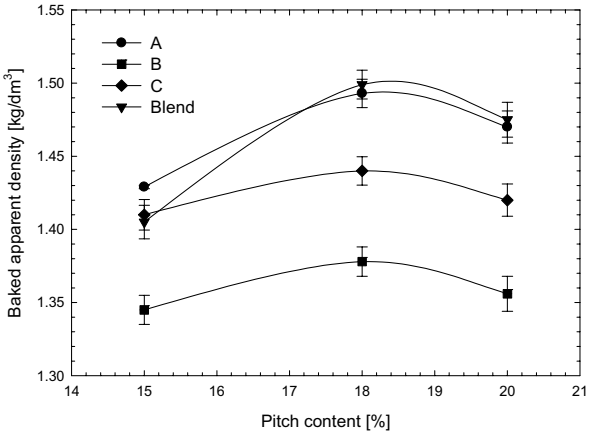

Dust size 94 %

Figure 6.17 Baked apparent density of anodes with 45, 63 and 94 % dust size.

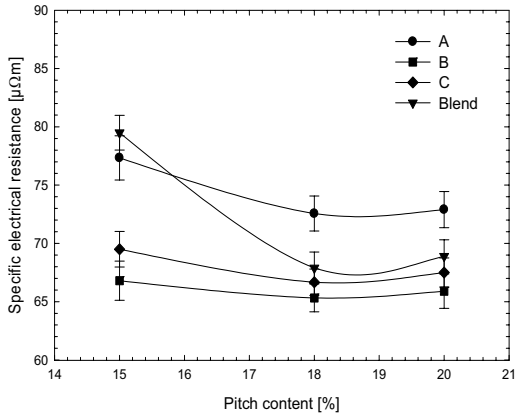

Dust size 45 %

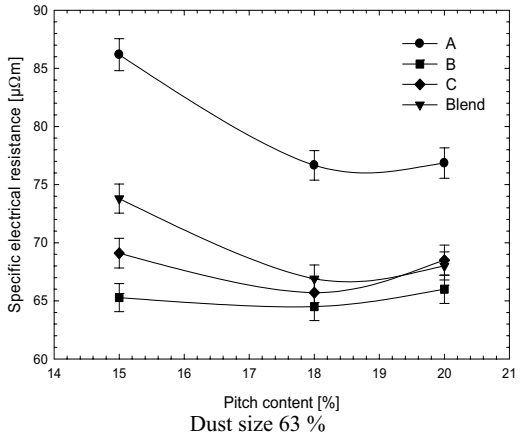

Dust size 63 %

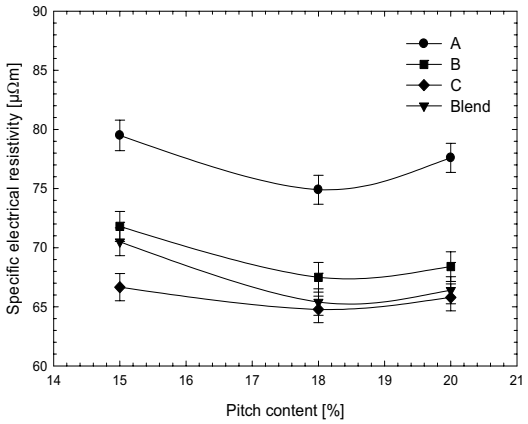

Dust size 94 %

Figure 6.18 Specific electrical resistance for anodes with 45, 63 and 94 % dust size.

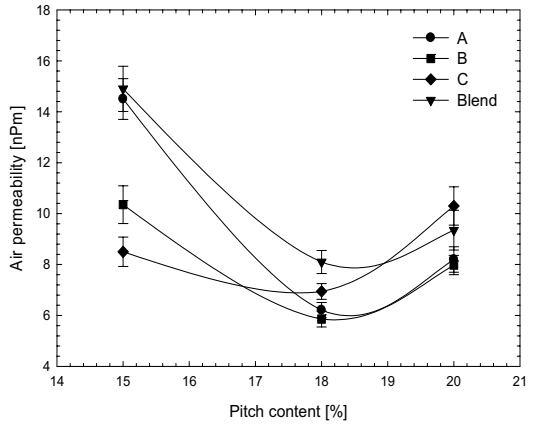

Dust size 45 %

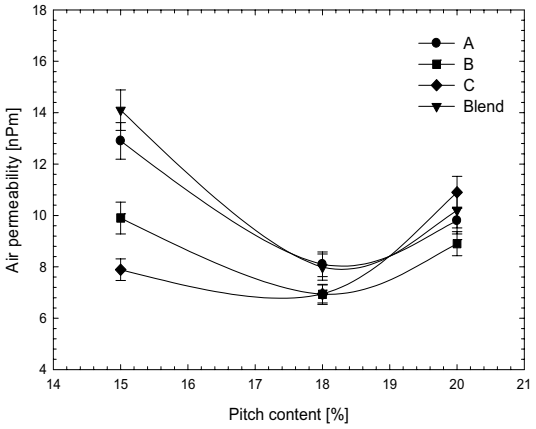

Dust size 63 %

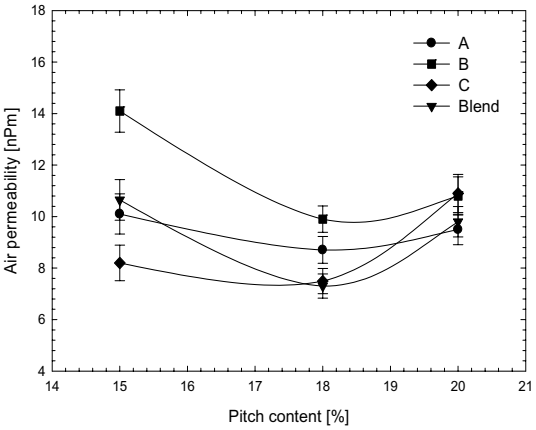

Dust size 94 %

Figure 6.19 Air permeability for samples with 45, 63 and 94 % dust size.

6. Concluding remarks

The ability to analyse the mechanical strength of the coke in the entire size range by the drop test gives a great advantage compared to other conventional methods in finding the size fractions which are suitable for grinding and/or just mixing directly in to the paste. The differences in the mechanical strength of cokes are significant and selective treatment of the coke from the initial state will contribute to a more stable and predictable anode production. The correlation between the drop test results and specific grinding energy can help provide a better understanding and control of the grinding circuit. The fine particles (below 148 μm) produced during the drop test indicates the necessity of additional pitch requirements to account for the generation of excess fines. Further improvement and optimisation of this method is recommended.

Better understanding and control of the grinding circuit, and thus production of the finest fraction, dust, can greatly contribute to the production stability, and consequently increase the grinding circuit capacity. Control of the sweeping speed and mill filling can affect the proportion of the finest particles in the product as well as the capacity. Implementation of on-line particle size control with subsequent regulation of the product size via an air classifier can considerably improve the product size stability, which will constantly produce a precise recipe for anode production. The particle shape of the dust varies according to the coke type and residence time in the ball mill. This factor can influence the ability of the paste to flow during forming and baking. It is recommended to investigate further the influence of the roundness factor on the anode properties.

Further development and improvement of the interpretation of results from the dilatometer showed the possibility to better characterise green anodes. Optimisation of the method found that there was a dependency on the sampling position, the effect of the heating rate and the influence of the packing material. Characterisation of green anodes by image analysis and a dilatometer showed possibilities for characterisation and quantification of anode properties, as for example; amount of dust, pitch content, porosity (green and baked state), shrinkage and baked density. It is recommended to continue with the work to characterise green anodes by the thermal dilation method.

This work contributed to a development of a new type of dilatometer which uses image analysis for the detection of the thermal dilation. The new dilatometer requires no correction/calibration, can measure thermal dilation in three dimensions, better control of the inert atmosphere, possibility to apply vacuum or toxic gases and better control of PAH removal.

The results showed that the shrinkage, dust size and pitch content could be analysed. The residual dilation expansion showed a very good correlation with the dust size. The measured differences in particle roundness of the dust could affect the flow ability of the paste during heating.

References

Akthtar R.J., Rabba S.A., Meier M.W., "Dynamic process optimisation in paste plant", Light metals 2006, p. 571 – 575

Allen T., "Particle size measurement, Volume 1, Powder sampling and particle size measurement", Chapman & Hall, ISBN 0412729504

Allen T., "Particle size measurement, Volume 2, Surface area and pore size distribution", Kluwer academic publishers, ISBN 0412753308

ASTM D5003-95, Standard Test Method for The Hardgrove Grindability Index (HGI) of Petroleum Coke, 1995

ASTM D5187-91 (2002) "Standard Test Method for Determination of Crystallite Size (Lc of Calcined Petroleum Coke by X-Ray Diffraction".

Aune F., Rørvik S., Støre A., "Pilot anodes: Optimum pitch content and mixing study", Technical report NTNU 1996, IUK-96-25

Austin L. G., Klimpel R. R., Luckie P. T., "Process Engineering of Size reduction: Ball Milling", 1984 American Institute of Mining, Metallurgical, and Petroleum Engineers, Inc.

Belitskus D., "Effects of butts content, green scrap, and used potlining additions on bench prebaked anode properties", Light metals 1980, p. 431-442

Bumiller M., Carson J., Prescott J., "A preliminary investigation concerning the effect of particle shape on a powder flow properties". Malvern Instruments, 2005

Carneiro R., Fong M.C. De Bango E.," Anodes made with 86 % butts", Light metals 1985, p. 935-955

Carter C. M., "An alternative ball mill feed controller", Light Metals 1979, p. 635-645

Chmelar J. & Sandvik, K.L., "Optimising dry autogenous grinding compared to conventional wet grinding", 10th European Symposium on Comminution, September 2002, Heidelberg, Germany

Chmelar J., Sandvik K.L., "A comparison of wet and dry autogenous grinding", International Mineral Processing Symposium, Mineral Processing on the verge of the 21st Century, Antalya 2000, Turkey, p. 35-39

Chmelar J., "Advanced fine particles processing and process optimisation", Nordisk Mineralsymposium 2001, Trondheim, Norway

Chmelar J., Bergstrøm T., Hellevik L.R., Laux H., Kolacz. J. "Improvement of the air classifier performance based on experiments and CFD simulations", Comminution 2004, Perth, Australia

Chmelar J., Breivik T., "Process control of an air swept ball mill circuit and jet mill using an on-line particle size analyser", Mineral Processing Conference, 2004, Luleå

Chmelar J., Foosnæs T., Øye H. A., "Thermal dilation of green anodes during baking", TMS 2006, p. 597 – 602

Chmelar J., Foosnæs T., Øye H. A., Sandvik K.L., "Coke quality effect on the grinding in an air swept ball mill circuit". Light Metals TMS 2005, p. 647-652

Dell M.B., Peterson R.W., "Dilatometry of pitch-anthracite mixes for carbon". Metallurgical Transaction, Volume 4 1973, p. 2077-2080

Dreyer C., Jouault C., Pinoncely A., Andre J.F., "The new AP-FCBA paste plant technology", Light metals 2003, p. 547 – 553

Edwards L., Vogt F., Wilson J., “Coke blending at Anglesey aluminium”, Light metals 2001, p. 689 – 694
Engvoll M.A., “Reactivity of anode raw materials and anodes for production of aluminium”, PhD thesis 2001, ISBN 8247153882
Fernandez R., “Petroleum coke, grades and production”, CarboMat seminar Trondheim 2003
Fernandez R., Meisingset H.C., Balchen J.G., “Mathematical Modelling of a rotary hearth calciner”, Light metals 1996, p. 491 – 497
Fishbane P.M., Gasiorowicz S., Thornton S.T., “Physics for scientist and engineers”, Prentice-Hall 1996, ISBN 0132311763
Fisher W.K., Keller F., Perruchoud C.R., “ Interdependence between anode net consumption and pot design, pot operating parameters and anode properties”, Light metals 1991, p. 681 – 686
Fisher W.K., Perruchoud C.R., “Bench scale evaluation of the mechanical and chemical behaviour of coke in anode manufacturing”, RDC Internal publication 1992
Fitzer E., Huettinger K.J., Megalopoulos A., “Dilatometric study of the baking behaviour of pitch bonded carbon artifacts”. Carbon 1973, p. 621-626
Foosnæs T., Naterstad T., in “Introduction to aluminium electrolysis”. Second edition, Grjotheim K., Kvande H., Editors, Aluminium Verlag, ISBN 3-87017-233-9, p. 87-138
Foosnæs, T., Kulset, N., Linga, H., Næumann, G.R., Werge-Olsen, A., “Measurements and Control of the Calcining Level in Anode Baking Furnaces”, Light Metals 1995, p. 649-652.
Franca G., Mesquita C., Edwards L., Vogt F., “Anode quality improvements at the Valesul smelter”, Light metals 2003, p. 535 – 538
Grjotheim K., Kvande H., “Introduction to aluminium electrlysis”, Aluminium verlag 1993, ISBN 3870172339
Hulse K.L., “Anode manufacture: Raw materials formulation and processing parameters”, PhD thesis 2000, ISBN 3952102857
Hulse K.L., Perruchoud R.C., Fischer W.K., Welch B.J., “Process adaptation for finer dust formulations: mixing and forming”, Light metals 2000, p. 467 – 472
Hume S.M., “Anode reactivity: Influence of raw material properties”, PhD thesis 1993, ISBN 3952102822
Hume S.M., Fisher W.K., Perruchoud C.R., “A model for petroleum coke reactivity”, Light metals 1993, p. 525 – 534
ISO 10142, “Determination of grain stability using a laboratory vibration mill”. 1996
ISO 14428, “Expansion and shrinkage during baking”, 2005
Jacobsen M., Log T., “Thermal conductivity of green carbon materials during baking”, Light metals 1995, p. 673 – 679
Johnson R., “Elementary statistics”, Duxburry Press 1992, ISBN 053492980X
Kolacz J., “Improving the fine grinding process in an air swept ball mill circuit”, PhD thesis, NTH 1995, ISBN 8271198572
Lavoie C., Bergeron E., “ALCAN ALMA new anode paste plant start-up and early operation”, Light metals 2003, p. 555 – 560
Letizia I., Calderone F., “Linear dimensional changes occurring during the baking of pitch-bonded green carbon bodies”. Carbon 1980, p. 297-301

Lossius L.P., “Vibration press manual with description and test results”, NTNU Report IUK-95-50, 1995
Lossius L.P., Holden I., Linga H., “The equivalent temperature method for measuring the baking level of anodes”, Light metals 2006, p. 609 – 613
Madshus S., “Thermal reactivity and structure of carbonized binder pitches”, Doctoral thesis at NTNU, ISBN 8247170418
Malvern Instruments, Technical manuals to on-line particle size analyser INSITEC, 1997
Marsh H., Heintz E.A., Reinoso F.R., “Introduction to carbon technologies”, Published by the University of Alicante 1997, ISBN 8479083174
Martirena H., “Laboratory studies on mixing, forming and calcining bodies”. Light metals TMS 1983, p. 749-764
Molin A., Pinoncely A., Andre J.F., Morfoise J., “Anodes plant – the next step”, Light metals 2006, p. 565 – 570
Narvekar R.N., Sardesai A., Prasad A.B., “Importance of granulometry in calcined petroleum coke”, Light metals 2003, p. 525 – 530
National Instruments, LabView manual, 2004, Available from Internet: http://www.ni.com
Nordberg, “Nordberg grinding mills, ball, rod an pebble”, Technical specification of grinding mills, 1970
Øye H.A., “Control of anode consumption during aluminium electrolysis”, Kluwer Academic Publishers 1991, p. 573 – 593
Ozkahraman H.T., “A meaningful expression between bond work index, grindability index and friability value”, Minerlas Engineering 18, 2005, p. 1057 – 1059
Perruchoud C.R., Fisher W.K., “Granular carbon mechanical properties: their measurement and influence on paste production”, Light metals, p. 695 – 700
Perruchoud R.C., Meier M.W., Fischer W.K., “Coke characterisation from the refiners to the smelters”, Light metals 2000, p. 459 – 465
Perry R.H., Chilton C.H., “Chemical engineering handbook”, McGraw-Hill 1973, ISBN 0070494789
Pharma Vision Systems, “System Manager’s Manual, BeadCheck 830”, Version 4, 2003
Proulx A.L., “Optimum content for prebaked anodes”, Light metals 1993, p. 657 – 661
Rørvik S., Lossius L.P., Øye H.A., ”Classification of pores in prebaked anodes using automated optical microscopy”, Light metals 2003, p. 531 – 535
Rørvik S., Øye H.A., Sørlie M., “Characterisation of porosity in cokes by image analysis”. TMS 2001, p. 603-609
Rørvik S., Ratvik A.P., Foosnæs T., “Characterisation of green anode materials by image analysis”, Light metals 2006, p. 553 – 558
Sandvik K. L., Digre, M., Malvik, T., “Oppredning av primære og sekundære råstoffer”, Tapir 1999 (in Norwegian)
Schneider J.P., Coste B., “Thermal shock of anodes: influences of raw materials and manufacturing parameters”, Light metals 1993, p. 611 – 619
Sigma mixer technical manual, 1991
Sinclair K.A., Sadler B.A., “Improving carbon plant operations through the better use of data”, Light metals 2006, p. 577 – 582

Smith M. A., Perruchoud R. C., Fisher W. K., “An evaluation of the effect of dust granulometry on the properties of binder matrix bench scale electrodes”, Light Metals 1991, p. 651 – 656.

Smith M.A., Perruchoud C.R., Fisher W.K., Welch B.J., “An evaluation of the effect of dust granulometry on the properties of binder matrix bench scale electrodes”, Light metals 1991, p. 651 – 656

Sørgård W., “Crushing resistance and crushability index of coke particles”, technical report, NTNU 1995, IUK 95-29

Taylor R.E., Ho C.Y., “Thermal expansion of solids”, Sindas data series on material properties 2003, ISBN 0871706237

Uhl V.W., Gray J.B., “Mixing, theory and practise”, Volume 2, Academic press 1967, ISBN 0127066020

Vogt F., Tonti R., Hunt M., Edwards L., A preview of anode coke quality”, Light metals 2004, p. 489 – 493

Wright K.B., Peterson R.W., “Pitch content optimisation model for anode mixes”, Light metals 1989, p. 479 – 488

Appendix

Light Metals 2005 *Edited by Halvor Kvande* ***TMS (The Minerals, Metals & Materials Society), 2005***

COKE QUALITY EFFECT ON THE GRINDING IN AN AIR SWEPT BALL MILL CIRCUIT

Juraj Chmelar[1*], Trygve Foosnæs[2], Harald A. Øye [2], Knut L. Sandvik[3]

[1] SINTEF Materials and Chemistry, NO-7465 Trondheim, Norway
[2] Norwegian University of Science and Technology, Department of Materials Technology, NO-7491 Trondheim Norway
[3] Norwegian University of Science and Technology, Department of Geology and Mineral Resources Engineering, NO-7465 Trondheim Norway

Keywords: "Petrol Coke, Fines, Grinding, Characterisation."

Abstract

Petroleum coke fines have been produced under varying operating conditions from four petrol coke qualities in an air swept computer controlled ball mill circuit with an online particle size analyzer. The aim of the work is to show how the coke quality influences the grinding process and the product quality. Enhanced awareness on the paste plant's ball mill operation and control is increasingly important in a petrol coke market characterized by scarcity of stable single source coke qualities. The use of coke blends (up to 20 sources in one cargo) is common.

The paper presents results obtained from the fines production with the following variables; different product size, air sweeping velocity/particle residence time in the mill, circulating load, mill throughput and specific energy consumption. The circulating load and air sweeping velocity/particle residence time has a critical effect on the particle size distribution steepness although the same top size product is produced.

Morphology analyses show that the product particle shape depends on the process control and the energy used for fines production.

Introduction

Due to the petrol coke supply situation multiple source blend cokes today often have to be used. Although specifications on sulfur and trace elements are met by blending, cokes with different chemical and mechanical properties have to be used. The challenge of the anode producer is thus to produce consistent quality anodes from a raw material that requires specialized paste plant operation. The fines for anode production are produced by ball mill grinding. Variation of the fines content and composition may cause anode quality fluctuations; hence control of the grinding process is of critical importance for the production of stable quality anodes. This study demonstrates how the ball mill circuit control can affect the product particle size distribution. Four different petrol cokes were investigated; one blended and three single source cokes. Each coke was ground under varying settings of the ball mill circuit controls. The products were analysed with respect to particle size, particle morphology and Blaine number. There are clear differences between the products due to their origins and processing conditions.

Experimental

All coke feed materials were prior to grinding sieved into several size fractions. The finest fraction, 0-2 mm, was the feed material to the ball mill.

Air Swept Ball Mill

The grinding experiments were carried out in a pilot scale air swept ball mill circuit at the laboratories of SINTEF Materials and Chemistry. The ball mill is rubber lined and equipped with lifters, has an internal diameter 0.56 m and a length of 0.8 m. The nominal power of the mill is about 3.5 kW. The mill is filled with steel balls (about 45 vol %) of different sizes (1/3 of 24 mm, 1/3 of 18 mm and 1/3 of 11 mm diameter). The particle size distribution of the balls was regularly checked and the necessary amount of new balls was added. The rotational speed of the mill is adjustable with a frequency inverter.

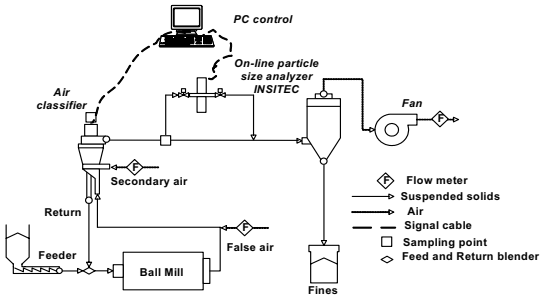

Figure 1. Air swept ball mill circuit with integrated air classifier and on-line particle size analyzer.

The flow sheet of the mill circuit, together with operating parameters to be controlled, is shown in Figure 1. A variable screw feeder supplies fresh feed coke to the ball mill. The ground product is pneumatically transported to the forced vortex air classifier. The material is classified into two size fractions, above and below a specified particle size. The cut size is adjusted by the air flow rate through the classifier and the classifiers rotational speed. Oversize material from the air classifier is returned to the mill via a mass flow meter, which measures the circulating load in the system.

The airflow rate of the classifier is adjusted by the speed of the fan. For improved classification efficiency the classifier is supplied with an additional air stream (secondary air) to clean the coarse material of the fines. The fines from the classifier are separated from the air in a filter. The filtered air enters the driving fan and is vented to atmosphere. Compressed air is periodically blown back through the filter cartridges to remove the filter dust.

The torque of the rotating shaft driving the ball mill is measured to determine the grinding power and energy. It is measured by

cradling the source (motor with chain transmission) and measuring the force of deflection. To determine the ball mill charge the mill unit is placed on a weighing platform, which directly measures the total mill weight. The fan creates the under pressure in the system for pneumatic material transport. The sweeping speed of the air in the mill is adjusted by the fan speed and/or by a false air valve. The change of the valve position does not affect the airflow through the air classifier and filter, only the sweeping speed inside the mill.

Figure 2 shows the inside of the mill towards the discharge grate. There are large steel balls on top with the coke material around. The lining and rubber lifters can also be seen.

Figure 2. Picture showing the inside of the mill.

Figure 3 presents an outline of the air classifier in the ball mill circuit. The material is introduced from the bottom of the classifier, through a vertical pipe directed at the lower section of the rotor. An inverted cone is attached to the mouth of this pipe for distributing the sample to the periphery of the rotor.

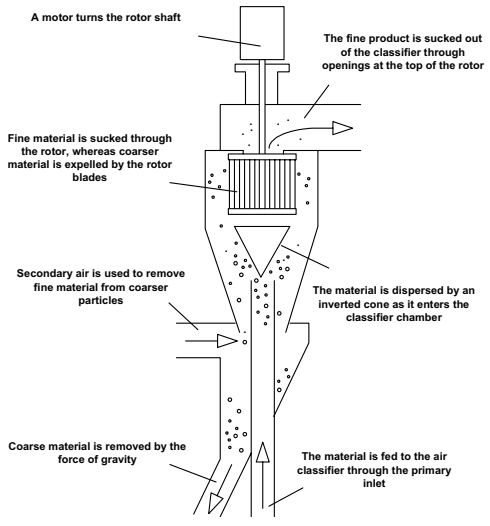

Figure 3. Overview of the air classifier.

The fine particles entering the rotor leave the classifier through the top outlet by the under-pressure applied to the classifier. The coarse particles follow the centrifugal and gravitational force and fall down to the bottom part through a conical section around the feed inlet. Before leaving this chamber, a secondary air inlet at the bottom part provides a rotating turbulent air current for rinsing this coarse product. Thus, fine particles entrapped or attached to the coarse material are re-introduced to the rotor area. The amount and proportion of the secondary air is adjustable by an external vane.

On-line Particle Size Control

In order to control the product particle size in the ball mill circuit an on-line particle size analyzer unit was installed (INSITEC, supplied by Malvern). The measuring principle is laser diffraction. Figure 4 shows INSITEC's general system layout.

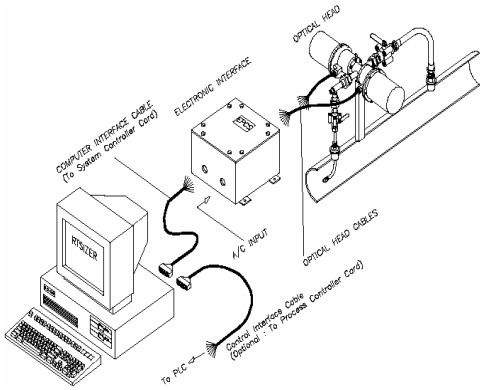

Figure 4. On-line particle size analyzer INSITEC (source: Malvern technical manual).

The stainless steel sampling flute shown in Figure 5 was installed at the air classifier outlet. The position was chosen after several sampling tests in order to ensure laminar flow and even material concentration at the sampling point. The sample is continuously transported from the process line into the analyzer and then returned to the system. Samples can be collected and analyzed up to 4 times per second.

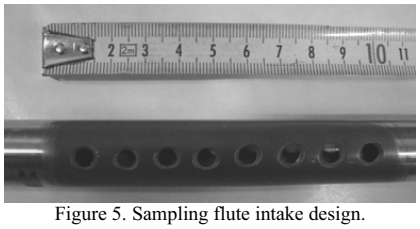

Figure 5. Sampling flute intake design.

The grinding circuit is PC controlled. The control program (LabView 6.1) communicates with the INSITEC program RTsizer via the ActiveX component. The control program can import/export any data from the INSITEC program RTsizer. The instrument control is done with Field Point modules from National Instruments.

The rotor speed of the air classifier can be adjusted through a frequency inverter in order to produce a specified product size. If the set point is for example 60 µm at d_{70} (d_{70} means that 70 % of the particles are finer than a set point which is 60 µm for this example), this value is kept by a PID regulator through the entire production period. If the product becomes coarser, then the PID regulator increases the rotor speed of the air classifier. Figure 6 presents the particle size control loop.

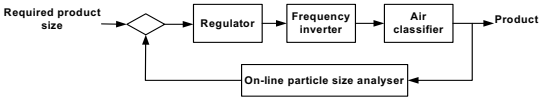

Figure 6. Product size control loop.

Particle Morphology Measurement

In order to demonstrate the effect of the residence time (sweeping speed) on the mill product, image analysis of the produced samples was carried out. About 1 million particles from the product sample are analyzed. The samples are taken at different times during grinding. This should ensure statistical validity of the measurements.

The measurements were focused on the particle roundness. Roundness is characterized on a scale between 0 and 1. If the particle has a roundness factor of 1 it is ideally round. However, if the value is close to 0 it is long and thin (splintery shaped). This investigation was performed using the Pharma Vision 830 equipment, based on the automated camera scanning principle. The sample is dispersed on a glass slide of dimension 100 x 100 mm by compressed air to create a particle mono layer. The glass slide with dispersed material is placed underneath a CCD video camera. A linear actuator automatically moves the camera across the sample and records digitized video images. It is possible to analyze particles in the size range of 3 – 2000 µm.

Roundness is defined as

$$R = \frac{\left|\lambda_1 - \lambda_2\right|}{\lambda_1 + \lambda_2} \tag{1}$$

where λ_1 and λ_2 are the eigenvalues of the covariance matrix M

$$M = \begin{pmatrix} I_{xx} & I_{xy} \\ I_{xy} & I_{yy} \end{pmatrix} \tag{2}$$

where

$$I_{xx} = \sum_{i,j} x_i x_j \; ; \; I_{xy} = \sum_{i,j} x_i y_j \; ; \; I_{yy} = \sum_{i,j} y_i y_j \tag{3}$$

where x_i and y_j are the coordinates of pixel p_{ij} of the object relative to the centre of gravity of the object. The major axis of the object is the eigenvector of the maximum eigenvalue of matrix M.

Results

Each coke type was separately processed in the air swept ball mill circuit. Approximately 2 tons of each was processed. It is necessary to process large amounts of the material in order to reach a steady state of the mill for each test. Table 1 presents specification of all coke types.

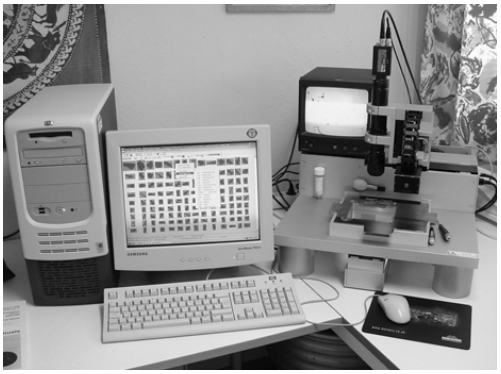

Figure 7. Picture showing the particle morphology measuring device.

Table 1. HGI data for the tested coke types.

Coke type	HGI
Single source A	35
Single source B	37
Single source C	34
Blended coke	36

The Hardgrove Grindability Index measurement is performed according to ASTM standard D409-71. This method indicates grindability/mechanical strength of the coke grains. The size fraction used for HGI determination is 1.18 – 0.600 mm, which is the major constituent in the 2 – 0 mm ball mill feed. The HGI tests indicate that coke C has the highest mechanical strength while coke B is the mechanically weakest.

Specific Grinding Energy Investigation

Three different grades of fines were produced for each type of coke. These fines will be used in a forthcoming investigation of prebake anode production. Sieve analyses were made for the feed fraction to the ball mill and results are shown in Figure 8.

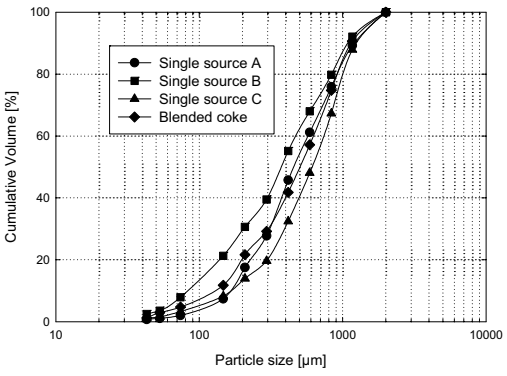

Figure 8. Particle size distribution of the feed material to the mill for four different cokes.

The particle size distribution of each coke is different. Single source coke C has the coarsest feed and single source B is the finest coke. During production the product size was controlled by the

on-line particle size analyzer. The set point of 60 µm at d_{70} was applied and calibration of the laser diffraction results compared to sieve analysis was carried out prior to testing.

All process parameters are measured/logged and the specific grinding energy is calculated. The mill torque is continually measured and an average value is calculated for each experiment. The grinding effect is then calculated according to formula (4).

$$P = \frac{2 \times \pi \times n \times T}{60} \quad (4)$$

P – power [W]
n – mill speed [rpm]
T – torque [Nm]

The production capacity is then used to calculate the specific grinding energy in kWh/t. Figure 9 presents the calculated specific grinding energy for each coke.

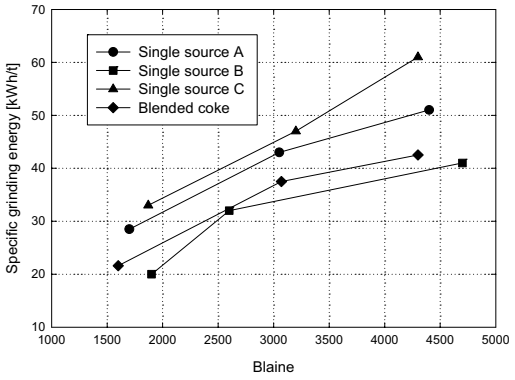

Figure 9. Specific grinding energy versus Blaine number for all tested cokes.

Each material behaves differently due to its mechanical properties. The single source coke C has the highest specific grinding energy for each product. However, single source coke B has the lowest specific grinding energy and thus is the easiest to grind in the ball mill. These results correlate well with the HGI tests which indicate that coke C has the highest grindability index, and coke B the lowest. The graph shows that there is a relation between the specific grinding energy and the Blaine number. The Blaine number was measured according to the ASTM standard C204-84.

Feed Size Effect

The composition of the ball mill feed material often shows large variation in the production of fines for prebake anodes. Recycled fines and/or filter dust from the paste plant are common additions to the primary ball mill feed. Also, material segregation in silos will contribute feed variation. Such a situation was simulated by placing two different size fractions in successive layers in the ball mill feeder. Figure 10 shows a feeder filled with two feed material types. The feed material fines had a particle size of 98 % at -74 µm and a Blaine number of about 4000. The circuit was run so that a 68 % of -74 µm (sieve analysis) was produced. The air classifier rotor speed was adjusted to this product size and no size regulation was applied. Six samples were taken at equal time intervals for further analysis. Figure 11 shows the variation in Blaine number and the amount of -74 µm particles. Particle sizes were measured by sieve analysis.

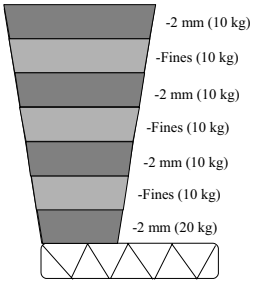

Figure 10. Feeder with two alternating material layers.

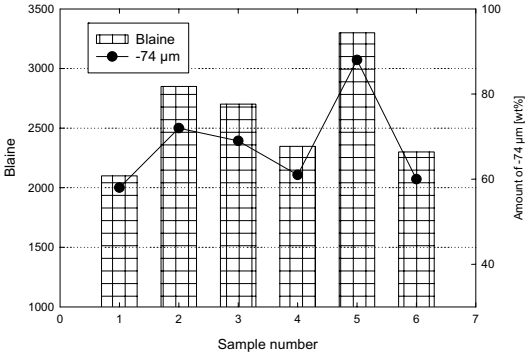

Figure 11. Graph showing the Blaine number and the amount of -74 µm particles (%) for six samples.

Figure 11 shows that there are large variations in the product size as well as in the Blaine number during the production. The variation in product size and Blaine number is also reflected in the process parameters, *i.e.*, the specific grinding energy as well as the return and the mill filling. The test was started at steady state conditions with specific grinding energy 33 kWh/t, mill weight 28 kg and return 31 %, respectively. During the experiment the specific energy, return and mill weight decreased as the fine fraction entered the mill. The feed rate was not adjusted to keep a fixed mill weight in order to demonstrate how the feed size variation can affect both the product quality and the process performance. At the end of the experiment the specific grinding energy was 25 kWh/t, the mill weight 20 kg and the return 15 %, respectively. Not only the product size and the Blaine number are affected but also the iron contamination in the fines fraction due to increased contact between uncovered steel balls.

The Effect of the Sweeping Speed

The residence time of the particle inside the mill determines the degree of contact between coke particles and the steel balls. In air swept ball mills the particles residence time can be regulated by the air sweeping speed. This speed can be regulated by applying false air at the mill outlet and thus not affect the total air flow rate of the circuit. Higher sweeping speed will remove coarser particles from the mill and thus shorten their residence time inside the mill. This will increase the amount of the returned material. If the

sweeping speed is low, the particles will be ground finer (more energy transferred). The amount of the return material will decrease. In order to investigate the effect of the sweeping speed three tests were performed. Figure 12 shows how the sweeping speed affects the Blaine number and the amount of return material. At low sweeping speeds the return is 27 % and fines with a high Blaine number of 3090 is produced. If high sweeping speed is applied, the return increases to 55 % and the Blaine number drops to 2100.

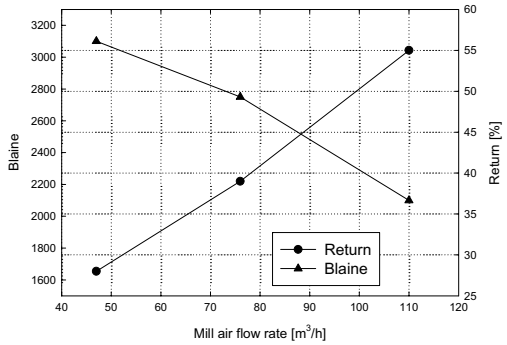

Figure 12. The effect of the sweeping speed on the Blaine number and the amount of return material.

Figure 13 presents particle size distribution of three products produced at different sweeping speeds. The lower sweeping speed gives more fines in the finest range and thus a flatter curve and a higher Blaine number despite that the top size is almost the same for all products. At the highest sweeping speed of 110 m^3/h less fines are produced in the finest range and the distribution curve is steeper compared with the lowest air flow rate.

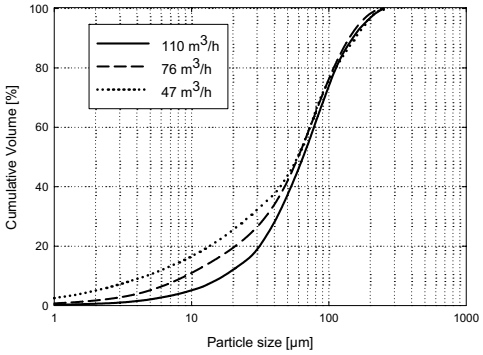

Figure 13. Particle size distribution of three products produced at different sweeping speeds (measured by laser diffraction analysis).

The Effect of Coke Mill Filling

The ideal mill filling level is the level where the lowest specific grinding energy is used for production of identical sized products. Figure 14 demonstrates how the mill charge affects the specific grinding energy. If the mill contains little material and the voids between the balls are only partially filled, the grinding is inefficient. In addition, higher iron content can be expected in the product. The mill filling was controlled by measuring the mill weight during the experiment. The optimum mill filling has to be determined for each coke and product size.

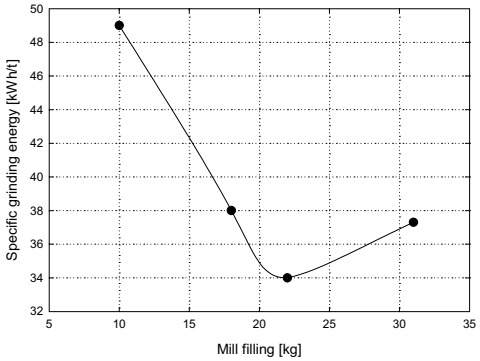

Figure 14. The relation between the mill filling of coke and the specific grinding energy.

Residence Time/Sweeping Speed Versus Particle Morphology

Samples extracted during the sweeping speed experiments were analyzed with respect to particle morphology.

Particle residence time in the mill affects the particle roundness, as the contact time between balls and particles and also between particles is longer at longer residence times. This causes rounded-off particles. Figure 15 shows a typical coke grain. The grain on the left has a very intricate shape with low roundness while the other grain is smooth and has a high roundness factor.

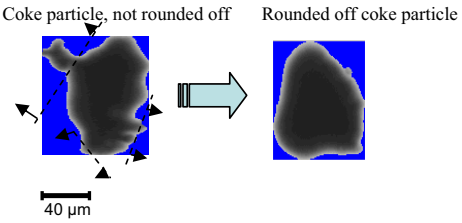

Figure 15. Particle roundness due to milling.

Prior to morphology analysis, the samples were sieved into several fractions. Figure 16 presents results from the morphology analysis of product samples produced with different sweeping speeds/residence times. This investigation was done only with the single source cokes. The roundness values are expressed in volume percent. The particle volume is calculated from formula (5).

$$V = \frac{2 \times a \times d}{3} \qquad (5)$$

where a is the object (particle) area and d is the mean object diameter.

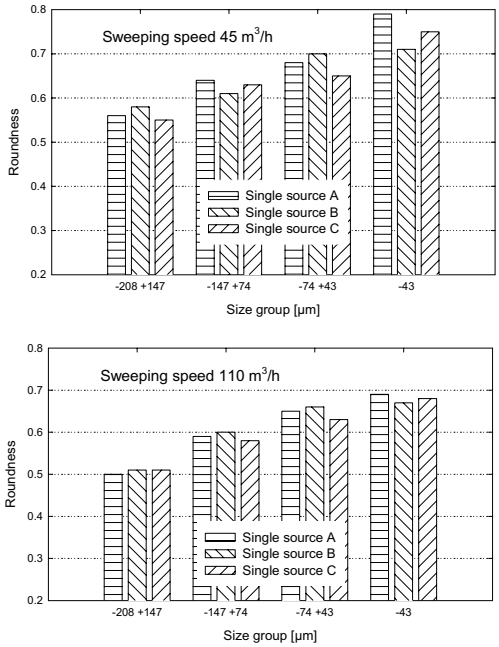

Figure 16. The relation between particle roundness factor and sweeping speed in the mill.

An average value of approximately 1 million measured particles from each sample is displayed in the graphs. Two graphs are shown in Figure 16, one for sweeping speed 45 m^3/h and the second for 110 m^3/h. Four size fractions were analyzed and the results show that a longer mill residence time gives rounder coke grains than a shorter residence time. There are also differences between each single source coke type due to their different mechanical strength.

Two different breakage mechanisms act during the mill grinding. The cascading mill charge movement causes attrition breakage which enhances fine particle production. However, the cataracting motion generates impact breakage which produces coarse particles. The higher amount of fines inside the mill is caused by a lower velocity of the sweeping air and thus a flatter screening curve (more fines) of the product results. Particle residence time controls the amount of fines but also their roundness. The cascading of particles and balls rounds off coke grains during grinding.

Discussion and Conclusion

This study demonstrates how different petrol coke materials behave during ball mill grinding under varying conditions. Single source C coke has the highest specific grinding energy (Figure 9) due it its mechanical strength which is also indicated by the HGI test. The specific grinding energy and mill capacity are proportional to the mechanical strength of the coke grains. The observed difference in the Blaine number is to be expected since the amount of return load to the mill also is changed. The Blaine number is related to the slope (amount of finest particles) of the particle size distribution curve (Figure 13). As the curve is flatter the Blaine number increases independent on the top size. If the curve is steeper (high circulating load and low particle residence time in the mill), then the Blaine number decreases. This corresponds to a situation with different coke types where the mechanical strength determines how much energy is needed to produce a certain product size. If higher energy is needed then there also will be a larger amount of coarse material going back to the mill as reject from the air classifier.

Results from the tests with inhomogeneous ball mill feed material show that the product size and its Blaine number change due to the feed size variation. The size variation also causes changes in the grinding circuit, e.g., decreasing mill filling which affects the iron content of the product, lower capacity and thus higher specific grinding energy. The size variation in the mill feed fraction is not only caused by recycling of filter dust from the paste plant but can also be due to segregation phenomena in the feed silo. It is critical to have a good control of the ball mill circuit in order to predict and avoid the variation in the mill product size and the Blaine number, respectively.

The mechanical strength of the coke grains is important for the resulting roundness factor. Mechanically stronger grains are resistive towards impact attrition breakage and therefore they will be more rounded. Single source cokes A and C are more rounded off in the finest range (- 43 µm) due to their higher grindability. Particle roundness will affect material compactness, porosity/permeability (voids filling), the Blaine number and the contact area between particles when compacted.

Industrial implications

Process variations introduced by raw materials (coke quality, feed fraction instability) and/or insufficient ball mill circuit control will cause unpredictable composition of the fine fraction. The pitch demand will hence fluctuate and the anode quality will deteriorate. Optimum ball mill circuit control will compensate for the variations and ensure stable fine fraction production.

Acknowledgement

Financial support from NFR and the Norwegian aluminium and ferro industries through the CarboMat program is gratefully acknowledged.

References

1. Smith, M. A., Perruchoud, R. C., Fisher W. K., “An evaluation of the effect of dust granulometry on the properties of binder matrix bench scale electrodes”, Light Metals 1991, 651 – 656.
2. Austin, L. G., Klimpel, R. R., Luckie, P. T., “Process Engineering of Size reduction: Ball Milling”, 1984 American Institute of Mining, Metallurgical, and Petroleum Engineers, Inc.
3. Kolacz, J., “Improving the fine grinding process in an air swept ball mill circuit”, PhD thesis, NTH 1995.
4. Sandvik, K. L., Digre, M., Malvik, T., “Oppredning av primære og sekundære råstoffer”, Tapir 1999 (in Norwegian).
5. Carter C. M., ”An alternative ball mill feed controller”, Light Metals 1979, 635-645.

Light Metals 2006 *Edited byTravis J. Galloway* ***TMS (The Minerals, Metals & Materials Society), 2006***

THERMAL DILATION OF GREEN ANODES DURING BAKING

Juraj Chmelar[1], Trygve Foosnæs[2], Harald A. Øye[2]
[1] SINTEF Materials and Chemistry, NO-7465 Trondheim, Norway
[2] Norwegian University of Science and Technology, Department of Materials Science and Engineering, NO-7491 Trondheim Norway

Keywords: Petrol Coke, Thermal Dilation, Characterisation

Abstract

Pilot scale anodes were made using three single source and one blended coke to determine how the green anode properties affect the final baked anode. Testing was performed in an improved vertical dilatometer using samples 50 mm in diameter and 50 mm long to determine the effect of different heating rates. No sample support was used, however the effect of packing material was evaluated. The sample shrinkage was calculated from the dilatometer data as the difference between the expansion at 550 °C and 950 °C. Dilatometric data for anodes prepared identically and with the same composition show differences due to varying mechanical properties of the cokes.

Introduction

After forming, the anode is baked to temperatures in excess of 1100°C. During this thermal treatment the anode can be subjected to significant stress, mainly due to thermal expansion, shrinkage and inherent temperature gradients, which can affect critical properties of the anode. Understanding these physical and chemical changes is important for both the economic viability of the process and optimal process control.

Dilatometric equipment was developed to study the dimensional changes during baking of green anodes, showing that these changes are influenced by sample orientation parameters (both parallel and perpendicular to the direction of forming), type of filler, specimen dimensions and heating rate [1].

Two studies [2, 3] point out that grain size distribution, pitch content, heating rate and the use of packing mass have significant influence on the dimensional changes during baking.

Description of thermal dilation

Figure 1 presents an example of thermal dilation of a green core sample 50 mm in diameter and 50 mm long, containing 15 % pitch. No packing material was used to support the sample. The sample was heated at 60 °C/h to 950 °C, then held for three hours under nitrogen.

The initial expansion at about 100 °C is due to release of residual stresses from the forming and cooling process. The sample expands further (up to 0.55 % of its initial height) because of trapped volatiles. A further increase in the temperature leads to slumping caused by the plasticity of the sample. The sample expands slightly at about 300 °C due to trapped light binder volatiles. There is a sudden height increase at about 400 °C which most probably is a consequence of the residual pitch expulsion from the coke pores. The sample height is then reduced after the release of volatiles and at about 450 °C the transition from a plastic to a solid matrix starts. The major release of non-coking volatiles takes place up to about 600 °C. The post coking process starts at about 600 °C and continues until 900 °C, followed by the release of cracked volatiles (methane, hydrogen) and sample height reduction. [4]

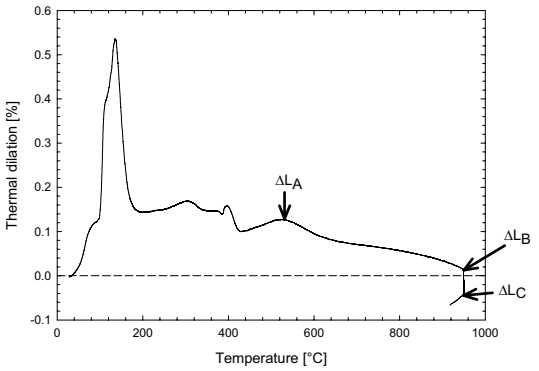

Figure 1. An example of thermal dilation measurement of a green sample versus temperature.

Standard method for determination of shrinkage during baking

The ISO 14428 standard describes the determination of expansion and shrinkage of ramming pastes during baking [5]. The standard describes the experimental procedure, equipment used for testing and how to calculate and interpret results.

In the current study the sample was packed in a mass of carbon particles (electro-calcined anthracite or graphite), then heated in nitrogen at 180 °C/h to 950 °C, where it was soaked for three hours.

The maximum thermal shrinkage before and after soaking at 950 °C were calculated from the following equations (Figure 1):

$$\Delta L_{before} = \Delta L_A - \Delta L_B \quad (1)$$

$$\Delta L_{after} = \Delta L_A - \Delta L_C \quad (2)$$

The distance measurements were corrected for the movement of the sample base by calibrating the equipment. However, the ISO 14428 method does not discuss the significant changes that occur before the sample reaches 450 °C.

Equipment

This investigation was performed in an improved vertical dilatometer, with a water cooled cylindrical furnace (Figure 2).

Two type S thermocouples were installed, one in the middle of the furnace to control the furnace temperature and the other from the bottom to measure the sample temperature. A core sample of 50 mm in diameter and 50 mm long was placed on a graphite washer inside the cylindrical quartz tube. A quartz push rod rested on top of the sample and followed the sample movements, which were then transferred to a linear transducer.

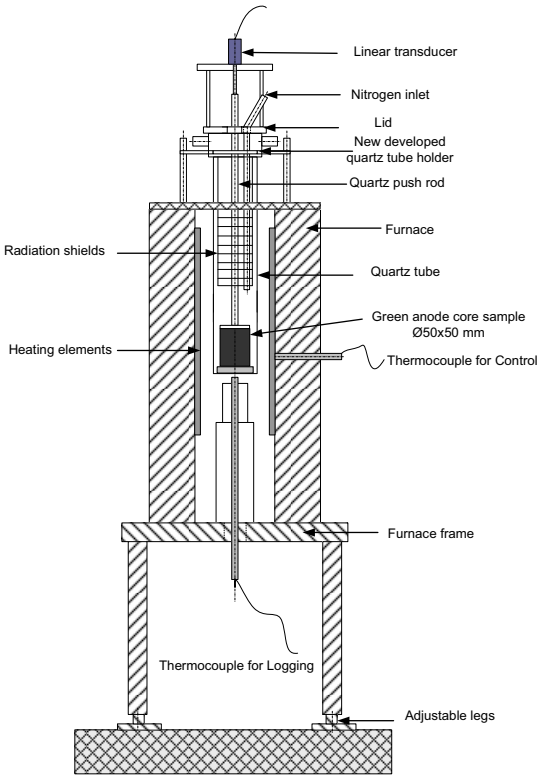

Figure 2. Schematic drawing of the dilatometer.

A quartz tube was suspended in the oven and kept in position with a holder suspended on four long bolts with nuts on the top of the oven. The top of the quartz tube was attached to a holder with two o-rings compressed between the quartz tube and the metal holder. This arrangement allowed the quartz tube to be positioned firmly in the furnace.

The new holder was additionally equipped with two ducts placed on opposites sides, but only one of them was used during the experiments for the outlet of the off-gasses. A rubber hose was installed on this duct and led to a vent pipe installed above the furnace. The under-pressure created by the rubber hose was sufficient to draw out the off-gasses, preventing condensation of volatiles on the push rod and linear transducer.

An enhanced nitrogen purging system was developed where a quartz tube of internal diameter 5 mm was mounted into the lid and through the radiation shields. The tube ended about 8 cm over the sample. This solution ensured nitrogen purging of the sample, prevented oxidation and also provided helpful circulation of the off-gasses from the green carbon sample. The nitrogen flow rate was approximately 40 l/h.

The furnace operation and thermal dilation measurement was controlled with LabView 7.1, a graphical programming language. The Human Machine Interface (HMI) allows the user to set the heating profile of the furnace as well as logging frequency, nitrogen purging and start/end of the water cooling. The sampling time can be defined between 0.5 seconds and 10 minutes.

Equipment calibration and dilation corrections

Prior to experimental testing the dilatometer was calibrated. The position of the quartz tube was adjusted so that the sample temperature was isothermal (± 2 °C). Subsequently, the quartz tube with the push rod was calibrated with a quartz reference sample (50 mm in diameter and 50 mm long; R&D Carbon).

Experimental and Results

Method optimisation

The aim of this investigation was to find an effect of the heating rate and the sampling position on the thermal dilation results. The shrinkage for each investigation is also presented.

The anodes were made from one coke type, one composition (coarse 17 %, medium 23.8 %, fines 34 % and dust 25.2 % with 63 % of -63 μm) and 15 % pitch content. The paste was mixed in a sigma mixer and formed in a vibration compactor. Core samples 160 mm in diameter and about 180 mm high were taken from the pilot scale anodes. Two core samples of 50 mm diameter were drilled from one green anode. The outer 15 mm of the samples was cut off in order to remove the outer inhomogeneous layer.

Influence of the heating rate

Four heating rates were investigated; 20, 60, 120 and 180 °C/h. The samples were free standing in the dilatometer and purged with nitrogen. The average for two samples is presented.

Figure 3 presents the thermal dilation curves for each heating rate. The maximum thermal expansion for the lowest heating rate (20 °C/h) was at about 120 °C, while the highest heating rate (180 °C/h) gives the highest maximum at 140 °C. The heating rates of 60 and 120 °C/h have a very similar curve profile. At the lower heating rates the dilation changes occur earlier than with the higher heating rates, except the initial expansion at a heating rate of 180 °C/h.

Calculated shrinkage ΔL_{before} and ΔL_{after} are presented in Figure 4. The highest shrinkage occurred for the heating rate of 180 °C/h, while the lowest shrinkage was found at 20 °C/h.

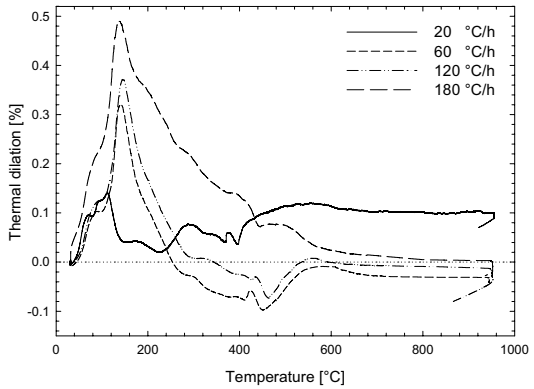

Figure 3. Thermal dilation of identical samples at different heating rates.

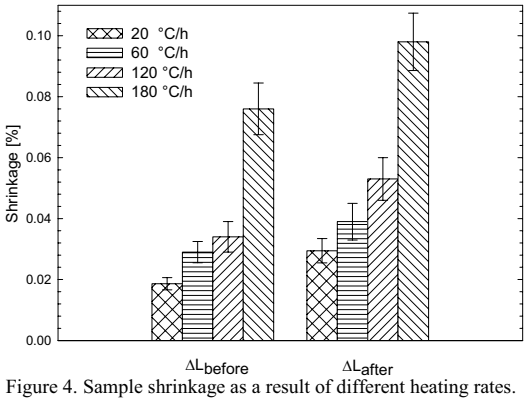

Figure 4. Sample shrinkage as a result of different heating rates.

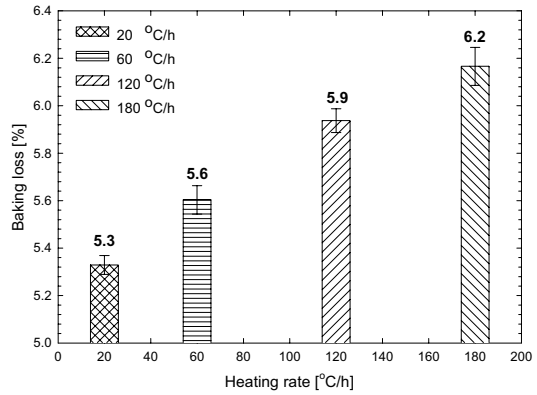

Figure 5. Baking loss of the samples at different heating rates.

The shrinkage results show how the heating rate can affect the final sample shrinkage and the tension in the samples thus created. This may have a critical effect on the final properties (air permeability, specific electrical resistance and Young's modulus) of the baked anodes. Measurements were only performed in the vertical direction (parallel to the vibration direction), thus there is limited information about the horizontal expansion/shrinkage of the sample.

Finally, the baking loss of the samples was measured and is presented in Figure 5. The baking loss increases with increasing heating rate.

Influence of the sampling position and packing mass

It was found that the sampling position in the anode was of critical importance for the behaviour of the sample during the thermal dilation investigation [1].

During forming the compaction force decreases with the sample depth, due to friction between the coke particles and between the paste and the mould. The force distribution corresponds to the thickness of the bridge layer of pitch between the particles. At the top of the sample the bridge layer will be thinnest while at the bottom the thickest. This can be seen after the forming process of the green anodes as a dark area at the top on the periphery due to pitch pressed out from the anode as a consequence of the pressure in this area.

Eight samples were tested in the dilatometer with a heating rate of 60 °C/h. Four samples were run with a graphite packing mass (graphite particles +0.5 mm to -1.0 mm) and the other four were free standing. Figure 6 shows the thermal dilation profile of the samples from the top and bottom positions. The drawn curves are the calculated average of two parallel measurements.

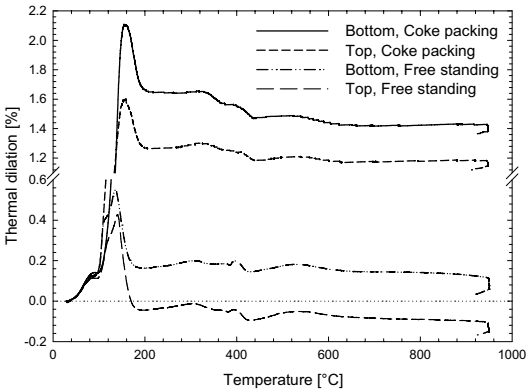

Figure 6. Thermal dilation of the graphite packed and free standing samples from the top and bottom of the green anode.

There is a significant difference in the thermal expansion when the sample is freely standing or packed. Much higher expansions are obtained when the sample is packed as slumping is minimized.

The bottom samples reached a higher maximum expansion than the top samples. The higher expansion maximum was caused by a higher pitch concentration between the particles in the bottom part of the green anode. The bottom samples of the anode have correspondingly slightly higher shrinkage than the samples from the top (Figure 7). Also, there is a difference between free standing and packed samples. The packed samples have lower values for both ΔL_{before} and ΔL_{after} due to the radial thrust on the sample from the packing mass.

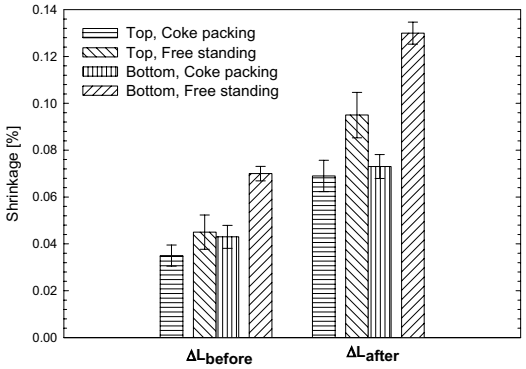

Figure 7. Shrinkage for samples with and without packing from top and bottom position.

Testing of three single source cokes

Anode samples from three single source cokes marked as SSA, SSB and SSC were investigated in the dilatometer. Table 1 presents the coke specifications. The cokes differ in sulphur content where SSC has the highest amount (2.89 wt%), SSA (1.09 wt%) and SSB (1.06 wt%). There is also a difference in the grain stability, where SSA and SSC are the mechanically strongest (87 and 85) while SSB is the weakest (66). Porosity was analysed with an image analysis technique on a 0.5 to 1 mm coke fraction [6]. The porosity was analysed with 3 µm cut-off size. The SSA and SSC cokes have a very similar total porosity of 16.8 and 17.1 %, while the SSB coke has the highest total porosity of 21.1 %.

Table 1. Coke specifications.

Properties	Method	Unit	SSA	SSB	SSC
Grain stability	ISO 10142	%	87	65	85
Total porosity	Image analysis	%	16.8	21.1	17.1
Sulphur	ISO 12980	%	1.09	1.06	2.89
		45*	0.60	0.72	0.62
Dust roundness	Image analysis	63*	0.67	0.76	0.66
		94*	0.74	0.87	0.76

* dust size expressed in % of particles passing a 63 µm sieve

Each coke was sieved separately in specified fractions for further recipe mixing (coarse 17 %, medium 23.8 %, fines 34 % and dust 25.2 %). The dust was produced by grinding the -2 mm fraction in an air swept ball mill [7]. Three different dust sizes were produced; Dust 45, Dust 63, and Dust 94, which corresponds to 45 %, 63 % and 94 % of the particles passing a 63 µm sieve, respectively.

The roundness of the particles was characterized by image analysis (Pharma Vision 830). Roundness is characterized on a scale between 0 and 1[7]. A perfect circle has a roundness of 1.0, while a very narrow elongated object has a roundness close to 0. Table 1 presents the mean dust size values. The differences in the mechanical strengths of the investigated cokes resulted in varying roundness of the produced fine particles. The SSB coke has higher roundness values compared to the SSA and SSC cokes. The standard deviation of particle roundness was about 5 % for Dust 45, 4.1 % for Dust 63 and 3.2 % for Dust 94. The differences in roundness can influence the powder flowability and internal friction [8]. The binder matrix using SSB coke is expected to flow more easily while in the SSA and SSC cokes the flowability was reduced due to irregularly shaped interlocking particles. However, the SSB coke has a similar roundness factor in Dust 45 as SSA and SSC have in Dust 94.

The anode paste (15 % pitch) was compacted in a vibrator at 170 °C. Core samples were drilled from identical positions in order to maintain the same testing conditions. The dilatometer was heated at 60 °C/h to 950 °C where it was soaked for three hours before cooling. All samples were run without a packing mass. Two samples were run for each test and an average of these is presented in Figures 8, 9 and 10. Figures 11, 12 and 13 show the measured shrinkage. Figure 14 presents four graphs where the first three (SSA, SSB and SSC) are plotted correlations between the dust size and the residual sample dilation (thermal dilation after the initial expansion when the height flattens out). The fourth graph presents the green apparent densities for each coke and dust size, and indicates that 15 % pitch is optimum for SSB coke with Dust 45, while the optimum for SSA and SSC cokes is Dust 63.

Dust 45 produced samples with a very similar shrinkage (Figure 11) despite a large expansion of the SSB coke, first at about 110 °C then strongly at 240 °C followed by slumping at about 350 °C (Figure 8). The expansion at 350 °C is probably caused by a denser matrix where binder volatiles were trapped and rounder particles produced higher flowability in the paste. At this dust size the SSB coke had the lowest shrinkage for both ΔL_{before} and ΔL_{after} and it seems that 15 % pitch is close to optimum for SSB at this grain composition (Figure 14). During the mixing process more fine particles were generated in the mechanically weak SSB coke, thus generating a higher surface area. It is expected that some of the largest grains in the coarse and medium fractions were crushed during mixing, thus reducing the samples overall strength.

The SSB coke with Dust 63 has a similar dilation profile (as with Dust 45); however both the initial expansion at 110 °C and the expansion at 350 °C are lower, although it reached the highest shrinkage of all cokes for this dust size. The lower expansion is considered by the larger surface area of the particles and thus a thinner binder layer with lower adhesion strength. The SSA coke initially expanded more to 160 °C with this size fraction after a significant residual stress release at 70 °C. The higher expansion is caused by a more dense structure with a higher volume of trapped volatiles in the voids and pores. The SSC coke with Dust 63 has nearly identical initial expansion (110 °C) as with Dust 45, however the whole thermal dilation profile is higher. Dust 63 produced the best composition with 15 % pitch content, considering green apparent densities (Figure 14) for both SSA and SSC.

The largest fine dust fraction of 94 % changed the thermal dilation profile of the SSB coke dramatically. The secondary expansion at about 350 °C (also observed with Dust 45 and Dust 63) was diminished and the sample shrunk extensively from 500 to 950 °C. For this composition visible cracks were observed at the periphery, which might contribute to the sample shrinkage. The sample became under-pitched with Dust 94 and thus no significant expansion occurred because of a limited amount of trapped volatiles in the voids and pores. The highest initial expansion is observed for the SSC coke at about the same temperature (160 °C) as measured with Dust 63. The higher thermal dilation might be caused by more trapped volatiles in a denser structure. However, the SSA coke does not have a large

initial expansion, but instead three subsequent peaks from about 70 to 190 °C. The highest shrinkage was found for the SSB coke, while the lowest for the SSC coke (Figure 13).

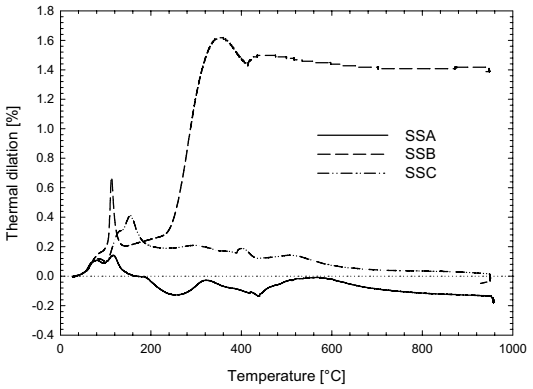

Figure 8. Thermal dilation of three single source cokes made with Dust 45 and 15 % pitch.

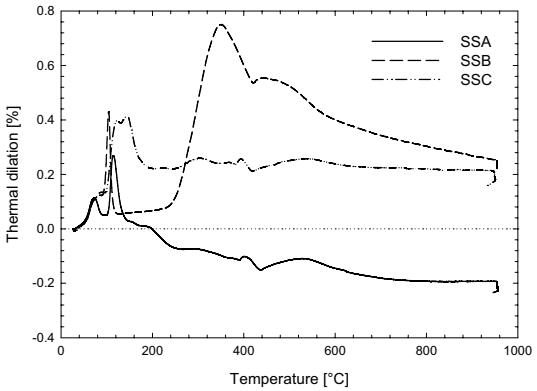

Figure 9. Thermal dilation of three single source cokes made with Dust 63 and 15 % pitch.

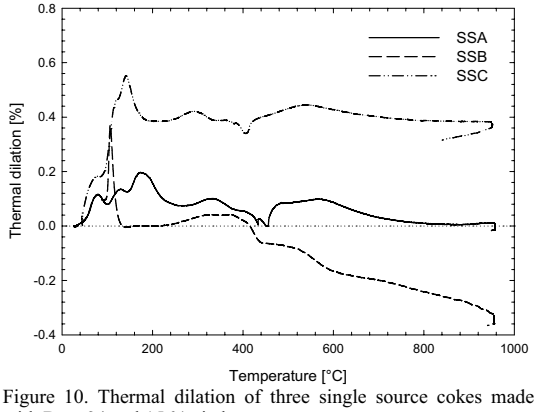

Figure 10. Thermal dilation of three single source cokes made with Dust 94 and 15 % pitch.

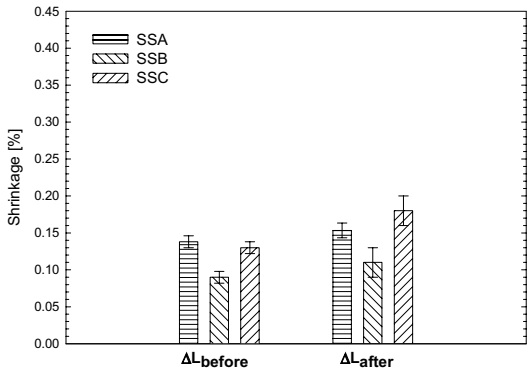

Figure 11. Shrinkage for three single source cokes made with Dust 45 and 15 % pitch.

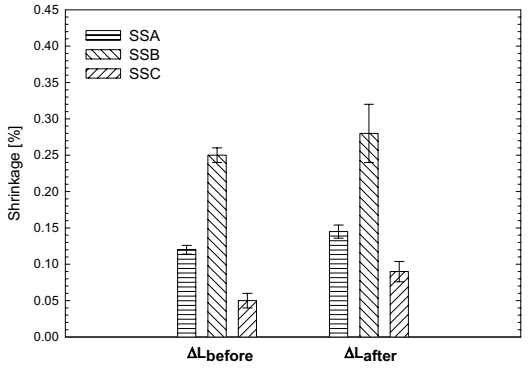

Figure 12. Shrinkage for three single source cokes made with Dust 63 and 15 % pitch.

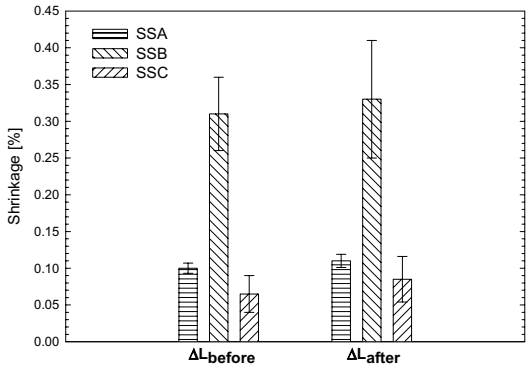

Figure 13. Shrinkage for three single source cokes made with Dust 94 and 15 % pitch.

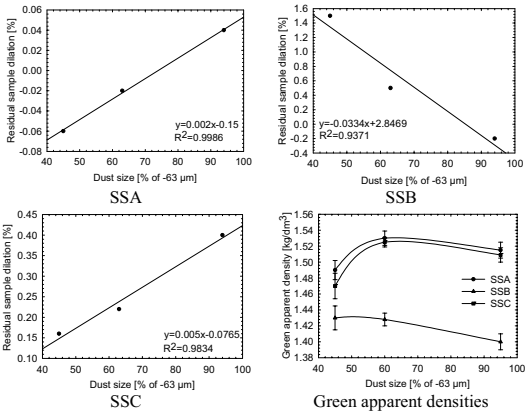

Figure 14. Residual sample dilation for SSA, SSB, SSC and green apparent densities versus three dust sizes.

The correlation between the residual sample dilation (thermal dilation after the initial expansion when the height flattens out) and dust size fraction in Figure 14 shows an increasing trend for the SSA and SSC cokes while it decreases for the SSB coke. The most probable reason why the SSB coke has a decreasing trend and lower green apparent density is the excess fines and lack of large coke grains, due to crushing during mixing, and thus a binder deficit resulting in reduced overall strength and crack formation.

Discussion and Conclusion

The new dilatometer construction showed an improvement in the reproducibility and measurement stability.

Four different heating rates were investigated with green core samples of identical pitch content and granulometry. An increase in the heating rate contributes to a larger initial expansion due to more trapped volatiles (at about 150 °C) and also to a higher final baking loss. The calculated shrinkage showed that the highest heating rate (180 °C/h) produces samples with the highest shrinkage, while the lowest heating rate (20 °C/h) had the lowest shrinkage. Additionally, changes in the early thermal expansion can be observed with a decrease in the heating rate.

The importance of the sampling position was investigated with the samples drilled from the top and bottom position of the green pilot anodes. Also, the difference between samples with graphite packing versus free standing samples in the dilatometer was investigated.

The distribution of the forming force inside the anodes is reduced with the height due to friction between the coke particles and between the paste and the mould. Therefore, an inhomogeneous binder distribution is generated in the anode's height and width. The results show that the bottom samples have a higher expansion due to a thicker pitch bridge layer while the top samples have reduced expansion. The sample packing contributed to a higher initial expansion due to the reduced free surface area for binder volatile release, and the calculated shrinkage was reduced because of the radial thrust from the packing material.

Anodes made from three single source cokes (SSA, SSB and SSC) were investigated in the dilatometer with the same pitch content and identical granulometry, but with three different dust sizes (45, 63 and 94 % of –63 µm). The SSA and SSC coke are the mechanically strongest and produced more irregular particle shapes (particles with lower roundness) during grinding in the ball mill, while the softer SSB coke has rounder particles for each size distribution. There is also a significant porosity difference, which is similar for SSA and SSC cokes (16.8 and 17.1 %, respectively) while SSB coke was 21.1 %.

The measurements show decreasing shrinkage with decreasing dust particle size (only for SSA and SSC cokes), while for the samples made of SSB coke the shrinkage increases.

The mechanically weak SSB coke had the highest green apparent density already with Dust 45, while the SSA and SSC coke had the highest density with Dust 64. This is due to an increase in the fines (surface area) and lack of large grains (coarse and medium fractions) by crushing during the mixing process.

Acknowledgment

Financial support from NFR and the Norwegian aluminium and ferro-alloy industries through the CarboMat program is gratefully acknowledged.

References

1. Fitzer E., Huettinger K.J., Megalopoulos A., "Dilatometric study of the baking behaviour of pitch bonded carbon artifacts". Carbon 1973, p. 621-626
2. Letizia I., Calderone F., "Linear dimensional changes occurring during the baking of pitch-bonded green carbon bodies". Carbon 1980, p. 297-301
3. Martirena H., "Laboratory studies on mixing, forming and calcining bodies". Light metals TMS 1983, p. 749-764
4. Foosnæs T., Naterstad T., in "Introduction to aluminium electrolysis". Second edition, Grjotheim K., Kvande H., Editors, Aluminium Verlag, ISBN 3-87017-233-9, p. 87-138
5. ISO 14428, "Expansion and shrinkage during baking", 2005
6. Rørvik S., Øye H.A., Sørlie M., "Characterisation of porosity in cokes by image analysis". TMS 2001, p. 603-609
7. Chmelar J., Foosnæs T., Øye H. A., Sandvik K.L., "Coke quality effect on the grinding in an air swept ball mill circuit". Light Metals TMS 2005, p. 647-652
8. Bumiller M., Carson J., Prescott J., "A preliminary investigation concerning the effect of particle shape on a powder flow properties". Malvern Instruments, 2005
9. Dell M.B., Peterson R.W., "Dilatometry of pitch-anthracite mixes for carbon". Metallurgical Transaction Volume 4 1973, p. 2077-2080
10. ISO 10142, "Determination of grain stability using a laboratory vibration mill". 1996